Polymer Modified Asphalt Evaluation at Desert Environment

BY

Khaleel J. Al-Adham

A Dissertation Presented to the

DEANSHIP OF GRADUATE STUDIES

KING FAHD UNIVERSITY OF PETROLEUM & MINERALS

DHAHRAN, SAUDI ARABIA

In Partial Fulfillment of the

Requirements for the Degree of

DOCTOR OF PHILOSOPHY

In

CIVIL ENGINEERING

December 2017

KING FAHD UNIVERSITY OF PETROLEUM & MINERALS

DHAHRAN- 31261, SAUDI ARABIA

DEANSHIP OF GRADUATE STUDIES

This thesis, written by **Khaleel J. Al-Adham** under the direction of his thesis advisor and approved by his thesis committee, has been presented and accepted by the Dean of Graduate Studies, in partial fulfillment of the requirements for the degree of **DOCTOR OF PHILOSOPHY IN CIVIL ENGINEERING.**

Prof. Hamad Al-Abdul Wahhab
(Advisor)

Dr. Salah U. Al-Dulaijan
Department Chairman

Prof. Ibnelwaleed A. Hussein
(Member)

Prof. Nedal Ratrout
(Member)

Prof. Salam A. Zummo
Dean of Graduate Studies

Dr. Ali Al-Gadhib
(Member)

29/1/13
Date

Dr. Hassan Al-Ahmadi
(Member)

I dedicate this work to my family; father, mother, brothers and sister. A special feeling of gratitude is to my loving wife Shahd and son Jawad.

I also dedicate this dissertation to my many friends at KFUPM community who have supported me throughout the study period.

ACKNOWLEDGMENTS

I would like to thank my advisor, Professor Hamad Al-Abdul Wahhab, for his countless hours of encouragement and patience during the past five years. I have learned a lot from him in life and academic issues. Thanks are extended to committee members; Professor Ibnelwaleed A. Hussein, Professor Nedal Ratrout, Dr. Ali Al-Gadhib and Dr. Hassan Al-Ahmadi for their help during the research period.

I would like to acknowledge and thank Dr. Salah Al-Dulaijan, the chairman of civil engineering department at KFUPM, for allowing me to conduct my research and for using its laboratories and machines. Special thanks go to Mr. Baig and Highway lab technicians and workers; Mansur, Ibrahim and Fathi in the "Advanced Highway Materials Laboratory" for their help in preparing samples and for their continued support.

TABLE OF CONTENTS

LIST OF TABLES

LIST OF FIGURES

LIST OF ACRONYMS AND SYMBOLS

AASHTO	American Association of State Highway and Transportation Officials
AMPT	Asphalt Mixture Performance Test
APA	Asphalt Pavement Analyzer
DSR	Dynamic Shear Rheometer
Jnr	Non-recoverable Creep compliance
MSCR	Multiple Stress Creep Recovery
Pb	Polybilt
PG	Performance Grade
PMA	Polymer Modified Asphalt
RTFO	Rolling Thin Film Oven
SBS	Styrene-Butadiene-Styrene
VMA	Voids in minerals aggregate
VFA	Voids filled with asphalts
$\%\mathbf{R}_{3.2\ kPa}$	Percent Recovery after applying 3.2 kPa repeated stress
$\mathbf{F_N}$	Flow Number
|E*|	Asphalt Mix Dynamic Modulus
$\boldsymbol{\eta}$	Binder Viscosity in poise
$\boldsymbol{f}$	Load frequency in Hz
$\mathbf{V_a}$	% air voids in the mix, by volume
$\mathbf{b_{eff}}\%$	Effective binder content, by volume
$\boldsymbol{\rho_{34}}$	% retained on the 3/4-in sieve, by total aggregate weight (cumulative)

ABSTRACT

Full Name : [Khaleel Jawad Al-Adham]

Thesis Title : [Evaluation of Polymer Modified Asphalt Exposed to Desert Environment]

Major Field : [Civil Engineering]

Date of Degree : [December, 2017]

New grading and evaluation process has been introduced to better characterize the modified asphalt binders utilizing Multiple Stress Creep Recovery (MSCR). Four polymer types commonly used in the modification of asphalt binders in local project are selected in this study. Styrene-Butadiene-Styrene (SBS), Crumb Rubber (CR), Polybilt (Pb) in addition to Eastman (EE2) were used. It is found that asphalt binder has significant contribution to the performance of the asphalt mix. Therefore, it is important to evaluate the rutting and fatigue performance of polymer modified mixtures to satisfy the latest Performance Grading (PG^{+}) system for asphalt binders at high temperatures and traffic loads.

SBS modified asphalt binders can sustain the change of Jnr value even at high service temperatures (76°C) which can resist rutting at Extremely Heavy Traffic when adding 6% of SBS and Heavy Traffic when 4% of SBS is added to local asphalt binders. The effect of 10% of crumb rubber (CR) on improving the Jnr is low compared to 6% SBS values. It can only withstand Heavy traffic at 70°C and Standard Traffic.

Local asphalt binders modified with 6% of Polybilt (PG 70(V)) are suitable for weather of 70°C temperature and very heavy traffic conditions. While 6% of EE2 modified asphalts are suitable for Heavy Traffic only at same weather conditions. None of the

plastomeric modified asphalt binders show significant improvement at 76°C temperature compared to SBS modified asphalts.

The performance of the modified asphalt mixes were evaluated in terms of the engineering properties related to the asphalt binder and mix. Samples were prepared using Superpave mix design which contains different types and amount of polymers. Three different dense-graded aggregate blends of wearing courses with different aggregate gradation within the same nominal maximum aggregate sizes (NMAS) were used in the design of thirty nine different concrete mixes.

A catalog of dynamic modulus values was developed and grouped by high temperature performance grade of the binders and aggregate gradations to evaluate and model the performance of the designed mixes. In addition, rutting resistance and fatigue properties were measured using Asphalt Pavement Analyzer (APA) and Flexural Beam Test, respectively. Test results indicated that dynamic modulus was sensitive to the PG actual temperatures and percent of course aggregate in the mix. Mixtures designed for PG^{+} and/or higher amounts of larger aggregates have higher dynamic modulus, lower rut depths and higher fatigue life at service temperatures.

Unmodified wearing courses showed rut depth of around 6mm after 8,000 load cycles, while modified mixes that contain 5% of polymer content can reduce rutting to less than 1.0 mm. The slope of the permanent deformation curves of unmodified mixes was 3-4 times higher than the slope of modified mixes. A multiple linear regression equation that predicts rut depth at 64°C after applying 8,000 loads cycles was developed utilizing mix properties that include actual PG temperature, polymer content, voids in mineral

aggregates effective polymer content and filler content. A correlation between laboratory measured and predicted rut depth was developed.

Fatigue tests were conducted on laboratory prepared mixes to develop fatigue life prediction models and used to characterize the behavior of different polymer modified asphalt concrete mixes that represent typical wearing courses of local pavements. Tests were carried out at intermediate temperature of 20°C and different strain levels. The analysis of variance showed that the impacts of strain amplitude, binders' actual PG temperature (T_{PG}), Polymer content (%P), voids in mineral aggregates (VMA), percent of course aggregate ($\rho 4$) and effective binder content to filler ratio have a significant effect on fatigue behavior. The developed models provide local pavement engineers the tool for accurate assessment of fatigue and rutting damage for different polymer modified asphalt concrete mixes. The results of this research show that with the use of polymer modification, thinner and less expensive roads can be constructed in Saudi Arabia.

ملخص الرسالة

الاسم الكامل: خليل جواد خليل الادهم

عنوان الرسالة: تقييم الخلطات الاسفلتية المحسنة في الاجواء الصحراوية

التخصص: هندسة مدنية

تاريخالدرجة العلمية: ديسمبر 2017

في الآونة الأخيرة، تم إدخال عملية تصنيف وتقييم جديدة لتحسين وصف الرابط الأسفلتي المعدل والتي تستخدم اختبار الاجهاد المتعدد واستعادة المرونة. إن التأثير الكبير لخصائص الرابط الاسفلتي على أداء الرصفات يزيد من أهمية تقييم أداء التخدد والاجهاد للخلطات الاسفلتية المحسنة باستخدام البوليمرات في درجات الحرارة العالية و حركة المرور المتزايدة.

في هذه الدراسة، تم تقييم أداء الخلطات الأسفلتية المعدلة من حيث الخصائص الهندسية المتعلقة بالرابط الأسفلتي والخلطات على حد سواء. حيث تم تحضير العينات باستخدام طريقة Superpave من أنواع وكميات مختلفة من البوليمرات. حيث شملت هذه البوليمرات على ستايرين-بوتادين-ستايرين (SBS)، المطاط المعاد تدويره (CR)، بوليبيلت (PB) بالإضافة إلى إيستمان إي-2 (EE-2). تم استخدام ثلاثة خلطات من الركام المتجانس التي لها نفس التدرج الاكبر والتي تمثل الطبقة السطحية المعتمدة من قبل وزارة النقل في المملكة في تصميم تسعة وثلاثين خلطة من الخرسانة الاسفلتية المختلفة. أثبتت نتائج اختبار الرابط الاسفلتي المحسن أن قيم معامل استعادة المرونة يمكن تحسينها حتى عند درجات الحرارة العالية والتي قد تصل الى 76 درجة مئوية وذلك عنداستخدام ستايرين-بوتادين-ستايرين بنسب مختلفة تتراوح بين 2 الى 6% من الوزن الكلي للاسفلت. أما عند استخدام المطاط المعاد تدويره، فقد تبين أنه حتى عند استخدام 10 % من هذه المادة فان الاداء للرابط الاسفلتي لن يتحسن كثيرا عند الحرارة العالية جدا، وانا يمكن استخدامه عند

درجة حرارة 70 مئوية و في الشوارع التي تمر فيها المركبات بنسب قليلة نسيبا. كذلك الحال بالنسبة للبوليبلت و الايستمان، فعند استخدام هذه لتحسين أداء الخلطات الاسفلتية عند درجات الحرارة العالية فان النتائج تشير أن التحسين سيكون غير مجدي اقتصاديا عند 76 درجة مئوية.

لقد تم الحصول على قيم معامل ديناميكية للخلطات الاسفلتية ومن ثم تصنيفها حسب درجة أداء الرابط الاسفلتي وتدرج الحصى المستخدم لتقييم ونمذجة أداء الخلطات المصممة، كما أشارت نتائج الاختبار إلى أن معامل الديناميكية يتأثر بشكل كبيربنوع ونسبة المواد المضافة الى الخلطات. بالإضافة إلى ذلك، تم قياس مقاومة التخدد وخواص الاجهاد باستخدام طرق تحاكي حركة المركبات في الموقع. حيث أوضحت النتائج أن الخلطات الغير محسنة ،والتي تناسب المناطق التي قد تصل درجة حرارة الاسفلت فيها الى 64 درجة مئوية، يمكن أن يصل فيها التخدد الى 6 مم مقارنة بالخلطات المحسنة بنسب عالية (5%) حيث تم قياس مقدار التخدد بأقل من 1 مم. وهذا مؤشر جيد على طريقة استخدام البوليمرات لهذا الهدف.

أما بالنسبة لمقدار الاجهاد الحاصل للخلطات الاسفلتية المحسنة عند درجة حرارة معتدلة (20 درجة مئوية) فانه تبين أن مقدار العمر الافتراضي لمقاومة الاجهاد يعتمد بشكل كبير على كل من أداء الرابط الاسفلتي المحسن و نسبة المواد المضافة و نسبة الفراغات بين الحبيبات و نسبة الحجم الخشن من الحصى و نسبة الاسفلت الفعلى الى نسبة المواد الناعمة في الخلطة. في نهاية العمل، تم انشاء نماذج رياضية تفسر أداء الخلطات المحسنة بناءا على خصائصها ومكوناتها بحيث يمكن استخدامها في تقييم الرصفات المستخدمة من المواد المحلية التي شملتها هذه الدراسة.

CHAPTER 1: INTRODUCTION

1.1. Background

Roads that have been built by high performance asphalts showed early signs of distress due to some reasons related to material properties. Lack of sufficient stiffness and elastic recovery under high pavement temperature in summer and flexibility under low temperatures in winter would most probably increase the chance for distress to occur. Proper improvement of asphalt mixes by selecting the right additive type reduces the maintenance frequency of the pavement structure and hence extends its life. Furthermore, proper evaluation and prediction of pavement performance produced from polymer modified asphalt binders is the key role for good roads.

Superpave performance grading (PG) [AASHTO M-320] has been used for many years in the evaluation process of asphalt binders to predict the performance of modified mixtures that would be used in harsh environments and high levels of traffic. Additional tests were introduced to fill the gap between the old procedures and the advancement in materials' properties, such as elastic recovery [AASHTO T-301] and forced ductility [AASHTO T-51]. These two tests are empirical and time consuming. Recently, a new grading and evaluation process has been introduced to better characterize the modified mixtures called Multiple Stress Creep Recovery (MSCR) [AASHTO M-322]. MSCR test is performed using Dynamic Shear Rheometer (DSR) at PG temperature using a constant stress creep of 1.0-second duration followed by a zero stress recovery of 9.0-second duration. The test is performed at two stress levels, 0.1 kPa and 3.2 kPa. Ten

cycles are run at each of the two stress levels making a total of 20 cycles. The stress and strain shall be recorded at least every 0.1 second for the creep cycle and at least every 0.45 second for the recovery cycle on an accumulated basis such that, in addition to other data points, the data points at 1.0 second and 10.0 second for each cycle's local time are explicitly recorded. There are no rest periods between creep and recovery cycles or changes in stress level. The total time required completing the two-step creep and recovery test is 200 seconds. Two parameters are calculated from this test; percent recovery (R) and non-recoverable creep compliance (Jnr). Percent recovery is the percent difference between the final strain (ε_{10}) and initial strain (ε_0) of the ten recovery curves while Jnr is the ratio between final strain (ε_{10}) and the applied stress.

Current methods for pavement structural design use viscosity (η) and complex shear modulus (G*) to predict the performance of the modified asphalt mixes. For polymer modified asphalts which should behave well at high performance temperatures (76°C), strain recovery properties including percent recovery (%R) and non-recoverable strain compliance (Jnr) should be considered in the prediction of the performance of the pavement.

In this research, the performance of the modified asphalt mixes were evaluated in terms of the engineering properties related to the asphalt binder and the mix. Samples were prepared using Superpave mix design and contain different types and dosage of polymers; Styrene-Butadiene-Styrene (SBS), Crumb Rubber (CR), Polybilt (Pb) in addition to Eastman (EE-2). Three different dense-graded aggregate blends with different aggregate gradation within the same nominal maximum aggregate sizes (NMAS) are used in the design of the asphalt mixes. The performance of asphalt mixes

produced from polymer modified asphalt binders were characterized by dynamic modulus (E*) which addresses rutting and fatigue [AASHTO TP-79]. Furthermore, rut resistance at high service temperatures was measured using Asphalt Pavement Analyzer test (APA) [AASHTO T-340]. The fatigue properties of the modified mixes at intermediate performance temperature were evaluated using Fatigue Beam Test [AASHTO T-321].

The analysis of the results in this research includes the evaluation of asphalt, aggregate and mix properties that affect rutting and fatigue resistance of the hot mix asphalts and to rank the mixes based on their performance using suitable statistical analysis and tools, then to correlate the performance results (rutting and fatigue) to their mechanistic properties. Performance prediction models were created from the collected data to simulate the behavior of pavement structure during its service life.

1.2. Problem Statement

The performance of asphalt concrete mixes is highly affected by high service temperatures of asphalt pavements and heavy traffic loadings. It is necessary to pay extra attention to material selection, mixture design and evaluation techniques. The use of polymers modification should be controlled by the selection of proper polymer type and polymer content in a cost effective way. Some polymers are expensive but perform better than others. There is a necessity to study the effect of polymer modification on fatigue and permanent deformation response of local asphalt concrete mixes and to explore the effect of performance grading (PG+) method of asphalt binders on the performance of the asphalt concrete mixtures. Mathematical models that correlate

fatigue and rutting of local mixtures to material's properties need to be developed for local applications.

1.3. Research Objectives

The main objective of this research is to study the effect of Superpave plus grading system of polymer modified asphalt binders on the performance of the asphalt mixes. Specific objectives are:

i. To improve the local asphalt binders by modifying with suitable polymer type and amount in order to achieve suitable performance grades (PG^{+}) for hot weather and heavy traffic loading.

ii. To evaluate the performance of the asphalt concrete mixes produced from modified asphalt binders at the targeted service temperatures and traffic levels, the evaluation is based on the properties of both the asphalt binders and aggregates.

iii. To develop mathematical models to predict fatigue and rutting performance based on measured engineering properties of polymer modified asphalt mixtures.

1.4. Research Methodology

In order to achieve the objectives of this research, an extensive literature review and a laboratory experiments have been conducted. The review includes binders' and mixtures properties that affect their performance in the field in addition to all experimental setups and procedures were used for that purpose. Samples were designed and prepared using Superpave procedures and recommendations. Two test procedures were conducted to evaluate the rutting of modified mixes; Asphalt Pavement Analyzer (APA) and Asphalt Mixture Performance Test (AMPT) flow tests. Rut depth and dynamic modulus test

results were correlated to asphalt binders' properties and regression models were developed. The engineering properties including the flexural stiffness and dynamic modulus of the modified asphalt mixtures were evaluated using Beam Flexural test and AMPT to characterize fatigue properties of the modified mixes. Figure 1.1 presents the experimental plan of this research.

1.5. Thesis Organization

This dissertation consists of six chapters. Chapter 1 provides an introduction to the new parameter of Jnr and its possible effect on pavement performance, including specific objectives. Chapter 2 focuses on previous studies and conclusions on each part of the experiment and materials' performance. Chapter 3 presents experiments' set-ups and selection of input parameters of each test. Performance evaluation of polymer modified asphalt binders using conventional and current methods are presented in Chapter 4. While in chapter 5, laboratory rutting and fatigue performance of polymer modified mixtures is discussed. Finally, in Chapter 6, a summary and conclusions of this study will be presented.

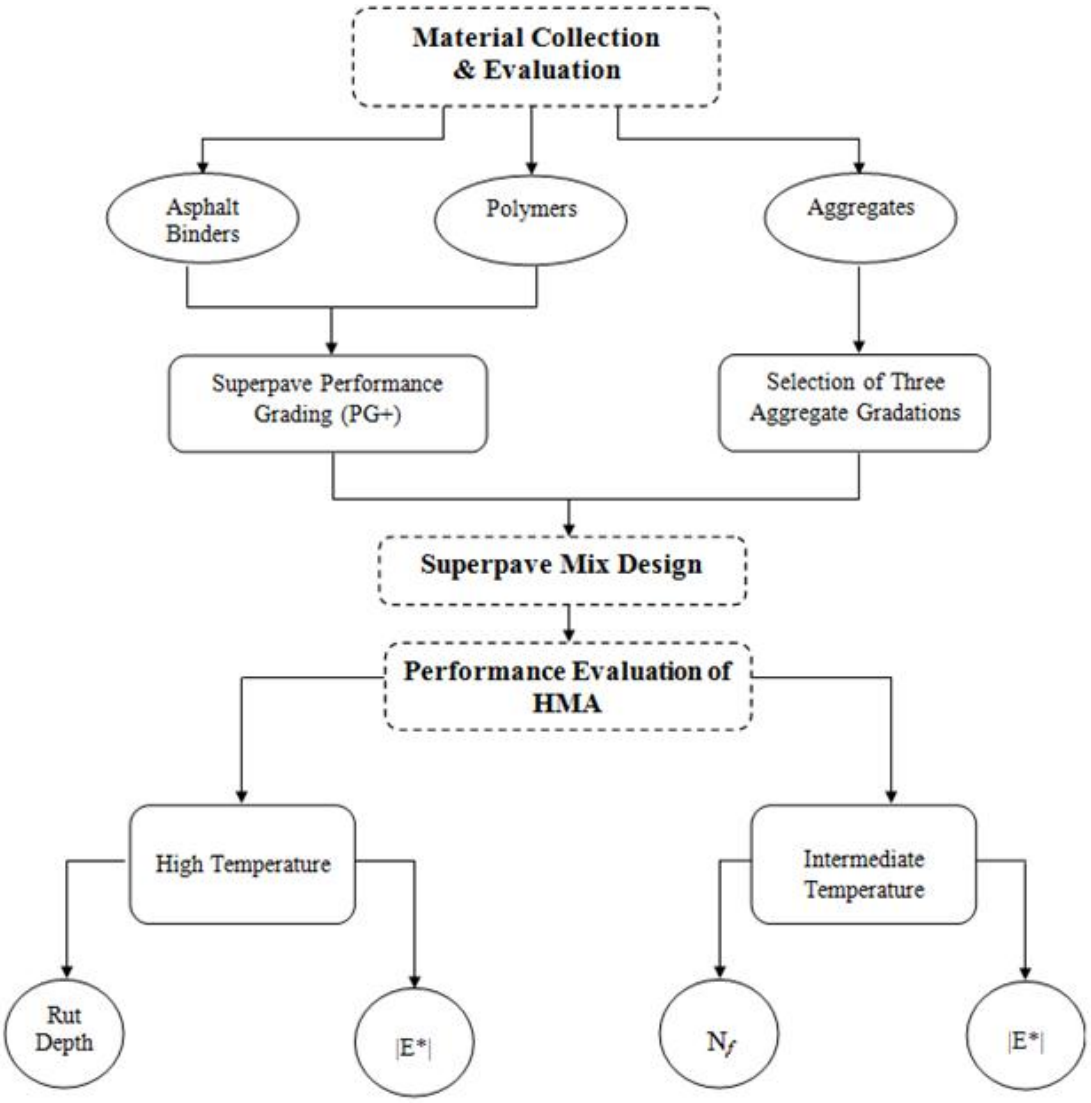

Figure 1.1Experimental Plan of the research

CHAPTER 2: LITERATURE REVIEW

2.1. Introduction

Fatigue and rutting performance of concrete asphalt mixes are affected by asphalt binders and aggregate properties at high service temperatures and heavy traffic loadings. In this chapter, performance evaluation methods of polymer modified asphalt binders and asphalt concrete mixes are discussed. Theoretical background of rutting and fatigue behavior is also explained.

2.2. Performance Grading of Polymer Modified Asphalt Binders

As a viscoelastic material, asphalt binders have been evaluated against rutting at high temperatures by measuring the G*/sinδ parameter and against cracking at intermediate and intermediate temperatures by measuring G*.sinδ [AASHTO M-320]. The resulted evaluation was used to grade the asphalt binders according to their peroformance. Most of the performance related properties of asphalt mixes are affected by the binder properties due to time and temperature dependence and its contribution to rutting and fatigue cracking of the pavement structure [Delgadillo and Bahia, 2010].

At desert environment, which is the dominant environment in Gulf Countries (GCs), temperature related distresses have higher chance to grow up and harshly affect the pavement structure. In 1998, [Al-Abdul Wahhab *et al*.] conducted a comprehensive study on the performance of Arabian asphalts. It was found that the asphalt binder, as used locally in the Gulf area, is only suitable for about 40% of the GCs area. In fact, there are only few types of crude that can produce good asphalts. Besides that, the plain

asphalts lack the viscoelastic behavior that usually exists when an effective elastic network is created by molecular association.

For this reason, asphalt binders should be modified with proper additive specially polymers due to compatibility properties with asphalt binders and resulted covalent bonds between the two materials. To achieve the required performance of the asphalt binder in an economical way, different polymer types have been used. It was shown that using polymers in modifying the asphalt binders is a convenient for road contractors. It is supposed to improve the high temperature permanent deformation [Wonga *et al.*, 2004] and improving their resistance to thermally induced cracking at low temperature [Isacsson and Zeng, 1998].

Among different types of available polymers, few are suitable for asphalt modification. About 75% of those polymers are elastomeric and 15% are plastomeric. [Airey, 2003]. Styrene–Butadiene–Styrene (SBS) is the most used polymer to modify asphalts, followed by reclaimed tire rubber [Becker, 2001]. SBS as a thermoplastic copolymer with radial structures increases the elasticity and moisture susceptibility of asphalt structures at high temperatures and reduces the fatigue cracking at low temperatures. [Yetkin, 2007].

Recycling of waste tires into modified crumb rubber (CR) for the asphalt applications has become a positive method to improve the asphalt properties, protect the environment and save resources. Crumb rubber has been used since 1960 in Arizona. However, the interest in use of crump rubber in asphalt pavements is increasing to improve the performance of the asphalt binder. Based on the literature, the modification of the asphalt binder by the crumb rubber could reduce noise [Paje *et al*., 2013] when used in

high amounts. It also increases the viscosity [Lee *et al.*, 2008; Jeong *et al*., 2010; Cong *et al.,* 2013; Presti, 2013], elastic recovery [Nejad *et al.,* 2012], complex modulus and decreases the penetration, ductility and phase angle of the CRM asphalt binders, [Cong *et al.,* 2013]. Crumb rubber modified asphalt as binder is currently being used or applied in a number of highways projects in Gulf countries as it is more economical than regular polymers and helps to protect environment.

The practice of using of recycled, instead of virgin, products helps reducing demand of extraction and easing landfill pressures without any environmental effect on surface and ground waters, air and soil [Huang et. al., 2007]. These practices have prompted the National Cooperative Highway Research Program (NCHRP) to research the possible impacts of waste materials on the surrounding environments. A comprehensive study on the environmental impact of using Crumb rubber in the modification of asphalt concretes has concluded that the asphalt concretes (AC) leachates contain a mixture of metallic and contaminants organic in low contents which are not affecting the surrounding soils and waters. These organic and metal compounds were readily removed from asphalt concrete leachates by the environmental processes of soil sorption, volatilization, and biodegradation. Metals, which do not volatilize or photo chemically or biologically degrade, were removed from the leachates by soil sorption [Azizian*et al*., 2003].

Some researchers have used a polyethylene based polymers. This group of material has a low molecular weight like Polybilt 101 and Eastman EE-2. A study was conducted on New Jersey pavements to evaluate the effects of EE-2 polymer on reducing the rutting found that adding 4% of this polymer can enhance the properties of asphalt

binders and the mixtures. [Bennert *et al*., 2003].Another study conducted on Arabian asphalts in found that EE-2 polymer can reduce the pavement stripping and fatigue cracking significantly [Al-Abdul Wahhab, 2004].

2.3. Superpave plus Performance Grading of Polymer Modified Asphalt Binders

Although the performance of asphalt binders have been evaluated using Superpave Performance Grading system (PG) [AASHTO M320] for the last 20 years, many researchers reported that the PG was not suitable for polymer modified asphalts. [Wasage *et. al*., 2011; Clopotel and Bahia, 2012].In this regard, a research study claimed that a parameter of $|G^*|/(1-(1/\tan\delta.\sin\delta))$ is more fundamental than conventional rutting parameter $|G^*|/\sin\delta$ and can predict the non-recovered strain on asphalt binders at high temperatures. [Aroon Shenoy, 2004].

To overcome that inconvenience in the evaluation process, Superpave has introduced additional tests to grade the polymer modified asphalt binders according to performance. Force Ductility [AASHTO T-51] and Elastic Recovery test [AASHTO T-301]. Both tests utilize the ductility bath and used to detect the elasticity of modified binders. Some researches revealed that any polymer modified asphalt have more than 60% of recovery can improve the rutting resistance at service [Batten *et al*., 2011; Clopotel and Bahia, 2012]. However, the empirical nature of this test reduces its use in the evaluation and leads to introduce the new fundamental test known as Multiple Stress Creep Recovery (MSCR) [AASHTO-M-332,].

MSCR test is currently used to evaluate the strain recovery properties of the asphalt binders. The test is conducted at targeted performance temperature and under two stress levels of 0.1 kPa and 3.2 kPa which cover all possible ranges of visco-elasticity; Linear and non-linear behavior or creep and recovery. The resulted parameters are recovery (R) and non-recoverable strain compliance (Jnr).

AASHTO TP-70 procedure requires that for each successful polymer modified asphalt binder, Jnr and %R values should lie above a standard function (curve) which is recommended by Federal Highway. While the other criteria of AASHTO MP-19 requires classifying Jnr values into four different grades based of traffic loading at high service temperature of the binder (standard, heavy, very heavy and extremely heavy). Table 2.1 shows the classification of traffic levels based on Jnr values.

Table 2.1Jnr values for each Traffic Levels [AASHTO MP-19]

Traffic Level	**Designation**	**Jnr (kPa^{-1})**	**Description**		
			Traffic Level (Million) ESAL		**Speed (kph)**
Standard	S	2- 4.5	<10	and	> 70
Heavy	H	1-2	10-30	or	20-70
Very Heavy	V	0.5 -1	>30	or	< 20
Extremely Heavy	E	< 0.5	>30	and	< 20

Since 2009, many researchers have applied the MSCR test on various polymer modified asphalt binders to evaluate their visco-elastic behavior and to compare between polymers when they are used as ant-rutting modifiers [Peng Y. *et al.,* 2012]. Some researchers extended their investigation to validate the MSCR non-recoverable

compliance Jnr to rutting testing using laboratory testers and actual roadways. They concluded that the MSCR test can provide better correlation to mixture rutting than the conventional Superpave performance grading (PG) [D'angelo, 2009; Wasage *et. al., 2011*].Effect of various polymer types on the MSCR test parameter have been studied in great depth by [Santagata *et al*., 2013; Wasage *et al*., 2011].

A research group has found that the non-recoverable compliance was sensitive to base binder and polymer type. They also found that the permanent strain calculated from the (MSCR) procedure is lower than non-recoverable strain measured at the end of 10 seconds [Shirodkar *et al*., 2012]. Creep-recovery results of MSCR test can be fitted into visco-elastic models to predict the rheological behavior of polymer modified asphalt binders when they are subjected to different stress levels and temperature values. A study used fractional models consist of spring and dash pots [Baglieri *et al*., 2017] to simulate the performance of asphalt binder to predict the strain response after applying an external loads. They found that the results of strain values were in a good agreement with the model and can be used for prediction.

2.4. Permanent Deformation of Polymer Modified Asphalt Mixes

Rutting (permanent deformation) is the depression of pavement layer/s under the vehicles' tires caused by the movement of materials due to lack of vertical strain of the subgrade or/and lack of shear strength of hot mix asphalt layers when roads are subjected to heavy traffic loads and high temperatures. Generally, rutting usually occur at the top 75 to 100 mm of pavement layers [Witczak *et al*., 2000; Stuart *et al*., 2001]. In desert environment, the high service temperature of pavement structures and heavy traffic loads increase the chance of rutting to occur.

2.4.1. Rutting Prediction Methods

Many tests have been used to measure rut-resistance of field and laboratory prepared asphalt mixes most popular ones are Hamburg Wheel Tracking Device (HWTD); French Pavement Rut Tester (FPRT) and Asphalt Pavement Analyzer (APA) [Skok *et al*., 2003; Zhang *et al*., 2013;Xe *et al*., 2014]. APA is the most accepted and practiced in pavement evaluation of field and laboratory samples [Jackson & Bladwidn, 2000; Choubane *et al*., 2000; Xu *et al*., 2014; Rushing & Garg, 2017].

It is described as a "thermo-statically controlled device to test the rutting resistance of HMA by applying linearly repetitive loads to compact cylindrical or beams specimens through pressurized standard nylon hoses via wheels" [AASHTO T 340-10, 2015]. The APA can simulate the field conditions (traffic load, temperature, etc.) of flexible pavements in the laboratory. Using the APA, a series of rut tests are performed on HMA mixes and these mixes are ranked based on their rut potentials.

One of the most recent methods for characterization of rutting is the Repeated Load Permanent Deformation (RLPD) also known as Flow number (FN) test. In this method, the repeated movement of heavy vehicles is simulated by applying repeated axial load on cylindrical asphalt mixes. The flow number is defined as number of cycles at which the material starts to flow. Many researchers found that flow number test is more correlating to binder's properties including the shear modulus |G*| and non-recoverable creep compliance Jnr [Domingos et al., 2017; Mehta & Nola, 2014].

The dynamic modulus |E*| and the phase angle is also used to characterize the ability of fundamental properties of asphalt mixtures as viscoelastic materials to resist rutting. Rutting parameter of $|E^*|_{54C,\ 5Hz}$ is usually used for materials' characterization

against rutting [Witczak *et al*., 2002].This test is currently conducted by utilizing the Asphalt Mixture Pavement Test (AMPT) by testing field or laboratory cylindrical samples at different temperatures and frequencies. Many studies have been conducted on modified asphalt mixes to evaluate their ability to resist rutting [Pellinen, and Witczak, 2002]. The results of dynamic modulus and phase angle are used to develop dynamic modulus |E*| master curve. These master curves are obtained by shifting the resulted dynamic modulus values at different temperatures and frequencies using the time-temperature superposition of viscoelastic materials.

2.4.2. Rutting (Permanent Deformation) Mechanism

In general, rutting is caused by two reasons; shear deformation and consolidation. When the volume of asphalt pavements changes due to repeated loads, the air voids between the compacted aggregate decreases significantly and rutting may occur if the limits are exceeded. On the other hand, when materials flow by rolling of rounded aggregates or sliding of flat particles, the shear rutting occurs [Cooley *et al*., 2001; Gramling *et al*., 1991].

The accumulation of permanent deformation on asphalt pavements consists of certain materials properties and subjected to different environmental and loading condition is defined in three well-defined stages [AASHTO Design Guide, 2002]. In primary stage, the volumetric changes cause a high level of rutting with decreasing rate of deformations. Smaller rates of deformations associated with volumetric change define the secondary stage. After the secondary stage ends, materials start to flow (i.e. high shear deformation) with no volume change, the tertiary stage has occurred [Kaloush and

Witczak, 2002]. Figure 2.1 shows the three stages of permanent deformation asphalt mixes.

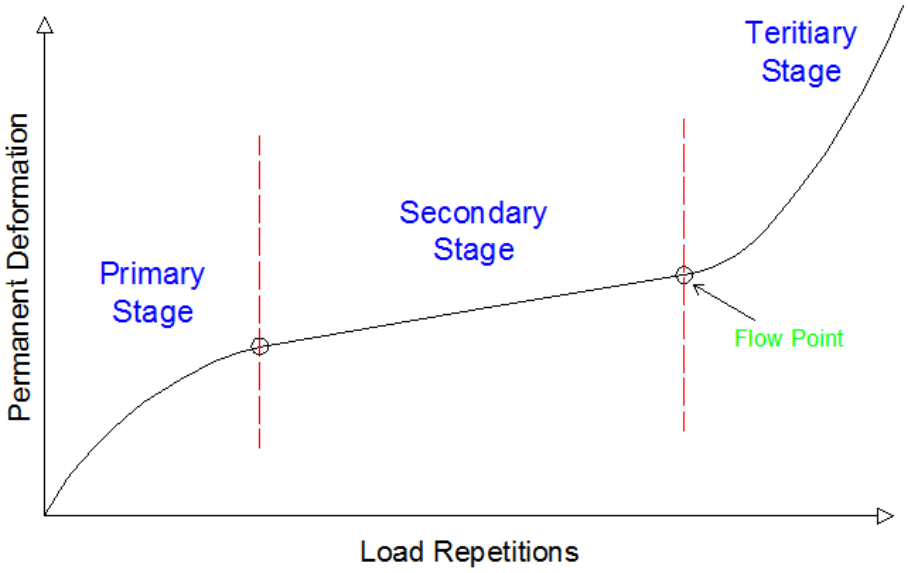

Figure 2.1Typical Permanent Deformation Behavior of pavement materials

APA is used to test rut-depths within the primary and secondary stages of permanent deformation. While at flow test, time and/or number of loading cycles defines the flow point and the initiation of the tertiary stage.

2.4.3. Influence of Mix Properties on Rut Resistance

Rut-resistance of hot mixes can be enhanced by increasing the thickness of the pavement layers or using more crushed-faced and angular aggregates in the mix and by properly design the hot mix asphalt for optimum voids filled with asphalt (VFA) and voids in the mineral aggregate (VMA) [Zhu *et al.*, 2016; Li *et al.*, 2014]. On the other hand, using polymers to enhance the properties of asphalt binders against rutting has been studied by many researchers. Some of them used polyethylene based-polymers [Brovelli *et al.*, 2015] while others used Crumb rubber [Fontes *et al.*, 2010]. All of those studies agreed

on improvement of rut resistance of modified materials without compromising other properties like mix stiffness and fatigue properties. It was found that polymer content and type are highly affecting the engineering and rheological properties of polymer modified asphalt at which a significant improvement in rut-resistance could be obtained [Khattak & Baladi, 2001].

Recently, Witczak prediction model have been used to estimate the dynamic modulus of asphalt mixes which involves the aggregate properties along with binders and volumetric parameters of the mix are required. The Witczak model could provide sufficiently accurate estimates of the dynamic modulus |E*| at different temperature and frequency for use in mechanistic-empirical pavement performance prediction and design [Witczak *et al*., 2002]. Witczak's prediction model uses a symmetrical sigmoidal function as shown in equation (2-1).

$$Log|E^*| = 3.750063 + 0.029232\rho_{200} - 0.001767(\rho_{200})^2 - 0.002841\rho_4 - 0.058097V_a - 0.802208\left(\frac{V_{eff}}{V_{eff}+V_a}\right) + \frac{3.87197 - 0.0021\rho_4 + 0.003958\rho_{38} - 0.000017(\rho_{38})^2 + 0.00547\rho_{34}}{1+e^{(-0.603313-0.313351\log(f)-0.393532\log(\eta))}} \quad \text{.....(2.1)}$$

Where

|E*|: Asphalt Mix Dynamic Modulus, in 10^5 psi

η: Binder Viscosity in poise

f: Load frequency in Hz

Va: % air voids in the mix, by volume

Vb_{eff}: % effective binder content, by volume

ρ34: % retained on the 3/4-in sieve, by total aggregate weight (cumulative)

ρ38: % retained on the 3/8-in sieve, by total aggregate weight (cumulative)

ρ4: % retained on the No. 4 sieve, by total aggregate weight (cumulative)

ρ4: % retained on the No. 200 sieve, by total aggregate weight.

The Hirsch model developed by Christensen is both simpler and rational and requires only binder modulus, VMA, VFA for predicting asphalt concrete modulus [Christensen *et al*., 2003]. The Hirsch model is given by equation. The maximum limiting modulus is estimated from mixture volumetric properties using the Hirsch model and a limiting binder modulus of 1 GPa (145,000 psi), Equations 2.2 and 2.3.

$$|E^*| = P_c\left[4{,}200{,}000\left(1-\frac{VMA}{100}\right)+3|G^*|\left(\frac{VFA\ xVMA}{10{,}000}\right)\right]+\frac{1-P_c}{\left[\frac{\left(1-\frac{VMA}{100}\right)}{4{,}200{,}000}+\frac{VMA}{3|G^*|(VFA)}\right]} \quad (2.2)$$

Where

$$P_c = \frac{\left(20+\frac{3|G^*|(VFA)}{VMA}\right)^{0.58}}{650+\left(\frac{3|G^*|(VFA)}{VMA}\right)^{0.58}} \quad (2.3)$$

$|E^*|_{max}$ = limiting maximum mixture dynamic modulus, psi

VMA = Voids in mineral aggregates, %

VFA = Voids filled with asphalt, %

Pc= Contact Factor

|G*|= Complex Shear Modulus of the binder, psi

It is observed that the dynamic modulus |E*| obtained from the Hirsch model is a function of binder and volumetric properties.

Recent studies pointed out that the new parameter of non-recoverable creep compliance (Jnr) is better correlating to rut depth and properly estimates pavement's life to

withstand permanent deformations [Meena and Biligiri, 2016; Rushing and Garg, 2017; Domingos *et al*., 2017].

2.5. Fatigue Properties of Polymer Modified Asphalt Mixes

This type of pavement's distress occurs in its later life stages when repeated tensile forces produce a gradual deterioration of the layered pavement structure which starts from the bottom of the pavement layers. The stiffness of the mixture tends to decrease due to accumulated damage of its layers under traffic loads at intermediate temperatures and fatigue cracks occur when fatigue limits has been exceeded. Many factors affect the fatigue cracking of pavement structures; such as thickness and materials' quality, position and magnitude of wheel loads and temperature of pavement layers. Other factors are due construction, like poor compaction and poor surface drainage. In order to resist fatigue cracking, stiff asphalt mixtures should be used in the design to withstand the deflection caused by repeated heavy loads. The enhanced stiffness of pavement materials could be achieved by using better aggregate and proper modified asphalt binders.

2.5.1. Fatigue Life Test Methods

Different methods have been used to evaluate the fatigue response of modified and unmodified asphalt mixes including Tri-axial Repeated Compression [Raithby and Ramshaw, 1972], Diametral Repeated Load Test [Khosla and Omer, 1985; Scholz *et al*., 1989], Simple Flexure Tests [Monismith, 1981] and Fracture mechanics testing [Tangella *et al*., 1990]. The four-point flexure fatigue test has been recently used for determining the fatigue properties and fatigue life of hot asphalt mixtures [Adhikari *et al.*, 2009; Abojaradeh *et al*., 2007; Hartman *et al*., 2004; Pais and Minhoto, 2010]. Some

factors should be considered during the fatigue test in order to properly characterize the fatigue properties of asphalt mixtures; mode of loading (stress or strain controlled), test temperature, and frequency.

2.5.2. Fatigue Mechanism

Most of fatigue models have been created by flexural test methods in which the specimen is repeatedly subjected to tensile strain or stress until it fails [Monismith, 1981]. These tensile forces are responsible for the initiation and then propagation of the cracks [Rao *et al.*, 1990]. The concern is to predict the fatigue life of any pavement structure based on laboratory results and then to estimate its performance in the field. Some models depend on test mode (stress-controlled or strain controlled) regardless of testing temperature and loading frequency.

Early researches on fatigue behavior were found that applied tensile stresses (σ_t) and strains (ε_t) are significantly correlated with fatigue life (N_f) of the mix [Shell 1978; Asphalt Institute, 1982]. These relationships are used to analyze and design the structure of the required pavements and characterized in Equations 2.4 and 2.5 as follows:

$$N_f = a\left(\frac{1}{\sigma_t}\right)^b \quad (2.4)$$

$$N_f = c\left(\frac{1}{\varepsilon_t}\right)^d \quad (2.5)$$

Where a, b, c & d are constants and can be determined from lab testing.

Other models consider the volumetric properties of the mix in the prediction of the failure point [Shell, 1978; Asphalt Institute, 1982; Shen and Carpenter, 2007].

Dissipated-Energy based methods are most commonly used in developing prediction models of failure point which suggested that the failure of pavement layer could happen when 40% of its initial stiffness was reduced by repeated load [Abojaradeh *et al*., 2007; Shen and Carpenter, 2007]. They both agreed that this method is less dependent on mode of loading in the fatigue test than traditional methods.

2.5.3. Effects of Polymers on Fatigue Properties

Stiffness of asphalt binders has a significant effect on pavement resistance to fatigue which can be improved by additives specially polymers. Many studied have concluded that adding polymer to asphalt binders could significantly extend the fatigue life of pavement layers [Al-Abdul Wahhab,1997; Kutay *et al*., 2008]. It was found that polymer content and type are highly affecting the engineering and rheological properties of polymer modified asphalt at which a significant improvement in fatigue life could be obtained [Khattak, & Baladi, 2001].

In 1997, [Al-Abdul Wahhab] used the flexural bending beam test to study the effect of different polymers on improving the fatigue cracking of Arabian asphalt mixes. He included SBS, EE-2 and Low Density Polyethylene (LDPE) polymers and both limestone and basalt aggregate blends in his study. Beam samples were tested at stress controlled mode and 20°C temperature. He concluded from his study that asphalt mixes contains PG 76-16 asphalt binders that were modified by elastomeric or plastomeric polymers have shown good fatigue resistance at a given stress level. One recent study was conducted to correlate the flexural modulus with tri-axial dynamic modulus of same material at similar conditions [Adhikari et al 2009] it was found that there is a good

linear relationship with the dynamic modulus was 30% higher than flexural modulus in most cases.

CHAPTER 3: METHODOLGY

3.1. Introduction

The proposed experimental work is performed based on current procedures and recommended specifications. Input and output parameters for each experimental set-up were selected to properly fulfill the stated objectives. The accomplishment of this requires the following tasks:

3.2. Materials Selection

Three basic components were used to prepare the modified asphalt mixes; asphalt binders, polymers and aggregates.

3.2.1. Asphalt Binders

Asphalt binders were collected from Riyadh and Ras-Tannura refineries. Samples were tested for basic engineering properties and for performance grading as shown in Table 3.1.

Table 3.1Properties of Asphalt Binders used in the study

Property	Standard	Criteria
Flash Point, °C	AASHTO T48	> 250
Rotational Viscosity at 135°C, cP	AASHTO TP48	< 3000
Ductility at 25°C, mm	AASHTO T 51	> 100
Performance Grade (PG)	AASHTO M320	PG 64, PG 70, PG 76 and PG 82

3.2.2. Polymers

Four common types of polymers used in local projects are selected in this study. Styrene-Butadiene-Styrene (SBS) was selected as an elastomer while Crumb Rubber (CR) as a low-cost waste material for asphalt modification. Eastman (EE2) and Polybilt (PB) were selected as they have plastomeric properties and have been used for many years in road construction projects in Gulf regions. The ministry of transportation in Saudi Arabia has no restriction on polymer type; however, the targeted PG^{+} grades should be achieved by designer and contractors.

Styrene-Butadiene-Styrene (SBS) is a thermoplastic block copolymer, polymerized in solution and has a radial structure a chemical composition of Butadiene/Styrene with 70/30 ratio. SBS is known as good oil absorption, good porosity and easy dispersion. Poly (styrene) is an organic compound with the chemical formula $C_6H_5CH=CH_2$ is a tough hard plastic, and this gives SBS its durability. While poly (butadiene) is rubbery and gives SBS its elasticity and considered as an important industrial chemical used as a monomer in the production of SBS polymers and has the formula of C_4H_6 [Cong and Liao, 2008].The properties of these two components that form SBS make it compatible with asphalt binders to improve the rheological properties of the new combination [Wang *et al*., 2010]. Figure 3.1 shows the SBS particles before lending with asphalt binders.

Figure 3.1SBS polymers used in the Study

Regardless of its high cost, SBS polymers have been used for many years in highway construction projects in Saudi Arabia. Crumb Rubber (CR) is produced from the recycled rubber obtained from automotive and truck scrap tires with different sizes. CR consists of five major components; Rubber hydrocarbon 50.5%, Natural rubber content 32.5%, Carbon black content 32.5%, Acetone extract 11% and Ash content 6%. These components gave the cumber rubber its elastomeric behavior when blended with asphalt binders [Davide Lo Presti, 2013]. Figure 3.2 shows typical particles of Crumb rubber.

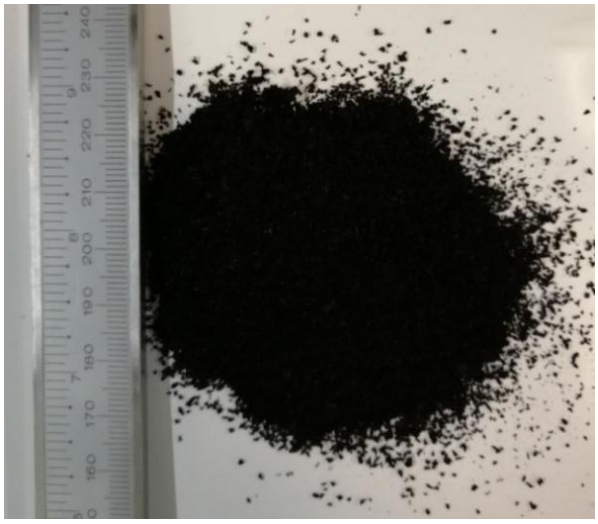

Figure 3.2CR Polymers used in Study

Crumb rubber, as a waste material, is currently used by most of contractors in Saudi Arabia due to its good performance and low cost. Eastman EE2 is a functionally modified Olefin, which is designed to be used as a high temperature modifier for road asphalt, was selected as a plastomeric in this study. It is produced from a simple alkene with the general formula of CnH_{2n} as a monomer. Figure 3.3 shows the (EE2) polymer used in the study.

Figure 3.3EE2 Polymers used in the Study

Low- density polyethylene resin that forms Polybilt 101 polymers were used a plastomeric in this study. It melts at low melting temperatures which make it easy for processing by the contractors. Pb polymers have been used to improve the stiffness of asphalt concrete mixes to resist fatigue and moisture damage. Figure 3.4 shows the Pb polymers used in the study.

Figure 3.4PB Polymers used in the Study

3.2.3. Aggregates

Aggregate was collected from local quarry in Summan Area on the Dammam-Riyadh highway which represents the limestone aggregates type in Eastern and central regions in the Kingdom of Saudi Arabia. These aggregates were evaluated for the standard tests specification as recommended by AASHTO, these tests include:, Coarse Aggregate Angularity (AASHTO TP 61), Fine Aggregate Angularity (AASHTO TP-304-A), Flat and Elongated Particles (ASTM D4791), Sand Equivalent (AASHTO T 176), Coarse Aggregate Specific Gravity (ASHTO T 85) and Gradation Test (AASHTO T 27) and Los Angeles Abrasion (AASHTO T 96). Figure 3.5 shows the aggregate used in the study. The physical characterization of aggregates is listed in Table 3.2.

Figure 3.5Aggregates used in the study

Table 3.2Properties of Mineral Aggregates

Property	Coarse Aggregate	Fine Aggregate	Filler	Criteria	Method
Bulk specific gravity	2.47	2.56	2.75	--	ASTM C127/C128
Apparent specific gravity	2.74	2.78	2.84	--	ASTM C127/C128
Los Angelis abrasion (%)	27%	--	--	⩽45	ASTM DC-131
Flat and elongated particles	0	--	--	⩽10	ASTM D4791
Coarse Aggregate Angularity	97/91	--	--	95/90	ASTM D5821
Fine Aggregate Angularity	--	45	--	⩾45	ASTM C1252
Sand Equivalent (%)	--	58	--	⩾45	ASTM D2419

Bulk and apparent specific gravity values are used in the design of concrete mixes which take into consideration the absorption of asphalt binders by aggregate particles.

Aggregate size and shape (i.e. elongation and angularity) are important to give more surface area and friction forces between compacted particles.

3.3. Preparation and Testing of Polymer Modified Asphalt Binders

The engineering properties of the modified and unmodified asphalts were characterized and evaluated for their fundamental properties. The polymer contents were selected at which the targeted Superpave performance grades (PG) were achieved. The grades included in this study are PG 64(for northern regions of the kingdom), PG 70(for western and central regions), PG 76 (for Eastern region) and PG 82 (special cases). Figure 3.6 shows the required temperature for each zone of the gulf area.

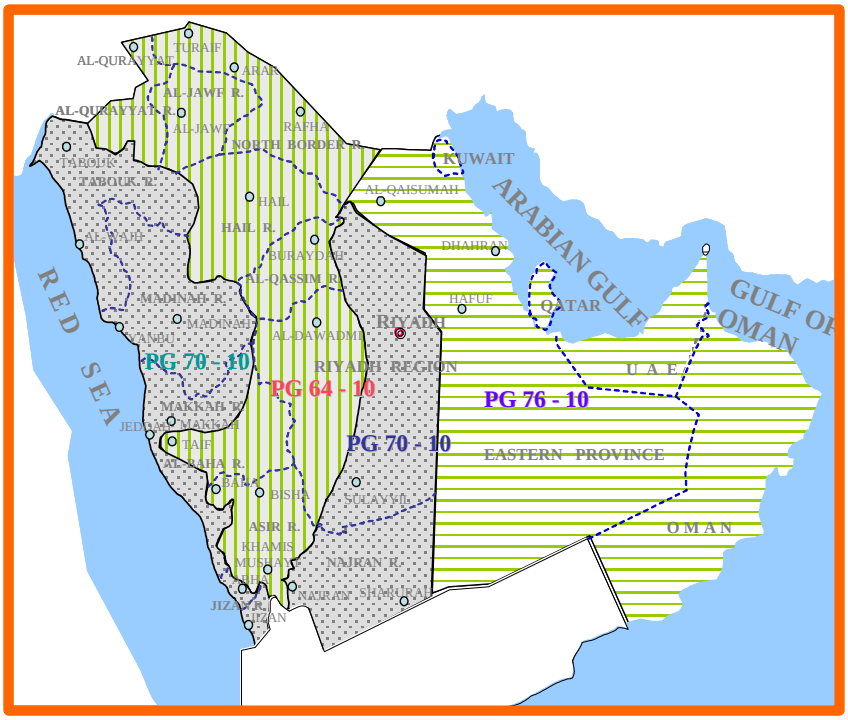

Figure 3.6Details of the temperature zones in the Gulf Area

The high performance grade of asphalt binders are also required in other gulf countries including, Kuwait, Qatar, United Arab Emirates and Oman. The experimental design of polymer modified asphalts included in this study is shown in Table 3.3. Both

conventional and newly proposed performance grading systems are used to characterize the asphalt binders.

Table 3.3Experimental designs for binder testing.

Asphalt Source	Polymer	Optimum Polymer Content	Viscosity	PG Grading	PG Plus Grading
Ras-Tannura Asphalt Binder	Styrene-Butadiene-Styrene (SBS)	✓	✓	✓	✓
	Crumb Rubber (CR)	✓	✓	✓	✓
	Eastman Olefin (EE2)	✓	✓	✓	✓
	Polybilt (Pb)	✓	✓	✓	✓
Riyadh Asphalt Binder	Styrene-Butadiene-Styrene (SBS)	✓	✓	✓	✓
	Crumb Rubber (CR)	✓	✓	✓	✓
	Eastman Olefin (EE2)	✓	✓	✓	✓
	Polybilt (Pb)	✓	✓	✓	✓

Optimum polymer contents were designed to obtain different performance grades of the asphalt binders. Dynamic Shear Rheometer test was conducted to obtain the rheological properties of the modified asphalts by measuring the dynamic shear modulus |G*| and phase angle δ at different aging conditions and testing temperature. The modified binders were graded based on the resulting rutting (|G*|/sinδ) and fatigue (|G*|.sinδ) parameters of the binders. In the second stage of binders' characterization, multiple stress creep and recovery test was conducted on PG graded asphalt samples to find the recovery (R) and non-recoverable creep compliance at different testing

temperatures and short-term aged conditions. Detailed procedures of the previous steps are described in the following sections.

3.3.1. Blending of Polymers in Asphalt Binders

Neat asphalt was mixed properly with polymers using a high propeller blade shear mixer shown in Figure 3.7. This closed container shear mixer is designed specifically in such a way that it reduces the oxidation of asphalt during blending. The mixing time, speed and temperature as required for both polymers based on their fundamental characteristics were selected and applied.

Figure 3.7Shear mixer used in the study.

Asphalt is heated to a uniform temperature, then polymers were added gradually with different dosages ranges as selected for the study. The polymers are simply addedto asphaltbinder and mixed for about an hour. For SBS polymers, mixing process is carried out at 180 ±2°C with high shear mixing and for crumb rubber at 190 ± 2°C. In case of CR, the prepared samples were stored overnight in an oven to mature the

networkbetween asphalt and CR. Samples were heated in an oven at 180 °C, and mixed for 15-20 minutes in the shear mixer before preparing the testing specimens. For plastomers; EE2 and PB, the blending was curried on at 160±5 °C for an hour.

3.3.2. Measuring the viscosity of the modified asphaltbinders

Viscosity (AASHTO TP48) was conducted on the modified asphalt binders to evaluate mixing temperature at which binder's viscosity is 0.170 ± 0.02 Pa.s and compaction temperature at which binder has viscosity of 0.280 ± 0.03 Pa.s.

3.3.3. Short Term Aging of the Asphalt Binders

Aging conditions of the modified samples that may take place during production, placement and compaction of asphalt mixes were measured by using the RTFO test (AASHTO T-240, ASTM D 2872). Figure 3.8 shows the RTFO machine and RTFO bottles before and after RTFO test. Thirty five grams of each asphalt binder was poured in cylindrical bottle horizontally and placed in a convection oven following the standard procedure of the test. This process created a thin film of asphalt on the inside of the bottles.

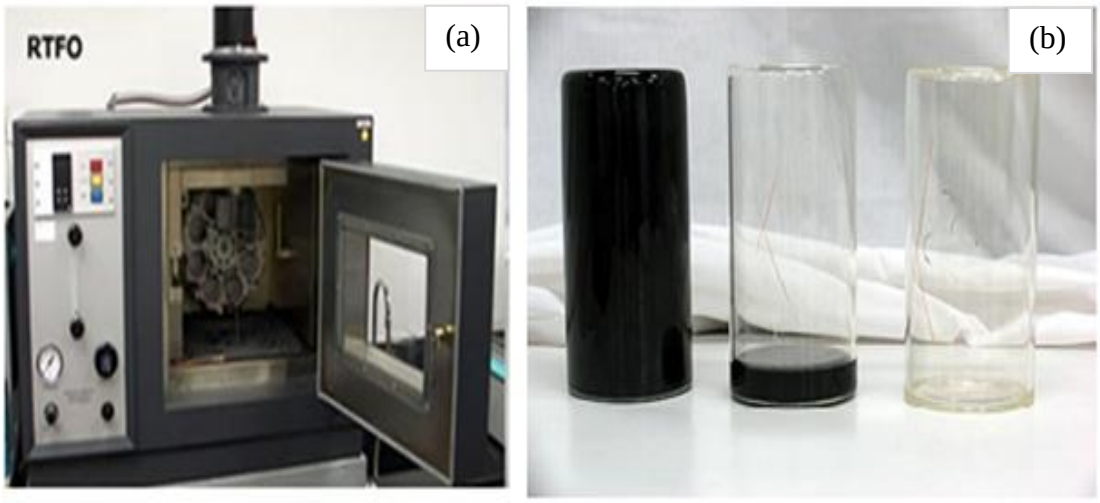

Figure 3.8Rolling Thin Film Oven Test

(a) Rolling Thin Film Oven (RTFO) machine, (b) RTFO bottles, bottle at left is after the RTFO test, the bottle in the middle is before the test.

3.3.4. Measuring the Rheological Properties of Asphalt Binders

Dynamic Shear Rheometer (DSR) testing was used to measure the rheological properties of modified and unmodified asphalt binders at both aged and fresh conditions Figure 3.9 shows the DSR used in the study. The Performance Grading (PG) system (AASHTO M320, ASTM D6373) was conducted to grade modified and unmodified asphalts based on dynamic shear modulus |G*| and phase angle δ. Tested samples, besides neat asphalt, have 2-6% of SBS, Pb and EE2 and 5-10% of CR as percent of the binder weight. Polymer modified asphalt binders were tested at different temperatures starting from 64 °C up to 82 °C for aged and fresh conditions.

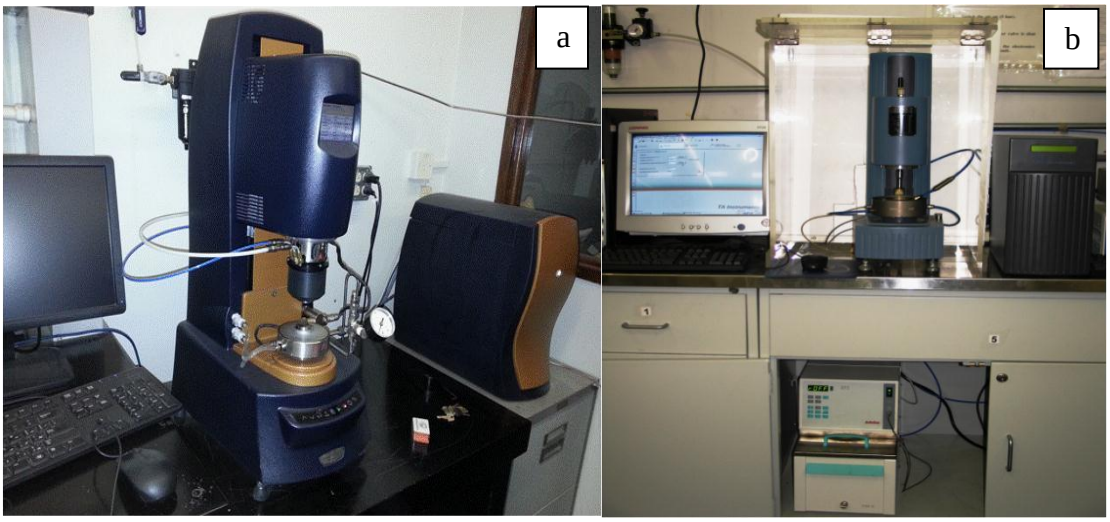

Figure 3.9Dynamic Shear Rheometer.
HR-3 Discovery Hybrid Rheometer (b) CSA II Rheometer.

3.3.5. Multiple Stress Creep Recovery (MSCR) test

One of the main objectives of this research is to study the effect of newly suggested binder Superpave plus specifications on the performance of local polymer modified asphalt concrete mixes, the modified binders were evaluated for strain recovery capabilities, represented by recovery (R) and Non-recoverable creep compliance (Jnr), in addition to classifying the tested samples into different traffic levels according to those parameters.

MSCR test is performed using Dynamic Shear Rheometer (DSR) at PG temperature using a constant stress creep of 1.0-second duration followed by a zero stress recovery of 9.0-second duration. The test is performed at two stress levels, 0.1 kPa and 3.2 kPa. Ten cycles are run at each of the two stress levels making a total of 20 cycles. The stress and strain shall be recorded at least every 0.1 second for the creep cycle and at least every 0.45 second for the recovery cycle on an accumulated basis such that, in addition to other data points, the data points at 1.0 second and 10.0 second for

each cycle's local time are explicitly recorded. There are no rest periods between creep and recovery cycles or changes in stress level. The total time required completing the two-step creep and recovery test is 200 seconds. Two parameters are calculated from this test; percent recovery (%R) and non-recoverable compliance (Jnr). Percent recovery is the percent difference between the final $\varepsilon_{10}$and initial $\varepsilon_0$strain of the tenth recovery curve while Jnr is the ratio between final strain ε_{10} and applied stress i.e. 3.2. Figure 3.10 shows typical 10 cycles of MSCR curves. Equations 3-1 and 3-2 show the calculation process for Recovery (%) and Jnr (1/kPa).

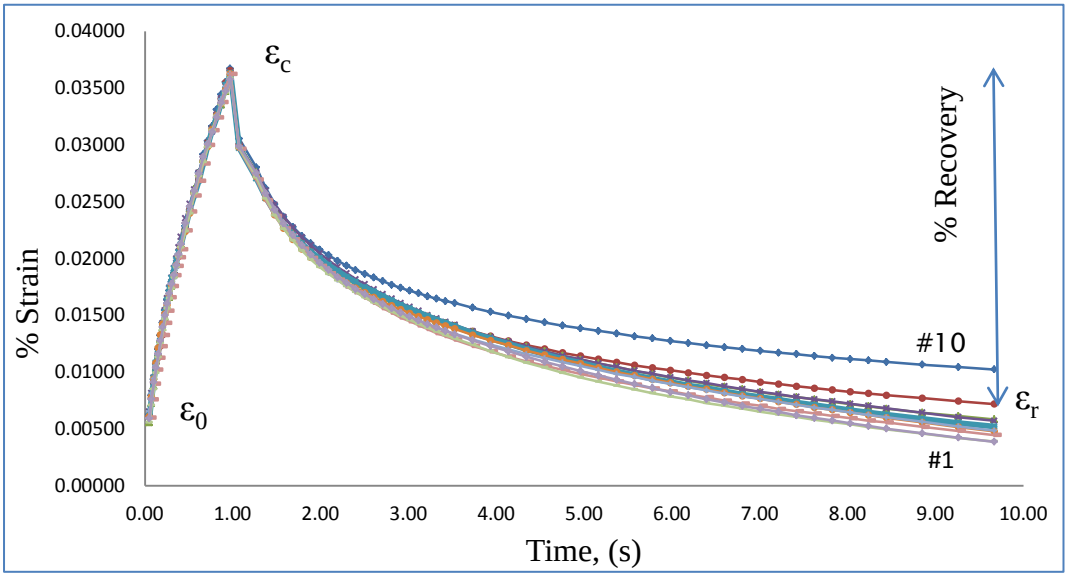

Figure 3.10MSCR test result after 10 cycles of creep and recovery

$$R = \frac{\sum[\varepsilon_r(S,N)}{t}, \text{ for N from 1 to 10} \qquad (3.1)$$

$$J_{nr}(S,N) = \frac{\varepsilon_r}{S} \qquad (3.2)$$

Where

R: is the recovery, %

Jnr: is the non-recoverable creep compliance, 1/kPa

ε_r: Strain value measured at the end of recovery curve.

S: the applied creep stress, kPa.

N: number of repeated cycles of the test.

T: the time of recovery test, seconds.

3.3.5.1. Strain Recovery Rate of Polymer Modified Asphalt binders

The MSCR curves are characterized and two distinct behaviors were defined along the recovery curve (1-9s). These two parameters are (1) the average near instantaneous recovery rate (RRNI) and (2) the average near steady state recovery rate (RRNSS) from the results of 10 creep-recovery cycles. It was found that the recovery rates (recovery rate of change) are different in those two locations. Figure 3.11 gives graphical description of the RRNI and the RRNSS.

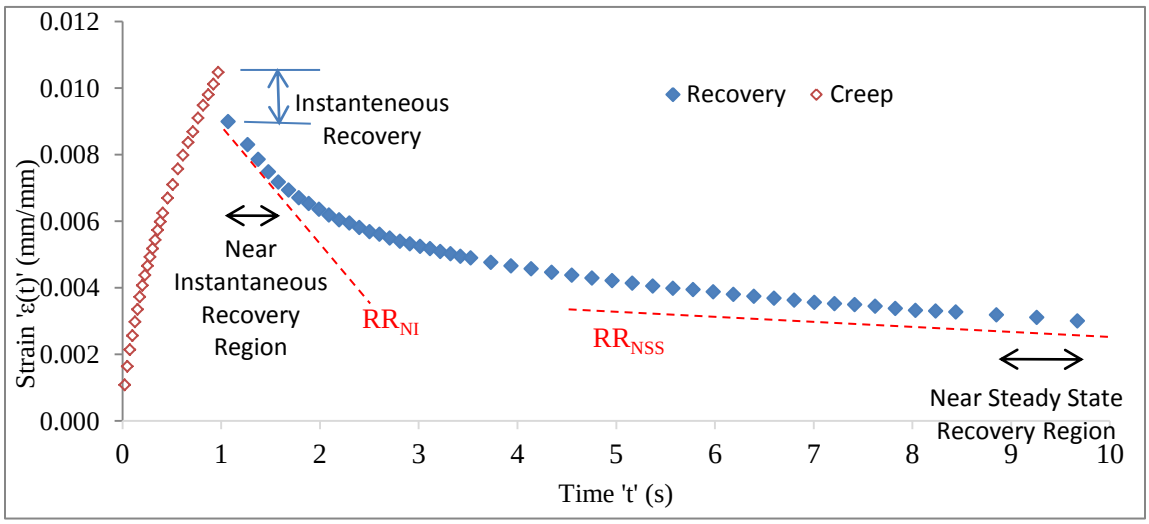

Figure 3.11 Typical Creep-Recovery Cycle

RRNI is the slope of the recovery curve obtained between t = 1 and t = 1.5 seconds, while RRNSS is the slope of the recovery curve obtained between t = 9 to t = 10 seconds of each creep-recovery cycle. These time intervals were adopted after careful study of the various PMA creep-recovery curves. Equation 3.3 and 3.4 represent mathematical interpretation of RRNI and the RRNSS.

$$RR_{NI} = \frac{\varepsilon(1)' - \varepsilon(1.5)}{0.5} \quad (3.3)$$

$$RR_{NSS} = \frac{\varepsilon(9) - \varepsilon(10)}{1} \quad (3.4)$$

Where

$\varepsilon(1)'$: Residual strain after the instantaneous recovery.

$\varepsilon(9)$: Non-recovered strain after 9 seconds.

Absolute percent recovery was obtained at near instantaneous (NI) and near steady state recovery (NSS) regions were determined. The absolute percent recovery at NI (%RNI) is the ratio of RRNI to $\varepsilon(1)$, while absolute percent recovery at NSS (%RNSS) is defined as the ratio of RRNSS to $\varepsilon(1)$. What makes these percent recoveries absolute is the common time unit denominator (per second) between RRNI or RRNSS and $\varepsilon(1)$.

$$\%R_{NI} = \frac{\varepsilon(1)' - \varepsilon(1.5)}{0.5 * \varepsilon(1)} * 100 \quad (3.5)$$

$$\%R_{NSS} = \frac{\varepsilon(9) - \varepsilon(10)}{\varepsilon(1)} * 100 \quad (3.6)$$

Average recoverable creep compliance rate at NI ($\dot{Jr}_{NI}$) and NSS ($\dot{Jr}_{NSS}$) were obtained by (3.7) and (3.8) respectively.

$$\dot{J}r_{NI} = \frac{\varepsilon(1)' - \varepsilon(1.5)}{0.5 * \text{AppliedStress}} \quad (3.7)$$

$$\dot{J}r_{NSS} = \frac{\varepsilon(9) - \varepsilon(10)}{\text{AppliedStress}} \quad (3.8)$$

These non-conventional parameters: RRNI, RRNSS,$\%R_{NI}$,$\%R_{NSS}$, $\dot{J}r_{NI}$ and $\dot{J}r_{NSS}$ were critically analyzed with the aim of establishing more insight on the recovery process of PMA, and establishing more versatile standard parameters. Pearson correlation coefficient (PCC) between the non-conventional parameters and conventional and between AC rut depth were statistically analyzed using MiniTab16^{TM}, at 5% significance level.

3.4. Preparation and Testing of Polymer Modified Asphalt Mixes.

Asphalt mixes were designed for optimum asphalt content based on Superpave method. Optimum asphalt mixes were prepared from three different aggregate gradations of typical Superpave wearing course (WC) layer and polymer contents and type.

3.4.1. Superpave Mix Design [AASHTO R 35].

Asphalts binders were modified with SBS, CR, EE-2 and Pb polymers at different polymer dosage to achieve the targeted binders' performance grades (PG) of the gulf area; PG 64-10, PG 70-10, PG 76-10 and PG 82-10. In order to study the effect of aggregate size on mix performance, three aggregate gradations with nominal maximum aggregate size (NMAS) of 12.5 mm recommended by Ministry of Transportation (MOT) and local municipalities in Saudi Arabia for wearing courses were used to prepare the asphalt concrete mixes. Figure 3.12 presents the criteria of selecting the 12.5 mm top size Superpave wearing course gradations.

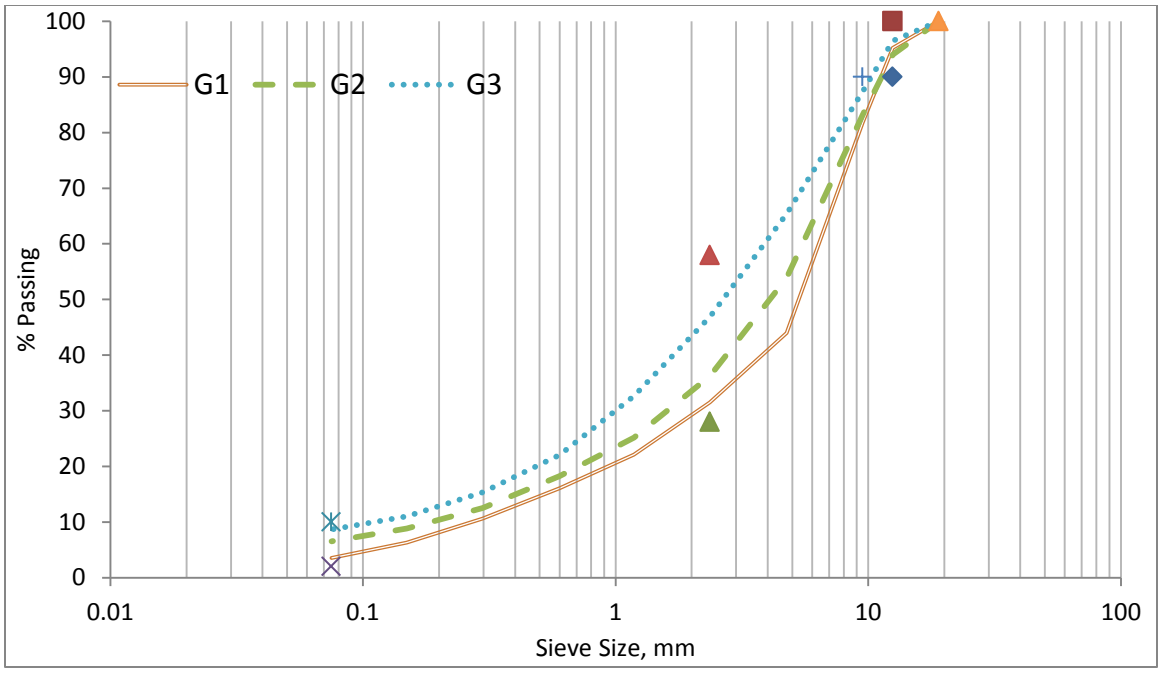

Figure 3.12Sieve size control points and the selected aggregate gradations

To differentiate between the three selected gradations, two specific aggregate sizes were selected to be significantly different; aggregate particles that are passing sieve no. 4 (coarse aggregates) and passing sieve no. 200 (fine aggregates). Table 3.4 shows the experimental variables that form the thirty nine mixes studied.

Table 3.4Experimental Plan of materials variables in the study

Mix	PG	PG 64	PG 70-10				PG 76-10				PG 82-10			
	Polymer	None	SBS	CR	EE	Pb	SBS	CR	EE	Pb	SBS	CR	EE	Pb
Gradation	G1	✓	✓	✓	✓	✓	✓	✓	✓	✓	✓	✓	✓	✓
	G2	✓	✓	✓	✓	✓	✓	✓	✓	✓	✓	✓	✓	✓
	G3	✓	✓	✓	✓	✓	✓	✓	✓	✓	✓	✓	✓	✓

In Superpave, Traffic is defined as the total anticipated project level equivalent single axle load (ESALs) on the design lane for a period of 20 years. Table 3.5shows Superpave criteria used to select the traffic classes.

Table 3.5ESAL and Traffic Designation

Class	Designation	ESALs	Applications
Very Light	VL	<0.3	Agricultural roads with light traffic , local and city streets without trucks
Light	L	0.3- 3	Agriculture, Feeder and collector roads
Medium	M	3-10	Main roads and city streets
Heavy	H	10-30	Highways and Expressway
Very Heavy	VH	>30	Heavily trafficked highways, industrial areas

3.4.2. Mix Coding.

Mix codes are given in the shape of (GxPPG) at which Gx represents the gradation number (1,2 & 3), while P represents polymer type (U for unmodified, SBS for Styrene-Butadiene-Styrene, CR for crumb rubber, EE for Eastman EE2& Pb for Polybilt 101). Finally, PG is the performance grade of the modified binder used to form the designated mix (PG 64, PG 70, PG 76 and PG 82). For example, an asphalt mix obtained with gradation number 2 and blended with optimum content of unmodified asphalt binder has mix code of G2U64. For a mix prepared with gradation number 3 and 10% of crumb rubber, the mix code is G3CR82.

3.4.3. Experimental Plan of Asphalt Mixes

The optimum contents of polymer modified asphalt binders obtained through Superpave mix design were used to prepare compacted cylinders and beams using the slab and

gyratory compactors. Table 3.6 shows the experimental design and required number of specimens per test for asphalt concrete testing.

Table 3.6Experimental plans for asphalt mixes testing procedure in the study

Test	AMPT	APA	Fatigue Test
Measured Parameter	Dynamic Modulus	Rut depth	Fatigue Life
Number of samples per combination	3	6	4
Sample shape	Cored and sawed Cylinder	Compacted Cylinder	Compacted Beam
Sample dimensions	H: 150mm D: 100mm	H:75mm D: 150mm	W: 63mm L: 380 mm H: 55mm
Total number of samples	39x3=117	39x6=234	39x4=156

Figure 3.13 shows the cored and sawed concrete samples used for dynamic modulus and flow tests. The aim of obtaining cored samples is to have better uniformity of air voids in the compacted samples. For rutting test utilizing the Asphalt Pavement Analyzer (APA), Superpave samples that have diameter of 150mm and 75mm height were used and shown in Figure 3.14. Beam samples were used for fatigue testing as shown in Figure 3.15.

Figure 3.13AMPT sample

Figure 3.14APA sample

Figure 3.15Fatigue test sample

3.4.4. Asphalt Mixture Performance Test (AMPT)

3.4.4.1. Measuring the Dynamic Modulus |E| of the mixes*

Asphalt concrete mixes were prepared for the performance grade of PG 64, PG 70, PG 76 and PG 82 and were compared to the unmodified asphalt binder. Samples for dynamic modulus (|E*|) were prepared in the laboratory by using Superpave design criteria and gyratory compactor, these samples has the 100 mm diameter and 150 mm height. AMPT samples were tested under various temperatures and loading frequencies using the Asphalt Mixture Performance Test. This test is recommended as the primary simple performance test for rutting. Figure 3.16 shows the AMPT test machine used in this study.

Figure 3.16AMPT Test Machine used in the study

For linear viscoelastic materials such as HMA, the stress- strain relationship under a continuous sinusoidal loading is defined by its complex dynamic modulus (E^*). This is a complex number that relates stress to strain for linear viscoelastic materials subjected to continuously apply sinusoidal loading in the frequency domain. The complex modulus is defined as the ratio of the amplitude of the sinusoidal stress (at any given time, t, and angular load frequency,ω), $\sigma = \sigma_0 \sin(\omega t)$, and the amplitude of the sinusoidal strain $\varepsilon = \varepsilon_0 \sin(\omega t - \varphi)$, at the same time and frequency, that results in a steady-state response is shown in Equation 3.9.

$$E^* = \frac{\sigma}{\varepsilon} = \frac{\sigma_0 e^{i\omega t}}{\varepsilon_0 e^{i(\omega t-\varphi)}} = \frac{\sigma_0 \sin(\omega t)}{\varepsilon_0 \sin(\omega t-\varphi)} \quad (3.9)$$

Where

σ_0: Maximum (peak)stress.

ε_0: Maximum (peak)strain.

φ: $phase\ angle, degress$

ω: $angular\ velocity, rad/sec$

t: $time, seconds$

Mathematically, the dynamic modulus is defined as the absolute value of the complex modulus,

$$|E^*| = \frac{\sigma_0}{\varepsilon_0}$$

For a pure elastic material, φ = 0, and it is observed that the complex modulus (*E**) is equal to the absolute value or dynamic modulus. For pure viscous materials, φ = 90°. Three LVDT's were used to measure the strain at different locations separated by 120° and the average value was used in the calculations.

3.4.4.2. Master curve for Dynamic modulus

Many models had been used to create the master curve calculations, the most representing and promising model is the visco-elastic model. For laboratory data obtained from AMPT, the Symmetrical Sigmoidal Function was used in this study. Arrhenius factor Equation (3.10) was used to shift the modulus values and to create the master curves.

$$\text{Log}_{10}\,[\text{a (T)}] = \frac{EA}{19.147\ (\frac{1}{T}-\frac{1}{T_r})} \quad (3.10)$$

Where

a (T): Function of time

EA: Activation energy

T: Testing temperature, Kelvin

Tr: Reference temperature, Kelvin

In this study, master curves for each designed sample of polymer modified hot mix asphalt were created from shifted modulus values. These master curves are used in the *Mechanistic-Empirical Pavement Design Guide* developed in NCHRP Project 1-37A, the modulus of HMA at all levels of temperature and time rate of load is determined from a master curve constructed at a reference temperature generally taken as 70°F (21.2°C). Master curves are constructed using the principle of time-temperature superposition. The data at various temperatures are shifted with respect to time until the curves merge into a single smooth function. The master curve of the modulus, as a function of time, formed in this manner describes the time dependency of the material. Figure 3.17 shows typical results of dynamic modulus and corresponding master curve.

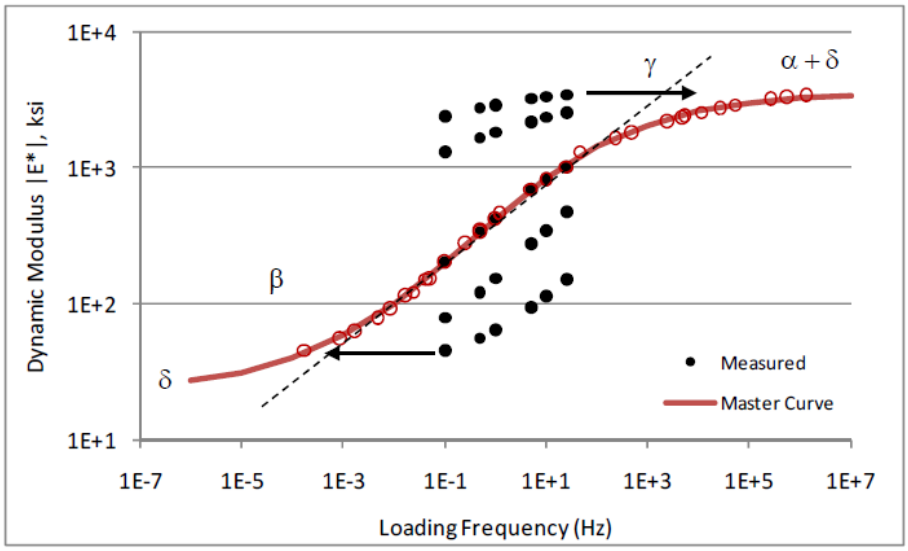

Figure 3.17Typical dynamic modulus master curve

Many models had been used to create the master curve calculations, the most representing and promising model is the visco-elastic model. For laboratory data obtained from AMPT, the Symmetrical Sigmoidal Function is used as shown in Equation 3.11.

$$\log(E^*) = \delta + \frac{(Max - \delta)}{1 + e^{\beta + \gamma\left\{\log(t) - \frac{\Delta E_a}{19.14714}\left[\left(\frac{1}{T}\right) - \left(\frac{1}{Tr}\right)\right]\right\}}} \quad (3.11)$$

E* = dynamic modulus

t = loading time

T = temperature, °K and Tr is the reference temperature.

Max = limiting maximum modulus

δ, β, γ and ΔE_a = fitting parameter

3.4.5. Rut depth Evaluation of Polymer Modified Asphalt Mixes

Rutting resistance of laboratory hot mixed asphalt samples was evaluated using Asphalt Pavement Analyzer (APA). Three mixes were chosen to be as control samples for the

sake of comparison and significance of polymer modification in improving the performance. Thirty six different laboratory produced mixes were tested and then ranked based on the results of rut depths.

APA samples were prepared by mixing the hot aggregates and modified asphalts together at corresponding mixing temperature targeted previously for each polymer type and content. The mixed materials then were conditioned at 135℃ for four hours in the oven. Then samples were compacted using Superpave Gyratory compactor at 7.0±1.0 % air contents. The volumetric properties were controlled by measuring the Bulk specific gravity G_{mb} AASHTO T 166 and maximum theoretical density G_{mm} AASHTO T 209 of asphalt mixes. The compacted specimens are conditioned for 6 hours at testing temperature (i.e. 64°C). The conditioned samples are then tested for rutting in the APA machine shown in Figure 3.18 and in accordance to AASHTO T 340-10 procedure. Table 3.7 shows the standard test parameters of APA test. The 7% air voids simulates field conditions of the pavement at its initial stage.

Table 3.7Input parameters for APA testing

Parameter	**Selected value**
Test Temperature, °C	64
Condition	Dry
Specimen Type	Cylindrical
Specimen size	150mm x 75mm (6”x3”)
Load N(lb)	445 (100)
Hose Pressure, kPa (psi)	689 (100)
Wheel speed m/s (ft/s)	0.6 (2)
No. of Cycles	8,000
Air voids %	7±1

Figure 3.18Asphalt Pavement Analyzer (APA) used in the study

All modified specimens were tested at same temperature (64°C) and then ranked according to the resulted rut depths. Figure 3.19 shows the arrangement of APA samples.

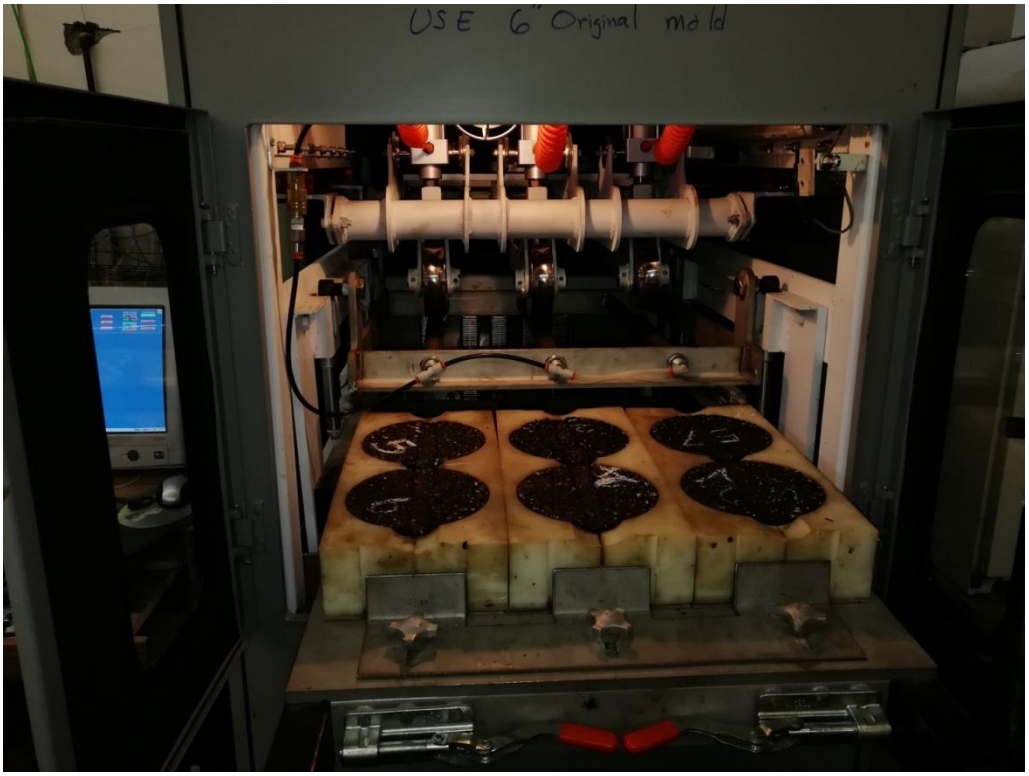

Figure 3.19Samples arrangement inside the APA

The rut depths results of all polymer modified asphalt mixes used in this study were compared and correlated to their properties related to asphalt binder, aggregate gradations and mix volumetric parameters. Although rut depth measurements obtained from APA test do not have mechanistic basis and cannot be directly correlated to field performance, the resulted stress-strain values can be used to generate prediction models for field rut depths. The average of three rut depth (mm) specimens were automatically recorded after 25, 4,000 and 8,000 cycles and reported for further analysis.

3.4.6. Evaluation of Fatigue Properties for Asphalt mixes

Fatigue life (N_f) of modified and unmodified asphalt mixes was evaluated using four-point flexural bending beam test (AASHTO T-312) was used. Slabs of hot mix asphalts contain different modified binder and aggregate gradations were compacted to optimum density at 4%±1 air-voids by using a slab compactor shown in Figure 3.20. The resulted

slab (380x300x50mm) was sawed to form 5 beams each has a dimension of 380x63x50 mm as shown in Figure 3.21. Samples were conditioned at 20°C for two days in closed chamber as shown in Figure 3.22.

The test was terminated when the stiffness of the mix reaches 40% of initial stiffness. Table 3.8shows the standard parameters of the test. The initial stiffness was automatically calculated after 200 cycles and reported. Each beam was tested under controlled stress mode at different stress value ranges from 400-1000 kPa.

Table 3.8Fatigue test parameters

Test Parameter	**Selected Value**
Test Temperature	20°C
Test Mode	Stress controlled
Strain Levels	Measured at each cycle
Frequency	10 Hz
Failure mode	40% of Initial Stiffness measured at 200^{th} cycle.

Figure 3.20Slab roller Compactor

Figure 3.21Beam Samples obtained from compacted slab

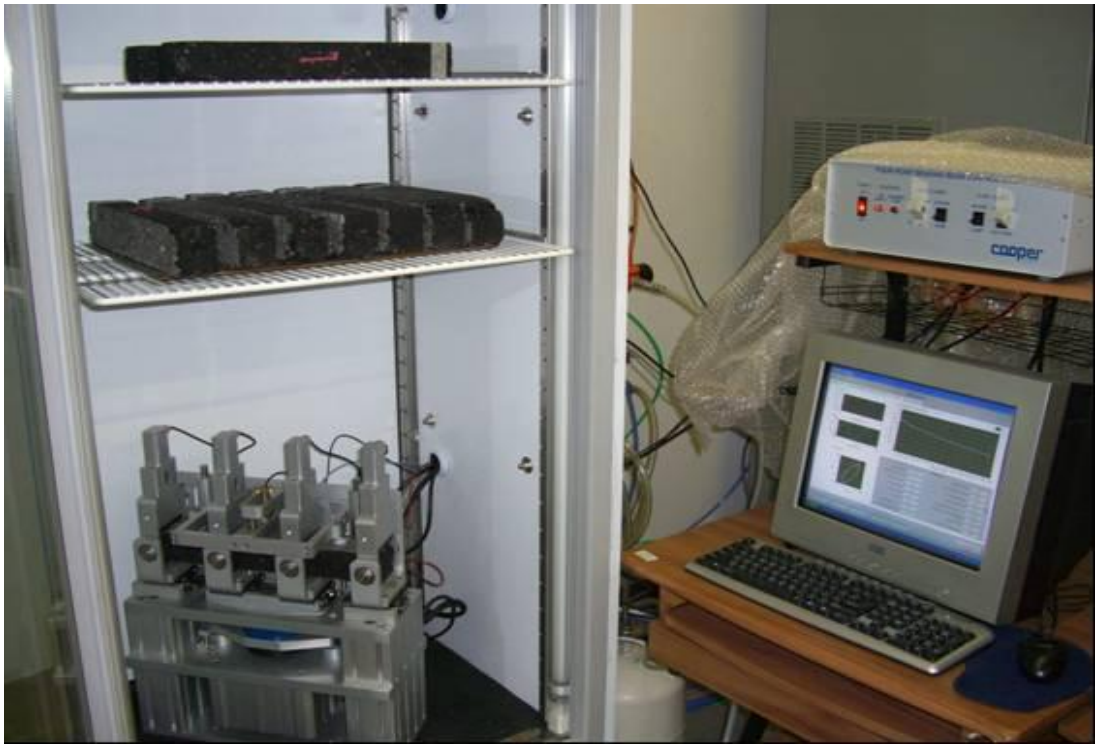

Figure 3.22Fatigue Beam test and conditioning Chamber

CHAPTER 4:
Performance Evaluation of Polymer Modified Asphalt Binders

4.1. Introduction

The performance of modified and unmodified asphalt binders to resist rutting and fatigue is based on their rheological properties and depend on temperature, loading time and aging. In this chapter, the Superpave performance grading (PG^+) methods of polymer modified asphalt binders are discussed in details. Furthermore, characterization of MSCR curves is also discussed in this chapter.

4.2. Superpave Performance Grading (PG^+) of Polymer Modified Asphalt Binders

The initial stage of performance grading requires the measurement of temperature at which the asphalt binder can sustain the applied shear stresses during its service life. Then the elastic recovery response of the modified binder is evaluated at that temperature using Multiple Stress Creep Recovery (MSCR) Test.

Dynamic Shear test [AASHTO TP5-93] is conducted by applying a repeated shear stress with an angular frequency of 10rad/sec and the resulting shear strain is measured at each cycle. The resulting shear modulus |G*| is defined as the ratio between maximum shear stress and maximum shear strain. Phase angle δ is the time lag between stress and strain during the test which gives an indication on the viscosity and elasticity of the material at different temperatures. In order to predict the performance of asphalt binder against rutting, a parameter $|G^*|/\sin\delta$ is measured for both aged and fresh (un-aged) conditions

at pavement high service temperature. Rutting Evaluation of Polymer Modified Asphalt Binders

At pavement service temperature, binder's rutting parameter should not be less than 1.0 kPa and 2.2 kPa for un-aged and short-term aged conditions, respectively. The PG upper temperature is the lowest among the two cases. Table 4.1 shows the PG temperature of SBS modified Ras-Tannura asphalt binders. Results of PG testing of all tested samples are listed in Appendix A.

Table 4.1Rutting parameter of SBS Ras-Tannura Modified Asphalt Binders

%P	Testing Temperature, °C	Un-aged		Aged		PG Grade
		|G*|/sinδ (kPa)	Actual PG Temperature	|G*|/sinδ (kPa)	Actual PG Temperature	
0%	64	1.012	65.28	2.598	64.1	PG 64
	70	0.485		1.191		
2%	64	3.174	76.20	8.009	74.93	PG 70
	70	1.713		3.875		
	76	1.018		1.938		
	82	0.738		1.043		
4%	64	6.123	85.9	14.49	81.96	PG 76
	70	3.641		7.519		
	76	2.239		4.035		
	82	1.343		2.192		
6%	64	9.072	89.6	19.43	83.08	PG 82
	70	5.569		14.86		
	76	3.46		8.264		
	82	1.948		2.691		

Results of dynamic shear test show that polymer content has significant effect on improving the resistance of shear stress at different temperatures. Aged results of G*/sinδ control the passing PG temperature, since it is lower than the un-aged

conditions for all levels of polymer contents. Adding 2% of SBS to Ras-Tannura asphalt binders has significantly improved the PG temperature to 76.20°C for fresh (un-aged) and 74.93°C for short term aged conditions. When same asphalt binders are modified by 4% of SBS, passing temperatures reach 85.90°C and 81.96°C, respectively. For higher content of SBS, the resulted temperature reaches 89.6°C and 83.08°C. The reported PG temperature is rounded down to whole number that matches 64, 70, 76 or 82°C.

It is concluded from this discussion, that 2% of SBS modified asphalt binders can be used to increase the chances of resisting rutting at locations which require PG 70 service temperature. Similarly, 4% is used to reach the PG 76.Figure 4.1 summarizes |G*|/sinδ values at fresh and short term aged conditions. Polymer type and content have significantly increased the rutting parameter at any testing temperature and aging conditions.

The Superpave specification parameter $|G^*|/\sin\delta$ was identified as the term to be used for high temperature performance grading of paving asphalts in rating the binders for their rutting resistance. The $G^*/\sin\delta$ of polymers modified asphalt binders display higher values and high rate of changes after short-term aging. The oxidation of asphalt is one of the principal factors causing the deterioration of asphalt pavements at which the mechanical properties and chemical structures of asphalt binders change with aging [Lu Xiaohu and Ulf Isacsson, 2002]. The aging include short term aging that occurs during the mixing, paving, compacting and during the service life in the pavement.

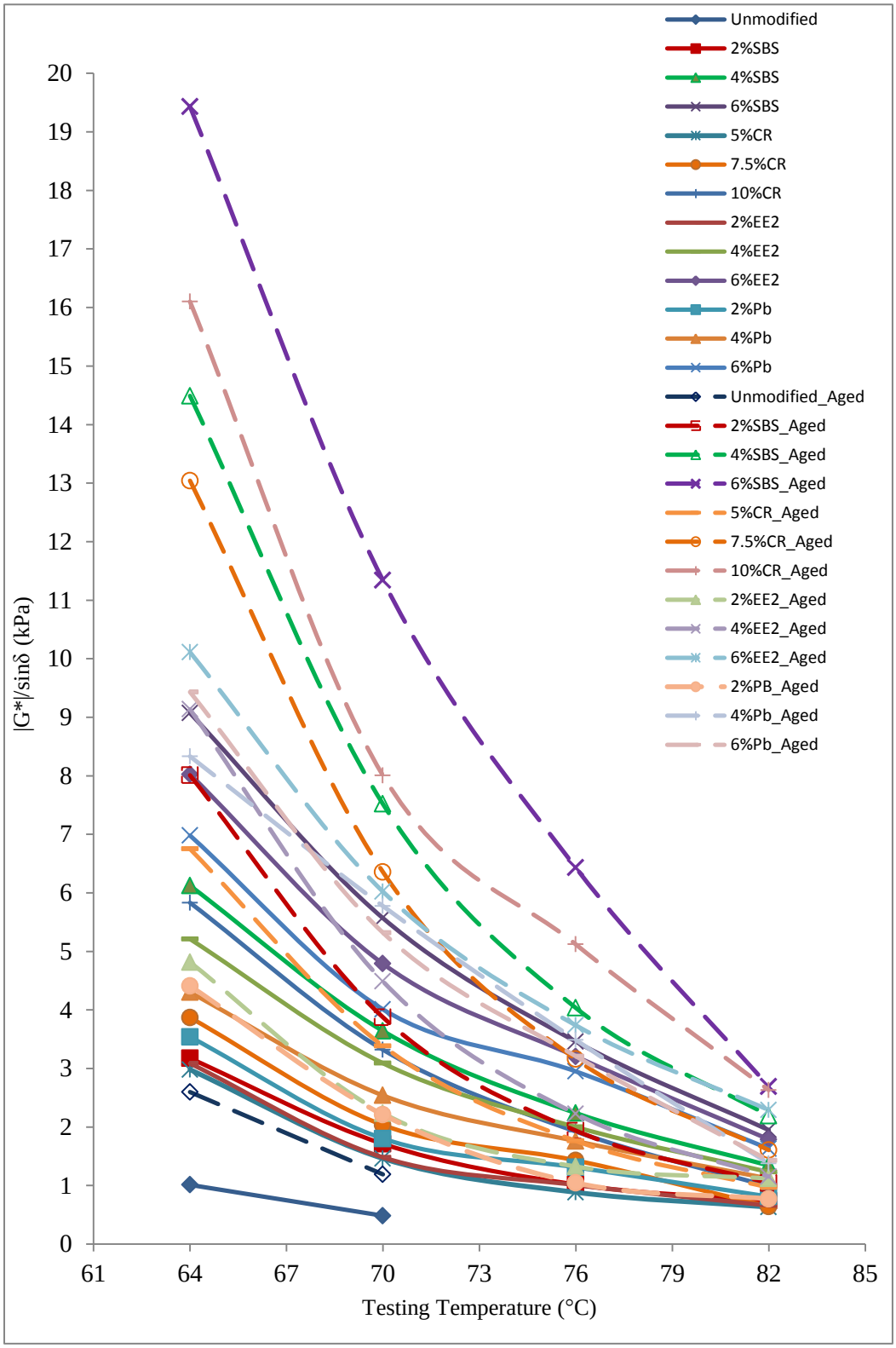

Figure 4.1Rutting Parameters for the Modified Asphalt Binders

It was clearly observed from Figure 4.1 that the $|G^*|/\sin\delta$ of asphalt binder increased when polymers were added and after aging. However, compared with the unmodified asphalt binder, the $G^*/\sin\delta$ of modified asphalt binder decreased remarkably with temperature increasing. As a result, the rate of change of the $G^*/\sin\delta$ curves increased with temperature increasing in a non-linear form. At high temperature testing i.e. 82°C, the change is less significant; however, at 64°C the effect of aging is clearly noticed at same polymer type and polymer content.

SBS modified asphalt binders have shown the highest values of |G*|/sinδ followed byEE2, Pb and CR. The chemical composition of each polymer type has a direct influence on its behavior against shear loading. Polyethylene based polymers have lower melting point and lower stiffness compared to SBS.

Performance grading (PG) of asphalt binder is determined based on rutting resistance at high service temperatures and fatigue resistance at intermediate and low temperatures. The fatigue parameter of binder termed by |G*|.sinδ is measured at intermediate temperatures that depend on passing actual high temperature. Finally, asphalt samples were subjected to long-term aging and the stiffness is measured accordingly. Table 4.2 below shows Fatigue parameter |G*|/sinδ of SBS Ras-Tannura Modified Asphalt Binders.

Table 4.2Fatigue parameter of SBS Ras-Tannura Modified Asphalt Binders

High PG temperature	Testing Temperature	G*sinδ (MPa)	Testing Temperature	Stiffness, S (Mpa)	Slope, m	PG Grade
64.1	28	1.2436	-6	45.699	0.4009	PG 64-16
	25	1.8291	-12	-	-	
	22	2.8478	-18	-	-	
	19	-	-24	-	-	
	16	-	-30	-	-	
74.93	34	-	0	30.06	0.3886	PG 70-16
	31	1.413	-6	63.0418	0.365427	
	28	1.97	-12	-	-	
	25	-	-18	-	-	
	22	-	-24	-	-	
81.96	37	0.549	0	-	-	PG 76-16
	34	0.821	-6	71.65	0.381	
	31	-	-12	-	-	
	28	-	-18	-	-	
83.08	40	-	0	-	-	PG 82-16
	37	0.431	-6	87.93	0.334	
	34	0.763	-12	-	-	
	31	-	-18	-	-	

Results obtained from fatigue test of asphalt binders show that modified samples have passed the intermediate and low temperatures as per Superpave procedures. All polymer modified asphalt samples in this study can resist fatigue up to -16°C. The high stiffness values measured on highly modified samples gives more fatigue resistance of the mix. It is concluded from the above discussion that the low temperature of -16°C is not a concern in desert environment and can be achieved easily.

4.2.1. Effect of Polymer Source on PG Actual Temperature

Asphalt binders are heavy product from the barrel of crude oil. It is produced from the fractional distillation of crude oil at 500–600 °C its properties are affected by source and production processes. Figure 4.2 presents a bar chart of PG actual temperature of Riyadh and Ras-Tannura asphalt binders modified by different polymer type and content.

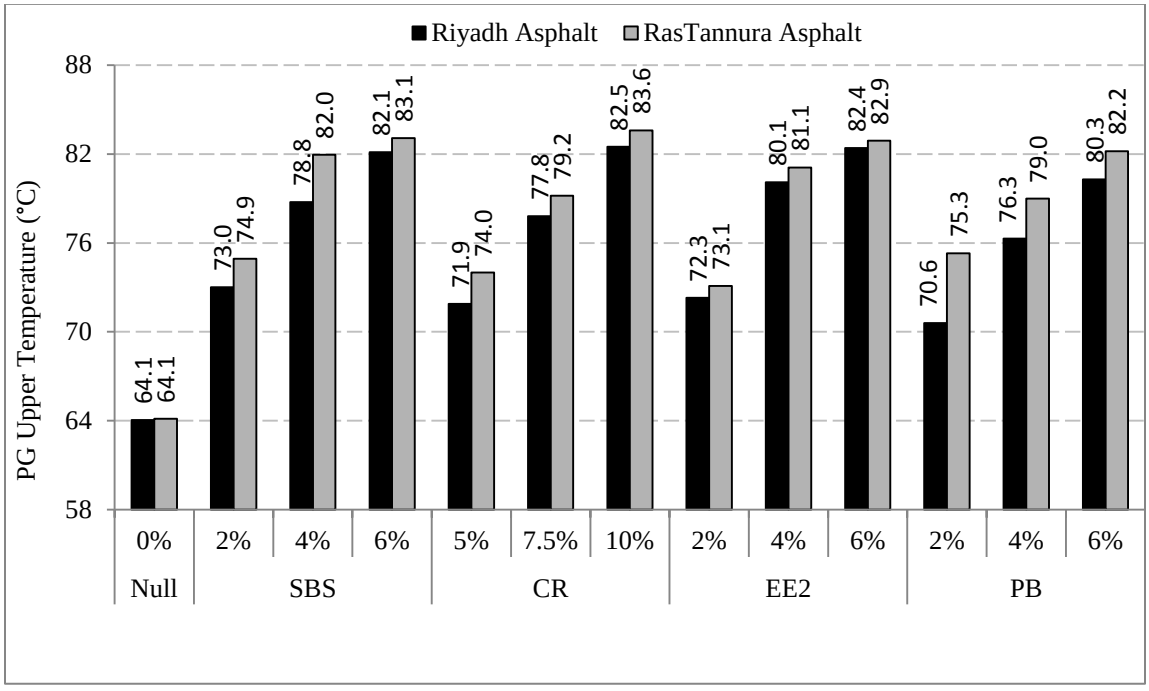

Figure 4.2Effect of Asphalt Source on PG Temperature

Figure 4-2 shows that Ras-Tannura modified asphalt binders have higher PG actual temperatures at high service temperatures than Riyadh asphalts. However, both asphalt sources have achieved the same PG grades (PG 64, PG 70, PG 76 and PG 82) when modified by same type and content of polymer.

Adding 2% of SBS, EE2 and Pb and 5%of CR polymer to Riyadh or Ras-Tannura asphalt binders can improve rutting resistance of asphalt pavements servicing at 70°C. While adding 4% of SBS, EE2 and Pb are required to improve rutting resistance at 76°C.

Highly modified asphalt binders (6% and 10%) are used at specific locations at which low speed and extremely heavy vehicles exist.

4.3. Stress Creep and Strain Recovery of Polymer Modified Asphalt Binders

All modified binder samples were tested after they have been short term aged under different temperature, starting from PG high value and ends when sample starts to flow and no more recovery is shown. Table 4.3shows MSCR results for SBS modified asphalt binders tested at different temperature and stress levels. Two stress levels were selected to cover the linear and non-linear recovery trends, and the difference as percent was calculated to find out how much the material is sensitive to stress. As recommended by [AASHTO M-322], the difference is preferably should not exceed 75%.

Table 4.3MSCR summary results for SBS modified Ras-Tannura asphalt binders

Polymer type	%P	Testing Temperature, °C	Recovery (%)		Diff. (%)	Jnr (1/kPa)		Diff (%)
			0.1	3.2		0.1	3.2	
Unmodified	0%	64	4.2	1.5	64.3	3.240	3.810	15.0
		58	10.0	3.6	64.0	1.290	1.480	12.8
SBS	2%	70	19.0	8.1	57.3	1.593	2.036	21.8
		64	28.4	18.7	34.0	0.635	0.875	18.1
		58	39.3	34.0	13.4	0.237	0.268	11.2
	4%	76	30.7	16.3	47.1	1.196	1.703	29.8
		70	42.1	29.2	30.8	0.499	0.685	27.2
		64	53.6	46.6	13.1	0.199	0.241	17.7
		58	66.1	62.2	5.8	0.069	0.079	12.9
	6%	82	54.8	43.2	21.2	0.542	0.708	23.4
		76	68.3	54.0	20.9	0.218	0.363	39.9
		70	75.4	67.7	10.3	0.088	0.128	31.6
		64	83.8	78.0	6.9	0.030	0.043	32.0
		58	91.3	85.0	6.9	0.010	0.015	32.4

Results of MSCR test show that recovery (%) and non-recoverable creep compliance (Jnr) have been improved by increasing the polymer content at any temperature and stress. At 76°C and 3.2 kPa, the elastic recovery of asphalt binders could reach 54.0% when 6% of SBS was used compare to 16.3% in the case of 4% of SBS. In addition, the non-recoverable creep compliance (Jnr) has been improved from 1.7 to 0.36 (1/kPa). It is important to mention that there is no specific threshold for recovery values of polymer modified asphalts, but those recovery results have been used to classify materials as an elastomeric or plastomeric. On the other hand, Jnr values are used to grade the performance of modified asphalts. The lower the Jnr values the higher traffic level that asphalt binders could withstand. Specifically, values less than 0.5 1/kPa can resist rutting even under extremely heavy traffic as targeted by the ministry of transportation and municipalities in Saudi Arabia.

Results presented in Table 4.3 show that 6% of SBS can satisfy the targeted value at any temperature (58-82°C) and any stress level (0.1& 3.2 kPa). While 4% of SBS modified asphalts could have good performance against rutting at any temperature lower than 70°C when same value of Jnr is targeted. MSCR of other tested asphalt binders are shown in Appendix B.

Figure 4.3 shows a comparison between the two asphalt binders when modified with 2%, 4% and 6% of SBS polymers. MSCR evaluation was conducted at different testing temperature to study the effect of temperature on the recovery of modified asphalt binders.

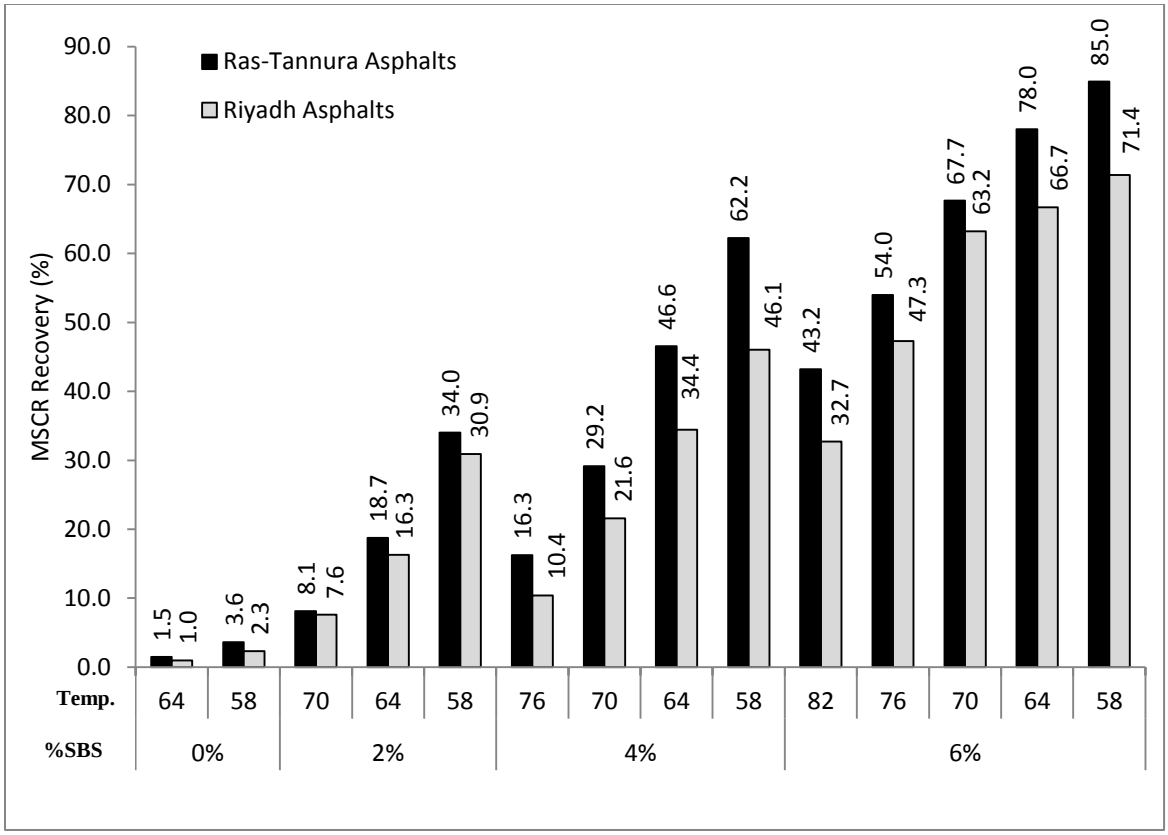

Figure 4.3Comparison of MSCR elastic recovery for different asphalt source

It is shown from the results of elastic recovery obtained by MSCR test that polymers can improve the performance of asphalt binders at any service temperature compared to unmodified asphalts. However, Ras-Tannura asphalt binders show higher values at any polymer content and testing temperature. This behavior can be explained by the chemical and physical components of the asphalts.

Figure 4.4 presents the effect of polymer type on improving the recovery property of asphalt binders grouped by polymer content and their PG actual temperatures.

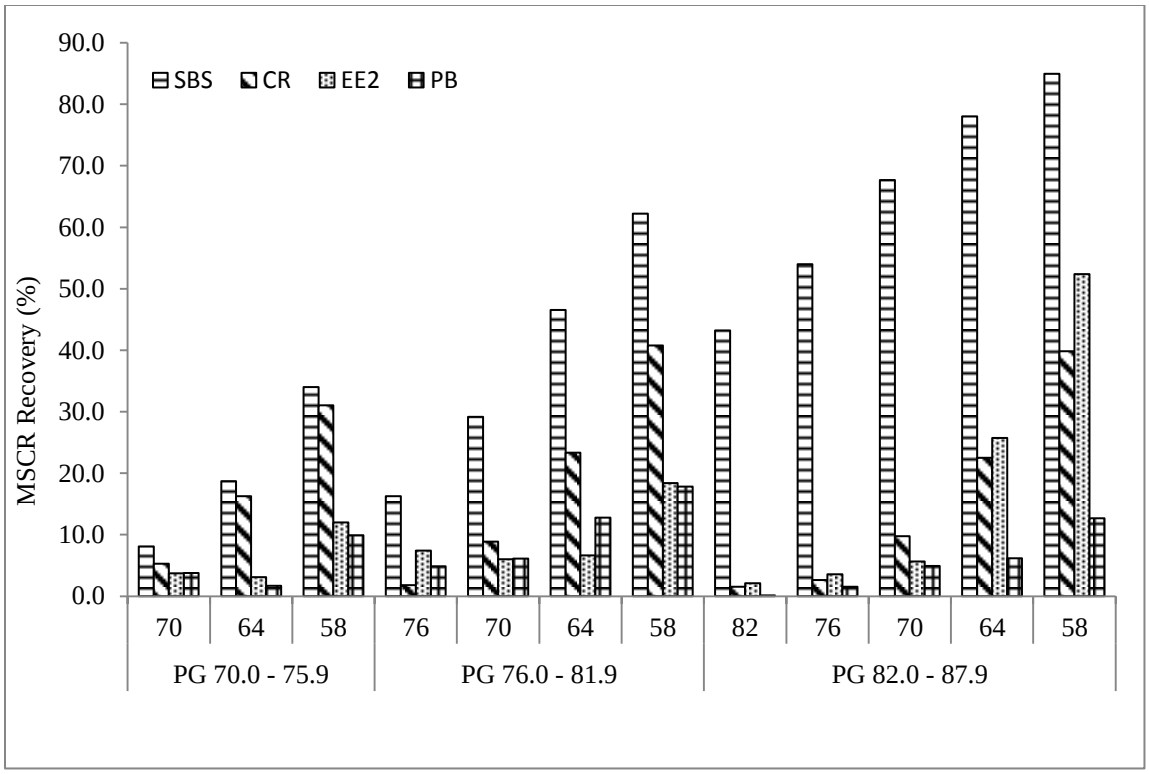

Figure 4.4Effect of Polymer Type on MSCR Recovery Property of Asphalt Binders

It is shown from the Figure that SBS modified asphalt binders showed significant improvement in recovery at any temperature and content. As an elastomeric material, it consists of butadiene that gives the copolymer its rubbery behavior. While Polyethylene based polymers (Pb) on the other hand, have lowest values of recovery and any testing temperatures. At 76°C, EE2 modified asphalt binder has higher recovery than CR. As a plastomeric, Polybilt is highly affected by temperature regardless of its content in the blend.

Ras-Tannura asphalt binders showed better performance than Riyadh asphalts to improve the PG actual service temperature and elastic recovery. Ras-Tannura asphalts are used in the rest of this research.

4.4. Effect of Temperature on MSCR Parameters

By plotting percent recovery (%R) and Non-recoverable strain creep compliance (Jnr) results on the standard curve (%**R**=29.4**Jnr**$^{-0.26}$) recommended by [AASHTO TP-70] for each polymer modified asphalt binder tested at 3.2 kPa stress and at different temperatures, the elastomeric property of that binder can be evaluated. If the data point of %R-Jnr at specific temperature lies above that line, the elastomeric behavior is highly expected at that condition when used in asphalt mix. Figures4.5 and 4.6 show the results of SBS and CR modified asphalt binders, respectively.

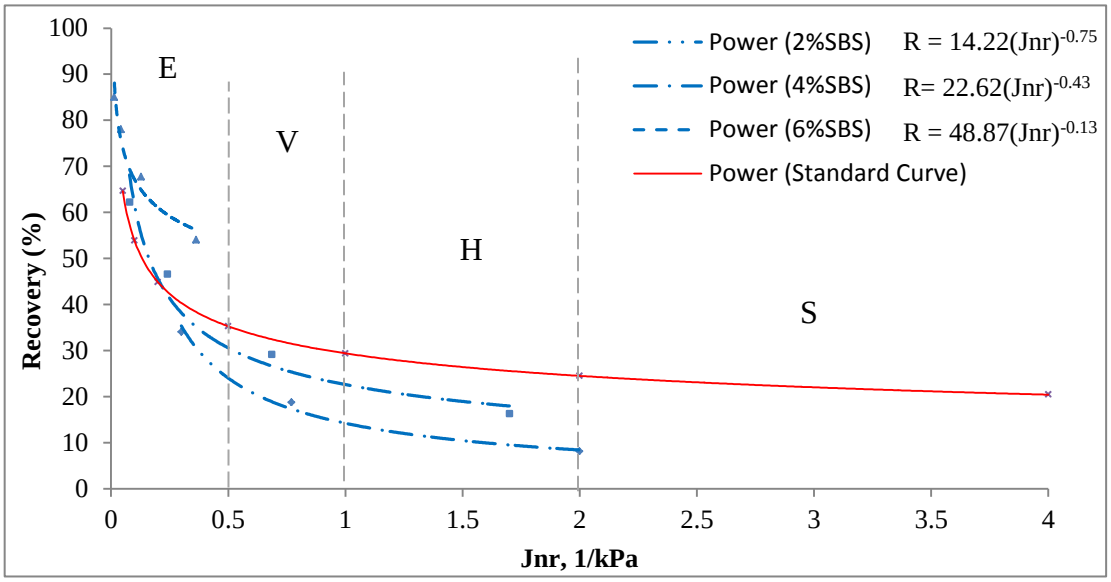

Figure 4.5Evaluation of Elastomeric behavior of SBS modified asphalts

Power-law curves parallel to the standard line of elastomeric behavior are generated as shown in the Figures. It can be shown from the Figure that 6%-SBS modified asphalt binder have a remarkable elastomeric behavior at any temperature. That means, number of polymer's molecules are sufficient to improve the elastic recovery for the system. While 4%SBS modified asphalt binders at lower temperature might reach a point at which signs of elastomeric behavior is reduced. There is a sign of

superposition of temperature and number of molecular interaction points between polymer and asphalt binders that improve the elastic recovery property of the system. With simple algebraic calculations the temperature at which elastomeric behavior starts can be estimated.

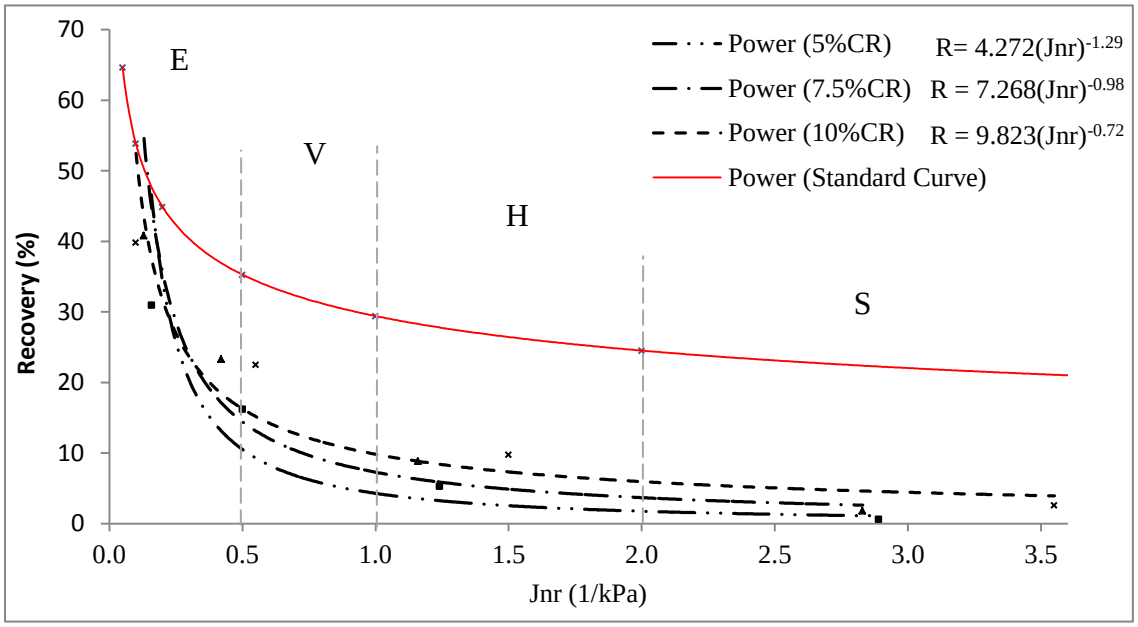

Figure 4.6Evaluation of Elastomeric behavior of CR

Similar behavior could happen for crumb rubber (CR) but the inversion could happen at very low temperatures which is undesirable situation at desert environment. For Polybilt (Pb) and Eastman (EE2)modified asphalt binders, the resulted curves are not reaching the elastomeric curve at high nor moderate temperatures, only the situation at which the required temperature is less than 58°C these modified binders could have some strain recovery. Figure 4.7 shows the results of EE2 modified asphalt binders at different temperatures while Figure 4.8 shows the PB results.

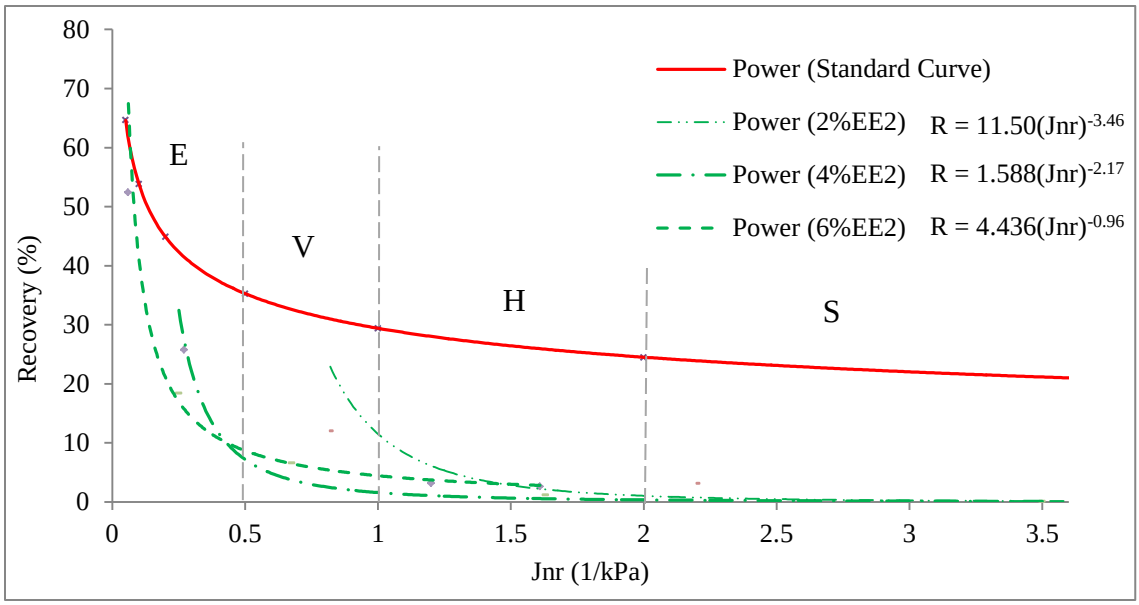

Figure 4.7Evaluation of Elastomeric behavior of EE2 modified asphalts

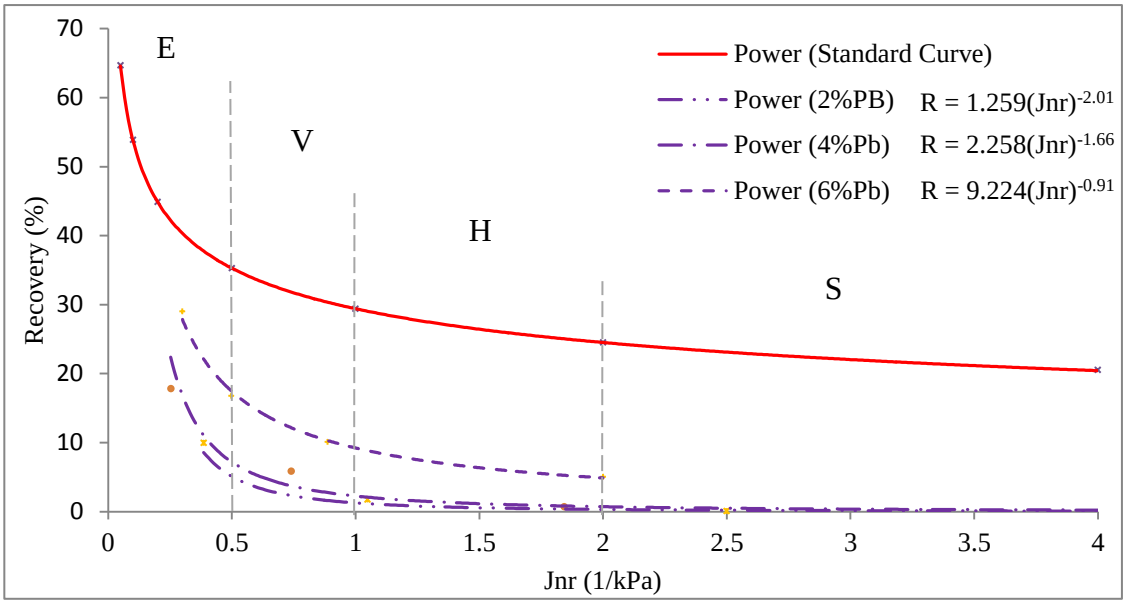

Figure 4.8Evaluation of Elastomeric behavior of PB modified asphalts

All polymer modified asphalt samples prepared in this study were tested at 3.2 kPa stress level and at different temperatures range from 58°C to 79°C in order to find a relationship between Jnr parameter and temperature and to create regression models

used for proper design of asphalt mixes and structures against rutting. Figure 4.9 shows the results of the four selected polymer modified asphalts that have three levels of polymer amount and performance grades tested at various temperatures.

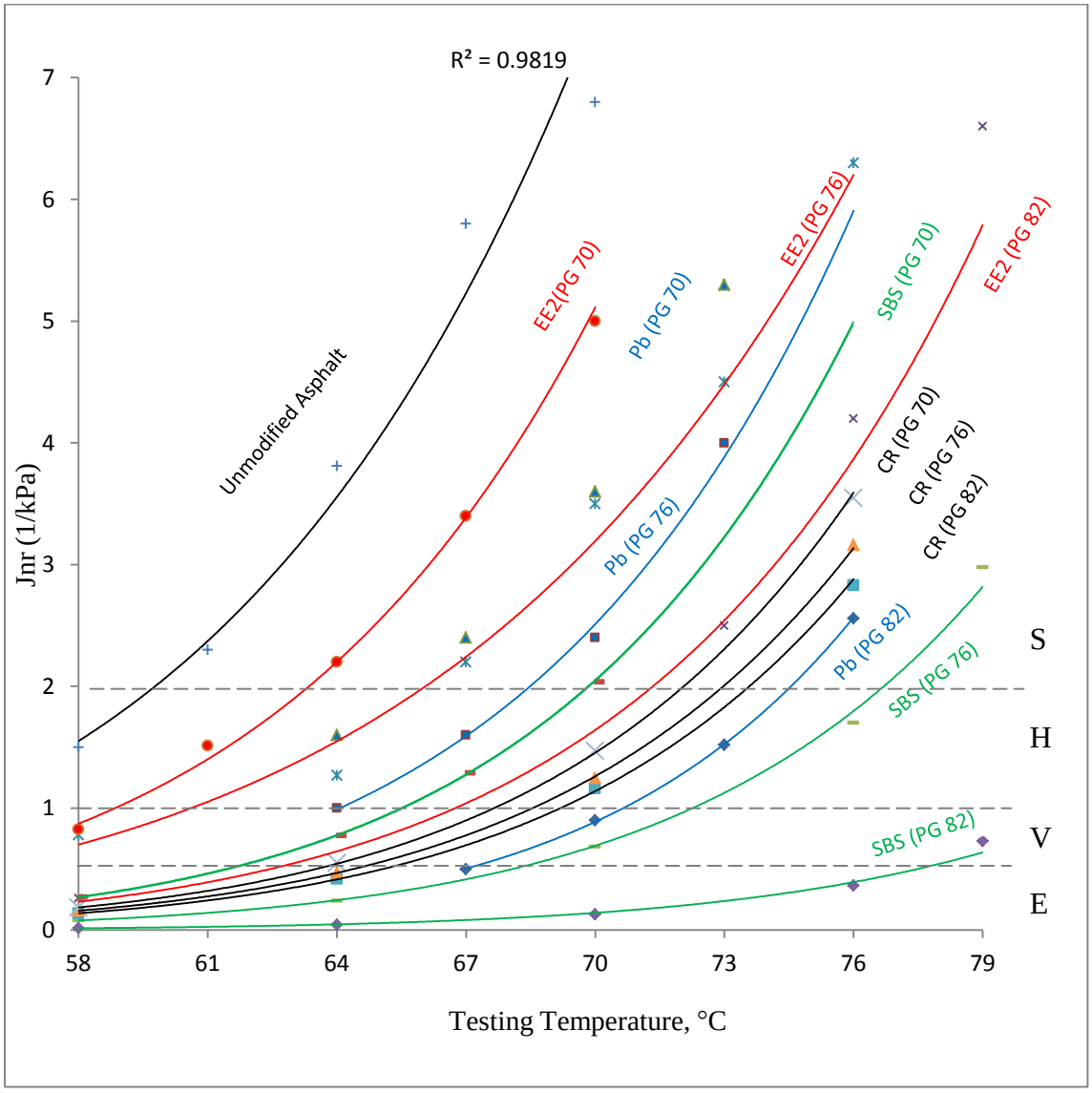

Figure 4.9Effect of Temperature on Jnr values

As shown from the Figure, the best relationship was found between Jnr and temperature follow the cubic trend while polymer content has a linear effect on Jnr values as presented in Equation4.1:

$$Jnr = a + b\,(T_{PG})^{n} – Di\,(\%P) \qquad (4.1)$$

Where

Jnr is the average of non-recoverable compliance (ε_{10}/τ) after 10 cycles tested under 3.2 kPa stresses.

T_{PG}: test temperature in Celsius

n: is the exponent of the power law equation

%P: Polymer content as percent from binders' weight.

a and b : constants differ with polymer type

Di is the dummy variable included for polymer type.

These curves can be used to estimate the required amount of polymer (as a percent of binder weight) at given traffic level (Jnr) and targeted service temperatures. Compared to unmodified asphalt binders, all tested samples in this study showed signs of strain recovery improvement when tested under high stress and different temperatures. Furthermore, a comparison between elastomer (SBS and CR) and Plastomers (Pb and EE2) modified samples was conducted to differentiate the effect of polymer type on the rate of change of Jnr when increasing the temperature. Table 4.4 shows the analysis of variance for the developed model Jnr.

Table 4.4ANOVA results for the Jnr prediction equation

	df	*SS*	*MS*	*F*	*Significance F*
Regression	6	32.56313095	5.427188492	145.3428	8.68029E-22
Residual	32	1.194899817	0.037340619		
Total	38	33.75803077			

These equations give direct prediction of Jnr values at required actual PG temperature of the project. The choice of using polymer type and content depends on

material availability and cost. Table 4.5 shows the significance test of included variables of Jnr model.

Table 4.5Significance test for included variables in Jnr prediction equation

	Coefficients	*Standard Error*	*t Stat*	*P-value*	*Lower 95%*	*Upper 95%*	*Lower 95.0%*	*Upper 95.0%*
Intercept	3.937412	0.384242	10.24723	1.24E-11	3.154737	4.720087	3.154737	4.720087
T^n	-4.8E-07	1.39E-06	-0.34652	0.731219	-3.3E-06	2.36E-06	-3.3E-06	2.36E-06
%P	-0.02856	0.061162	-0.46699	0.643668	-0.15315	0.096021	-0.15315	0.096021
D1	-3.35454	0.188787	-17.7689	3.87E-18	-3.73908	-2.96999	-3.73908	-2.96999
D2	-3.07064	0.221176	-13.8832	4.29E-15	-3.52116	-2.62012	-3.52116	-2.62012
D3	-2.94607	0.175168	-16.8186	1.91E-17	-3.30288	-2.58927	-3.30288	-2.58927
D4	-2.55516	0.155895	-16.3903	4.00E-17	-2.8727	-2.23761	-2.8727	-2.23761

The grading procedure of polymer modified asphalt binders was done in successive stages. Based on $|G^*|/\sin\delta$ and Jnr values. Results show that PG 70(H) can be obtained by adding 3% of SBS, while 4% of SBS is required to reach PG 76(V) grade. In case of CR modified asphalts, adding 5%, 7.5% and 10% of CR can achieve the PG+ grade of 70(H), 76(H) and 76(V), respectively. The results obtained from MSRC testing procedure using the four polymers (i.e. SBS, CR, EE2 & Pb) were further evaluated.

Local asphalt modified with all the three different dosages has attained the PG+ requirements, by satisfying at various levels of high temperature grade and traffic levels. The PG+ grading results obtained shows that the local unmodified (plain) asphalt having a PG 64-10, cannot reach the PG+ standard at 64 (V). Indicating that in order to satisfy PG+ criteria modification of local asphalt is necessary. As the local agencies is targeting to have a Superpave plus performance grade of 76(E) for a major portion of kingdom highways. To achieve this targeted PG+ requirement, 4% of SBS or 10% of CR is needed. The previous requirement of improvement never occurs when using Plastomers

in the modification process and could be used in low traffic highways (S-H) or regions where required PG temperature is less than 76°C like northern or central provinces of the Kingdom. Table 4.6 shows summary results of grading system SBS modified asphalt Binders. While Tables C.1 to C.3 in Appendix C show the results of the other polymer modified asphalt.

Table 4.6PG and PG+ grading of SBS Modified Asphalt Binders

%P	Performance Grade (PG)(AASHTO M320)	Performance Grade Plus (PG^+) at 3.2 kPa stress and PG temperature(AASHTO TP70)			
		Testing Temperature, °C	Percent Recovery, %	Non-recoverable compliance (Jnr), 1/kPa	Performance Grade (PG+)
2	PG 70	70	8.1	2.04	70 (S)
		64	18.7	0.78	64 (V)
		58	34.0	0.27	58 (E)
4	PG 76	76	16.3	1.70	76 (H)
		70	29.1	0.68	70 (V)
		64	46.5	0.24	64 (E)
6	PG 82	82	24.4	1.37	82 (H)
		76	54.0	0.46	76 (E)
		70	67.7	0.13	70 (E)

It is shown from Figure 4-9 and Table 4-6 that SBS modified asphalt binders can sustain the change of Jnr value even at high service temperatures (76°C) which can resist rutting at Extremely Heavy Traffic E (Jnr<0.5 kPa^{-1}) when adding 6% of SBS (PG 82) and

Heavy Traffic H (1>Jnr>2) when 4% of SBS (PG 76) is added to local asphalt binder. The effect of crumb rubber (CR) on improving the Jnr is low compared to SBS values. It can only withstand Heavy traffic (Jnr 1-2 kPa^{-1}) at 70°C and Standard Traffic (Jnr 2.0-4.0 kPa^{-1}).

Local asphalt binders modified by 6% of Polybilt PG 70(V) are suitable for weather of 70°C temperature and Very Heavy Traffic conditions. While 6% of EE2 modified asphalts are suitable for Heavy Traffic only at same weather conditions. None of the plastomeric modified asphalt binders show significant improvement at 76°C temperature compared to SBS modified asphalts.

4.5. Strain Recovery Rate of Polymer Modified Asphalt binders

Three factors that influence the PMA characteristics and its response to loading, namely performance grade, applied loading stress and service temperature was analyzed. The effect of these factors on the rate of strain recovery for the various types of PMA is consistent, both at NI and NSS. (Full data is presented in Appendix D). Higher levels of applied stress and temperature have induced a correspondingly greater rate of strain recovery both at NI and NSS. Similar but slightly less obvious trend was observed for the higher PG level for higher stress level.

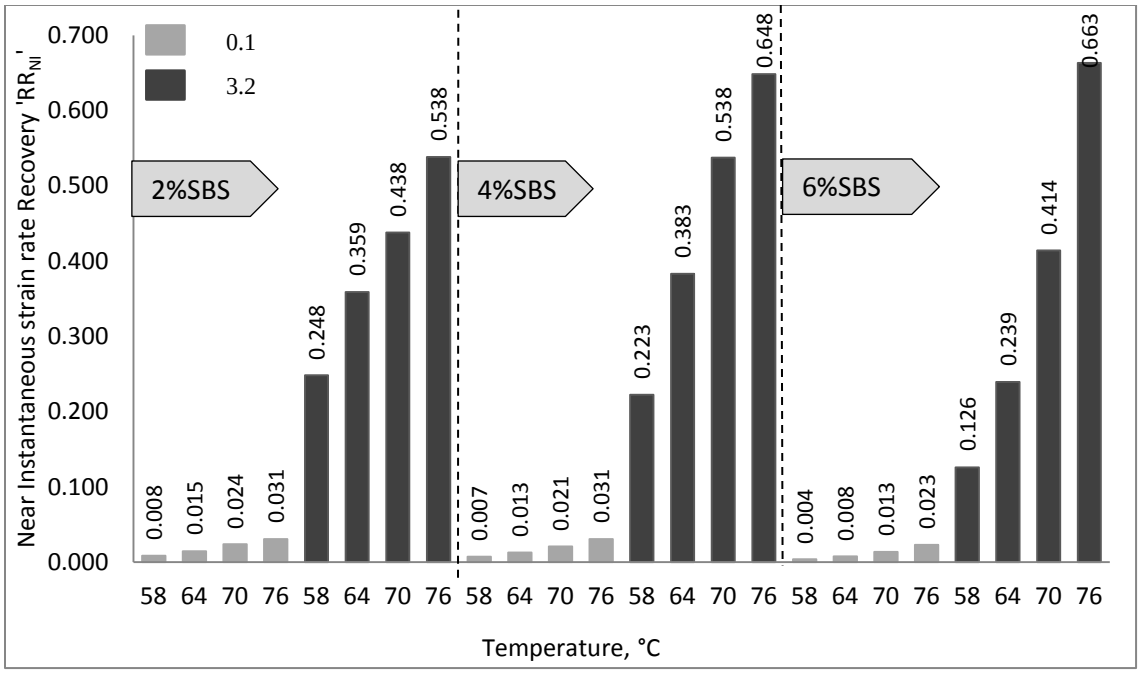

Figure 4.10Strain Recovery Rate near Instantaneous region for SBS

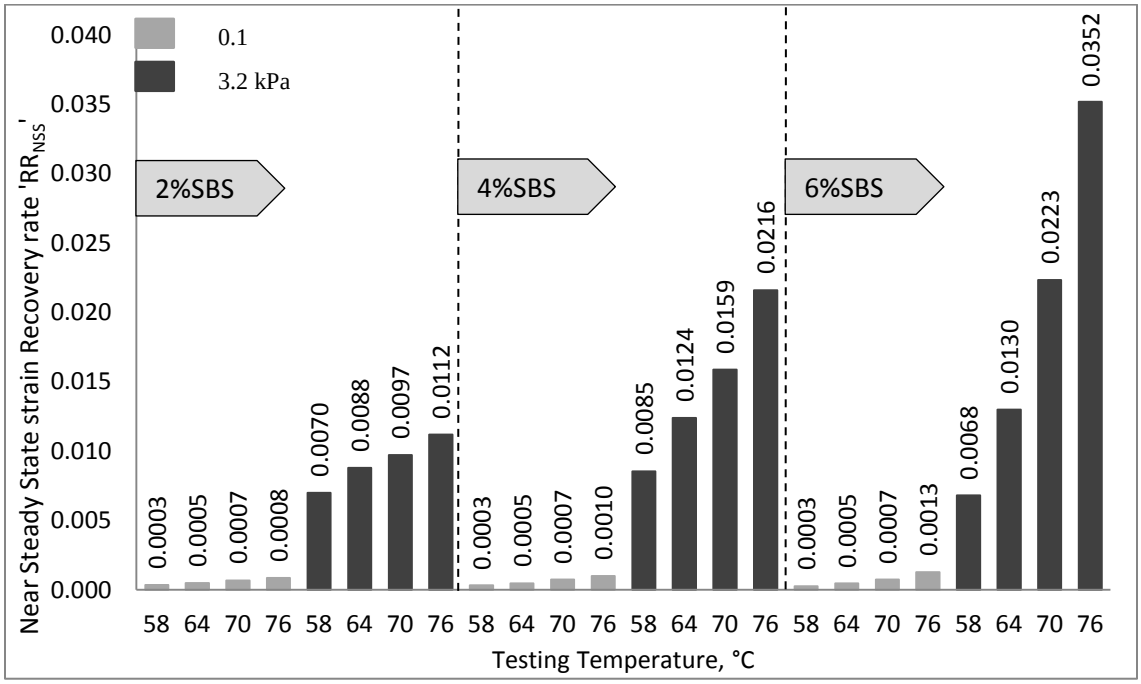

Figure 4.11Strain Recovery Rate near Steady State region for SBS

There is however no consistent trend of PG level effect for lower stress loading. The first cases of higher stress at a given temperature and higher temperature at a given stress translate in to additional accompanying strain. Therefore, the corresponding

rebound energy is relatively higher than those in the reverse scenarios. In the case of increased PG level, the corresponding surge in the recovery rate can be attributed to the improvement in the viscoelastic properties of the PMA [Al-Abdul Wahhab, Dalhat, & Habib, 2016; Dalhat & Al-Abdul Wahhab, 2015].

Percent recovery at NI ($\%R_{NI}$) and NSS ($\%R_{NSS}$) are termed absolute percent recovery. The term absolute is adopted here to describe the nature of the percent recovery of polymer modified asphalts as a function of its strain recovery rate (per-second), not as the function of recovered strain after a given time (greater than 1 second), as it is the tradition. The advantage of doing this is that the relative effect of time on the estimated percent recovery has been eliminated in case of $\%R_{NI}$, and minimized in the case of $\%R_{NSS}$. For example, the current standard percent recovery (%R) is obtained as the ratio of the recovered strain after 9 seconds of rest period to the total sustained strain after the 1 second loading. The numerator has a unit of strain/9seconds, while the denominator has a unit of strain/second. It is convenient to present the results without taking the time aspect in to consideration for easier comprehension, but it is inconsistent. In absolute reality, the traditional %R is exaggerated by a factor of 9. Plus the traditional %R varies over time due to the viscoelastic nature of PMAs. On the other hand, $\%R_{NI}$ and $\%R_{NSS}$ possessed a normalized function, with the numerator (RR_{NI} or RR_{NSS}) having a unit of strain/second and the denominator ($\varepsilon(1)$) also having a unit of strain/second. This is a consistent mathematical expression of unit-less percentage. The RR_{NI} and RR_{NSS} of a given PMA will relatively remain constant for any given period of rest time. By taking the strain accumulation rate as well as the recovery rate into account, only perfectly elastic

material could possess a 100% or 100+% absolute recoveries. In addition RR_{NI} can be obtained from less than 20% of the creep-recovery test data. This means RR_{NI} has the potential of reducing the current test duration by up to 80%.

4.6. Life Cycle Cost Analysis of Polymer Modified Asphalt Binders

The use of polymer additives could reduce the life cost of pavement construction and rehabilitation, selection of proper type and content of polymer should be controlled by the targeted performance grade (PG+) and material cost. In this section, cost analysis of polymer modified asphalt binders used in this research is discussed for PG 76 (S-E), PG 70 (S-E) and PG 64 (S-E). Table 4.7 shows the current unit price of local asphalt binders and polymers in metric tons.

Table 4.7 Unit prices of polymers

Material	Asphalt Binders	SBS	CR	EE2	Pb
Cost SR/Ton	450	3,500	900	1,400	1,200

The current material costs were obtained from main suppliers in Saudi Arabia. Polymer content (%P) as percent of binders' weight and total cost of polymer modified asphalt binders in metric ton are calculated and listed in Table 4-8. All studied asphalt binders are grouped based on PG temperature (°C) and traffic level (E, V, H and S) noted by T_{PG} and L_{PG}, respectively.

Table 4.8Cost Analysis of different polymer modified asphalt binders

T_{PG}	L_{PG}	Item	SBS	CR	EE2	Pb
76	E	%P	5.8	N/A	N/A	N/A
		Cost SR/Ton	626.9			
	V	%P	5.2	9.5	6.2	6.7
		Cost SR/Ton	608.6	492.75	508.9	500.25
	H	%P	3.5	7.0	5.3	5.9
		Cost SR/Ton	556.75	481.5	500.35	494.25
	S	%P	3.5	7.0	5.3	5.9
		Cost SR/Ton	556.75	481.5	500.35	494.25
70	E	%P	4.9	N/A	N/A	N/A
		Cost SR/Ton	599.45			
	V	%P	3.9	6.8	5.1	5.8
		Cost SR/Ton	568.95	480.6	498.45	493.5
	H	%P	2.0	5.0	3.3	3.9
		Cost SR/Ton	511	472.5	481.35	479.25
	S	%P	2.0	5.0	3.3	3.9
		Cost SR/Ton	511	472.5	481.35	479.25
64	E	%P	3.0	5.0	2.2	2.5
		Cost SR/Ton	541.5	472.5	470.9	468.75
	V	%P	1.2	4.2	1.8	2.3
		Cost SR/Ton	486.6	468.9	467.1	467.25
	H	%P	0.7	2.0	1.3	1.6
		Cost SR/Ton	471.35	459	462.35	462
	S	%P	0.0	0.0	0.0	0.0
		Cost SR/Ton	450	450	450	450

It is observed from the cost analysis shown in Table 4.8 the following:

- There are four polymer options can be selected to achieve the targeted PG+ grades of asphalt binders used in the designed pavements. The selection of polymer type is controlled by required polymer content and polymer unit price.
- In all cases, crumb rubber modified asphalt binders at any targeted performance grade are more cost effective than other polymer type.
- PG 76(E) and PG 70(E) can only be fulfilled by adding 5.8% and 4.9% of SBS, respectively. While adding any content of CR, EE2 and PB do not improve the Jnr values and hence the measured PG traffic level (L_{PG}).
- No additive is required for PG 64(S), since the performance unmodified asphalt pavement at PG 64 and standard does not require any modification. While minor polymer contents are required to improve the asphalt performance grades from PG 64(S) to PG 64(H).
- Although the actual performance grade of asphalt binders is 64°C, polymer modification is required to enhance their elastic recovery at the targeted service temperature. This enhancement can be obtained by adding 3% or 5% or 2.2% or 2.5%, respectively.
- In all cases, crumb rubber modified asphalt binders at any targeted performance grade are more cost effective than other polymer type. While least required polymer contents are found for SBS.

CHAPTER 5:

Rutting and Fatigue Characterization of Polymer Modified Asphalt Concrete Mixes

5.1. Introduction

Thirty nine polymer modified asphalt mixes were prepared using four polymer types at different contents to satisfy the performance grades (PG^+). These asphalts were mixed with three different aggregate gradations to prepare Superpave wearing course blends. The performance of the modified asphalt mixes against rutting and fatigue are evaluated and related to their physical properties. Three evaluation processes are conducted including the dynamic modulus, rutting and fatigue resistance of asphalt mixes.

5.2. Superpave Mix Design of Asphalt Concrete Samples

Asphalt concrete samples were prepared and compacted using Superpave mix design procedures [AASHTO R35]. Volumetric properties of designed samples were measured and reported. Table 5.1 shows the results of the three control (unmodified) mixes used in this study. The optimum asphalt content of each mix was obtained at air voids (Av) of 4% as per Superpave procedure. This involves the calculation of bulk specific gravity of the three aggregate blends (G_{sb}), the bulk and maximum specific gravity of the mix (G_{mb} and G_{mm}), the resulted voids in mineral aggregates (VMA) and voids filled with asphalt (VFA).

Table 5.1Job mix formula of the three control (Unmodified) mixes in the study

Mix ID	P_{bi}	G_{sb}	G_{mm}	G_{mb}	Av %	VMA %	VFA %	OAC %
G1U64	4.2	2.61	2.46	2.3	6.61	15.63	57.69	4.8
G1U64	4.7		2.45	2.34	4.37	14.58	70.06	
G1U64	5.2		2.43	2.36	2.87	14.29	79.92	
G1U64	5.7		2.41	2.39	0.83	13.51	93.85	
G2U64	4.2	2.63	2.47	2.3	7.04	16.28	56.76	5.0
G2U64	4.7		2.46	2.34	5.18	15.33	66.2	
G2U64	5.2		2.45	2.37	3.1	14.57	78.73	
G2U64	5.7		2.42	2.39	1.24	13.69	89.19	
G3U64	4.2	2.65	2.52	2.27	10.06	17.96	43.99	5.2
G3U64	4.7		2.48	2.32	6.67	16.69	60.04	
G3U64	5.2		2.46	2.36	3.9	15.47	74.81	
G3U64	5.7		2.42	2.41	0.71	14.22	90.44	

Same procedure of mix design has been applied on the other combinations; the variables are polymer type, polymer content and gradations. It is found that higher optimum asphalt contents were required for (1) stiffer polymers (i.e. crumb rubber compared to Polybilt), (2) higher polymer contents (6% compared to 2%) and for higher contents of passing sieve no. 200 (gradation#3). Detailed volumetric properties of prepared mixes are presented in Appendix E In this research the effect of aggregate size and distribution in asphalt mix on the performance of the studied asphalt mixtures has been considered in the experimental design. The aggregate used in all mixes consists of 100% crushed limestone. The thirty nine different mix designs which were evaluated included aggregate having gradations that contained different quantities of aggregate sizes retained on sieve no. 3/8, 4, and 200. The asphalt content for all mixes was selected to provide an air voids content of four percent under a compactive effort in the gyratory machine following Superpave mix design method.

Test results indicated that mixes with larger aggregate designed with an air voids content of four percent were generally stronger that mixes prepared with smaller aggregate. The mixes with more content of course aggregate (retained on sieve no. 4) required lesser asphalt due to decreased total surface area of the particles.

5.3. Evaluation of Dynamic Modulus |E*|and Phase Angle φ to Predict Rutting

Three replicate specimens were used to generate a full catalogue of the dynamic modulus |E*| and phase angle δ when tested at four temperatures (20, 37.8 and 54.4°C) and four frequencies (0.1, 1, 5 and 10 Hz). Results of dynamic modulus and phase angle for the thirty nine mixes are shown in Appendix F. The aim of selecting 20°C for |E*| testing is to simulate the fatigue behavior of the mixture at intermediate temperature and 54.4°C was selected to evaluate the rut parameter ($|E^*|_{54.4°C,\ 5Hz}/\sin\varphi$) of the mixtures and to discuss any possible correlation with binders' rutting parameter like |G*| or/and Jnr. This parameter involves the phase angle φ in the evaluation and is expected to correlate well with binder and mix properties [AASHTO 1972]. Higher values of rutting parameter indicate that the mix can sustain the applied loads and resist rutting at high service temperatures and frequent traffic loading.

Figure 5.1 shows the rutting parameter of asphalt mixes grouped by their binders' high PG temperature while Figure 5.2 compares the same mixes but grouped by aggregate gradations. The effect of both factors (PG and Gradation) on of $|E^*|_{54.4°C,\ 5Hz}/\sin\varphi$ values are discussed.

Figure 5.1 shows and compares the effect of binders grades on rutting parameter ($|E^*|_{54C,\ 5Hz}/\sin\phi$) that predict the mechanistic properties of the mix to resist rutting. The descriptive statistics of the results for rutting parameter ($|E^*|_{54.4°C,\ 5Hz}/\sin\phi$) obtained

from PG 64-16, PG 70-16, PG 76-16, and PG 82-16 modified mixes are listed in Table 5.2. General observation can be found from this comparison that the mixtures had higher values of $|E^*|_{54.4°C,\ 5Hz}/\sin\phi$ when having higher PG grade.

One-way ANOVA test was conducted on all grouped values and it was found that the mean values are significantly different within 5% significance level.

Table 5.2Statistical results of mixes' rutting parameter for different PG grade

PG actual Temperature	Range (ksi)	Average (ksi)	Standard deviation
64.0 – 69.9	66.96 ~ 84.18	74.22	±8.92
70.0 – 75.9	129.11 ~ 249.57	183.28	±46.67
76.0 – 81.9	143.95 ~ 286.19	220.57	±55.40
82.0 – 87.9	152.24 ~ 363.33	242.53	±64.31

It can be concluded that polymer type and quantity is significantly affecting the stiffness of the binder (i.e. $G^*/\sin\delta$ and corresponding PG) and hence the concrete mixes. Results shown in Table 5.2 can be used as a guide to rutting parameter related to their PG actual temperatures.

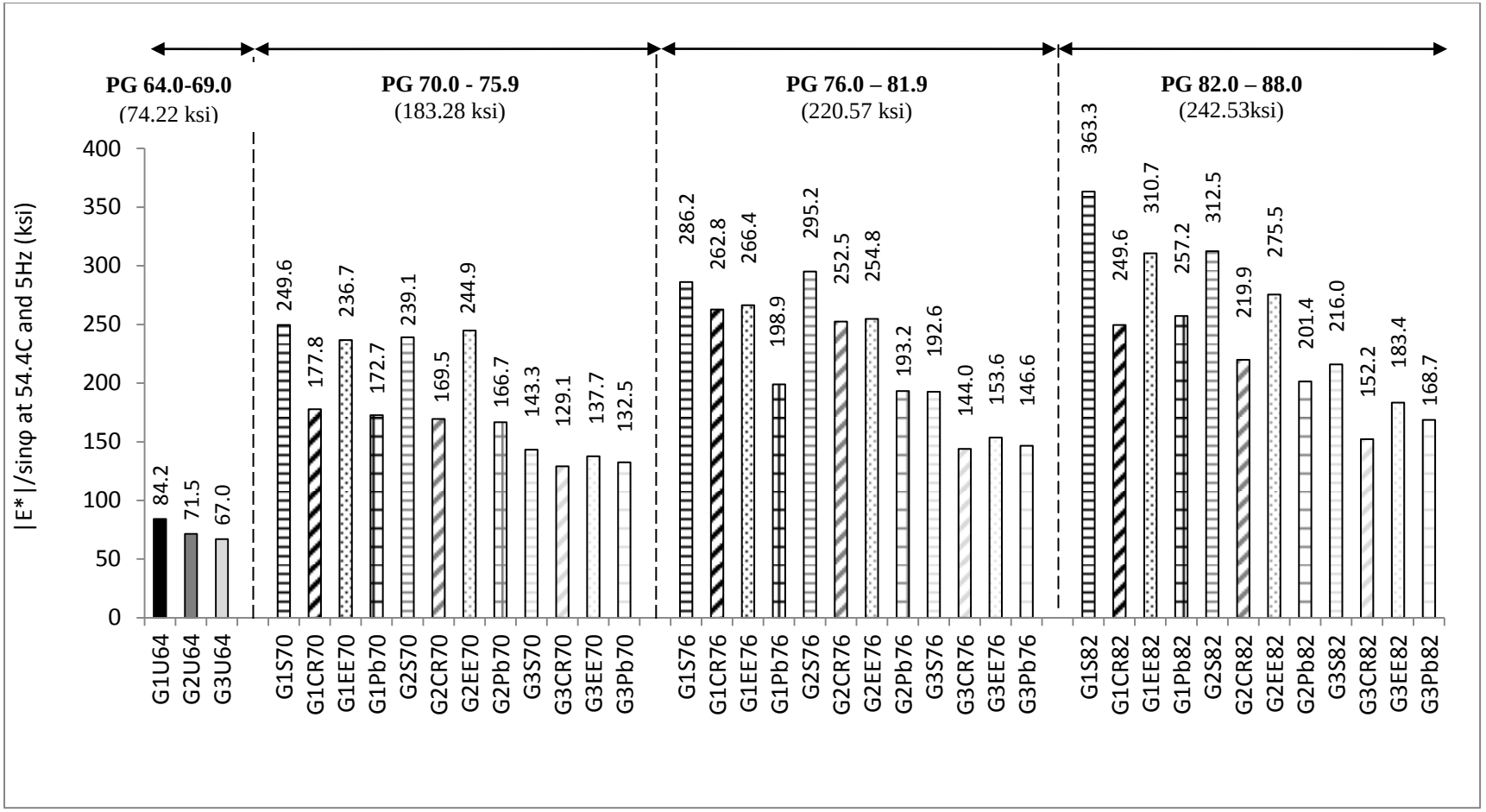

Figure 5.1Mixtures' Rutting Parameter Grouped by PG high temperature

Figure 5.1 summarizes the results of rutting parameter grouped by binder's PG grades. Actual performance temperature of asphalt binders were used to grouped the tested samples which have a range of 6°C. For example, samples graded at PG 70 could contain asphalt binders that have actual PG temperature ranges between 70.0 to 75.9°C; this applies to other PG grades.

SBS modified asphalt mixes have greater effect than other polymer types at all PG levels. EE2 and CR seem to have approximately similar effect, while PB is showing least effect on the modification of the mixes. Mixes contain higher contents of coarse aggregates showed higher values of $|E^*|/\sin\phi$ at same PG grade of asphalt binders, polymer type and polymer content. The highest value of rutting parameter was shown for 6% SBS modified asphalt mix prepared from coarser gradation (i.e. G1) this value reaches 363.3 ksi.

The second classification of the result was conducted based on aggregate blends. Table 5.3 summarizes the descriptive statistical results of this classification. For gradation#1, the average was (252.66 ksi) which is little bit higher than the case in gradation#2 (235.43 ksi). Significantly lower values of rutting parameters averaged by 158.30 ksi were obtained for gradation#3. It can be concluded from the one-way ANOVA that there are differences among the means at the 0.05 level of significance.

Table 5.3Statistical results of mixes' rutting parameter for different gradations

Gradation*	Range (ksi)	Average (ksi)	Standard deviation
G1	84.18 ~ 363.33	252.66	±54.12
G2	71.53 ~ 312.46	235.43	±46.84
G3	66.96 ~ 215.98	158.30	±26.66

* G1 represents the coarse aggregate blends followed by G2 and G3.

This difference could be due to higher amount of fine aggregates, specifically passing sieve No. 200 (ρ_{200}), and lower amounts of course aggregates (ρ_4) in the design of the aggregate structure when compared to gradation#2 and #3.

5.3.1. Effect of Mix Properties on Rutting Parameter |E*|/sinφ

Rutting performance of asphalt concrete mixes is affected by different variables. These variables are related to binders including the binder's rutting parameter (|G*|/sinδ) and non-recoverable creep compliance at high stress (Jnr). Aggregate sizes are considered in the comparison and correlation which includes passing sieve No.4 (ρ_4) and passing sieve No. 200 (ρ_{200}) which represents the limits of coarse and fine aggregate sizes in the three graduations, respectively. Finally, overall mix properties are also involved by including the voids filled with asphalt (VFA) and voids in the mineral aggregate (VMA).

Pearson correlation (PC) method was selected to find the most affecting factors on rutting parameters. A correlation coefficient (PCC) and significance level (p-value) are obtained between |E*|/sinφ and all parameters involved in the correlation. Table 5.4 shows the PCC and p-values for all included variables in the correlation. The PCC value ranges from -1 to -1, with 0 meaning absence of linear correlation. Negative value of PCC indicates an inverse variation, while positive PPC value means a direct

proportional variation. The closer the absolute value of PCC to 1, the stronger the correlation. Absolute value of PCC below 70% is considered weak correlation. P-value above 5% implies absence of statistical evidence that linear correlation exist between the paired parameters.

Table 5.4Pearson Correlation Coefficients to predict Rutting Parameter

	PG	%P	P	G*/sinδ	Av	VMA	VFA	Pbe/filler	H
PCC	0.663	0.406	0.154	0.618	*	0.191	0.154	0.790	0.609
p-value	0.005	0.01	0.761	0.000	*	0.243	0.349	0.004	0.01

* Constant variable for all mixes

PG is the actual performance temperature of asphalt binders, which covers the effect of %P and G*/sinδ on mix properties. Air voids content (Av) has no effect on rutting parameters because all samples were designed at constant value of 4% as per Superpave mix design [AASHTO R 35].

A linear regression model is attempted to predict the rutting parameter from the above mentioned parameters as shown in Equation 5.1 and the statistical analysis of the generated model is presented in Tables 5.5 and 5.6. Only significant independent variables were considered in the equation (i.e. p-value ≤ 5%).

$$E^*/\sin\phi = -651 + 10.8\,T_{PG} - 7.65\,\%P - 3.96\,\rho4 + 4.74\,VMA - 84.2\,Pbe/f \quad (5.1)$$

Where:

|E*|/sinϕ: is the mix's rutting parameter obtained at 54.4°C and 5Hz (as per standard)

T_{PG}: is the actual service temperature at targeted PG grade, °C

%P: is percent of polymer from binders' weight.

VMA: is the Voids in Mineral Aggregates (%)

ρ4; is the content of coarse aggregate in the mix (%)

Pbe/f: is ratio between effective binder content and filler content

All studied variables have an effect on the rutting parameter of the mix. The analysis of variance (ANOVA) of the created model is shown and summarized in Table 5.5

Table 5.5ANOVA results for the model

Source	DF	SS	MS	F	P
Regression	5	99366	19873	8.12	0.000
Residual Error	33	80779	2448		
Total	38	180154			

Although viscosity of modified asphalt binders has good correlation coefficient and significant p-value, its contribution did not improve the overall correlation model.

The p-value of the model obtained from F-test is less than 0.05 which indicates a significant prediction of $|E^*|/\sin\varphi$ from the selected predictors (variables). The determination coefficient (R^2) of this model is 0.852 which is very good.

5.3.2. |E*| Master Curves

Asphalt mixtures dynamic moduli |E*| obtained at various temperatures and frequencies are shifted horizontally using Arrhenius equation (time-temperature principle) which and combined into a master curve. The shifted dynamic modulus curves can be modeled by Sigmoidal function. Figure 5.2 shows typical master curve and its components.

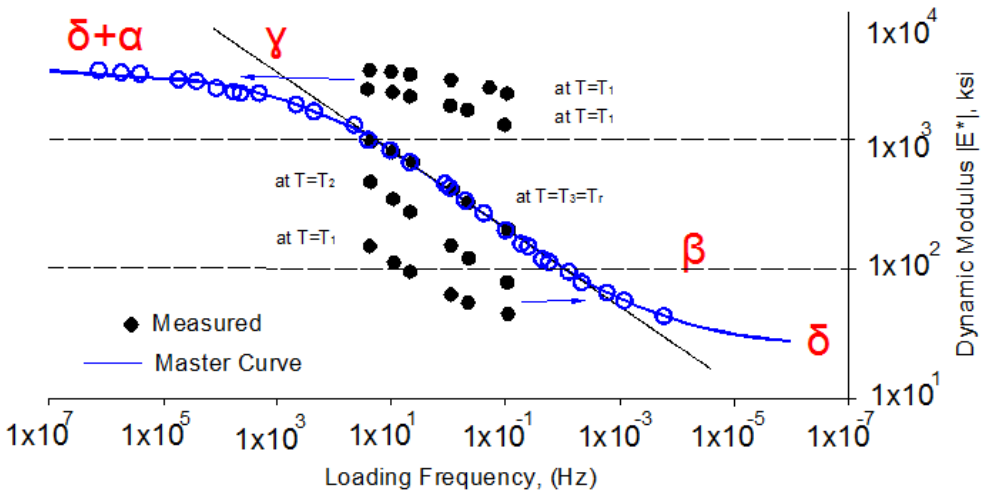

Figure 5.2Typical Master curve

The lower and upper limits of the master curve are described by α+δ and δ, respectively. This corresponds to the dynamic modulus of asphalt mixtures at low frequency/high temperature (lower bound) and high frequency/low temperature (upper bound) testing conditions. The upper bound of the Sigmoidal curve is the maximum modulus of the mixture, which is dependent on the limiting stiffness of the binder at low temperatures [Pellinen, Witczak, AAPT 2002].In this study all the mixtures had the same low temperature binder grade of -16ºC. Therefore, as expected, all the master curves seem to converge at the upper end (corresponding to low temperature/high frequency test condition) of the graph. At the lower bound, compressive loading at high temperature causes the binders' stiffness and aggregate blends to be more dominant.

Mixture samples contain PG 82 asphalt binders have shown higher dynamic modulus at any frequency level, this resulted due to stiffness significant improvement of the binder that resist the applied dynamic loading. Some PG 76 mixes showed lower dynamic modulus than PG 70 and happened because of one of two reasons; weaker aggregate gradation or/and softer asphalt binder involved in the modification. Table 5.6

summarizes master curves parameters and classifies them based on performance grade of the asphalt binders

Table 5.6Ranges of the master curve parameters

Parameter	64.0 – 69.9	70.0 – 75.9	76.0 – 81.9	82.0 – 87.9
δ	0.440 ~ 1.44	0.907 ~ 1.545	0.915 ~ 1.594	1.122 ~ 1.683
$\alpha+\delta$	3.37 ~ 3.45	3.49 ~ 3.57	3.58 ~ 3.63	3.65 ~ 3.77
β	-1.214 ~ -0.241	-0.905 ~ -0.373	-0.968 ~ -0.336	-1.317 ~ -0.320
γ	0.557 ~ 0.604	0.580 ~ 0.740	0.573 ~ 0.738	0.470 ~ 0.803

Similar comparison is discussed when results are classified based on aggregate gradation included in asphalt mixtures as shown in Figures 5.3 to 5.5. When the effect of aggregate gradation is separated from the comparison, the effect of binders dominates.

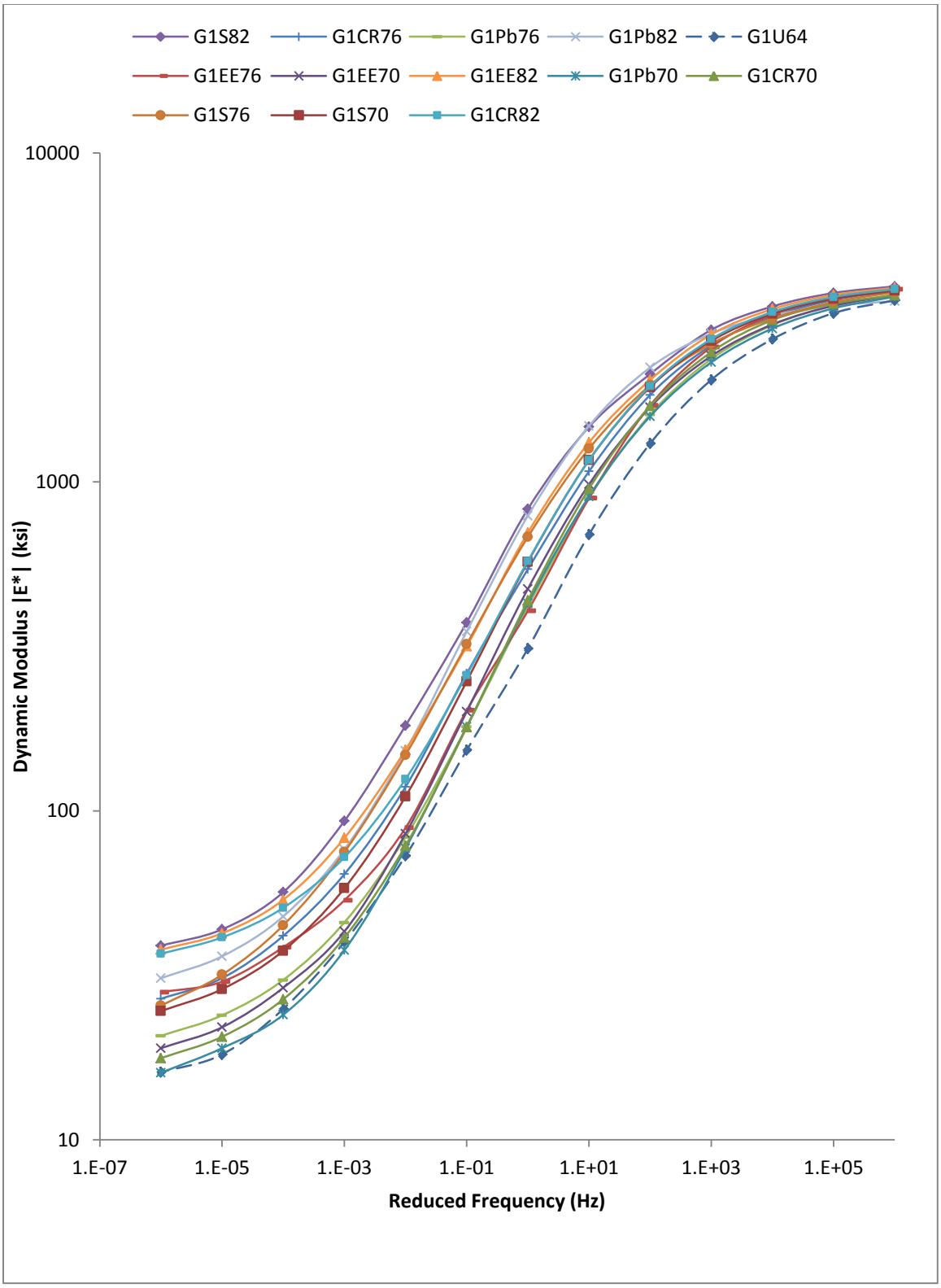

Figure 5.3Dynamic Modulus Master Curves for Mixes have gradation#1

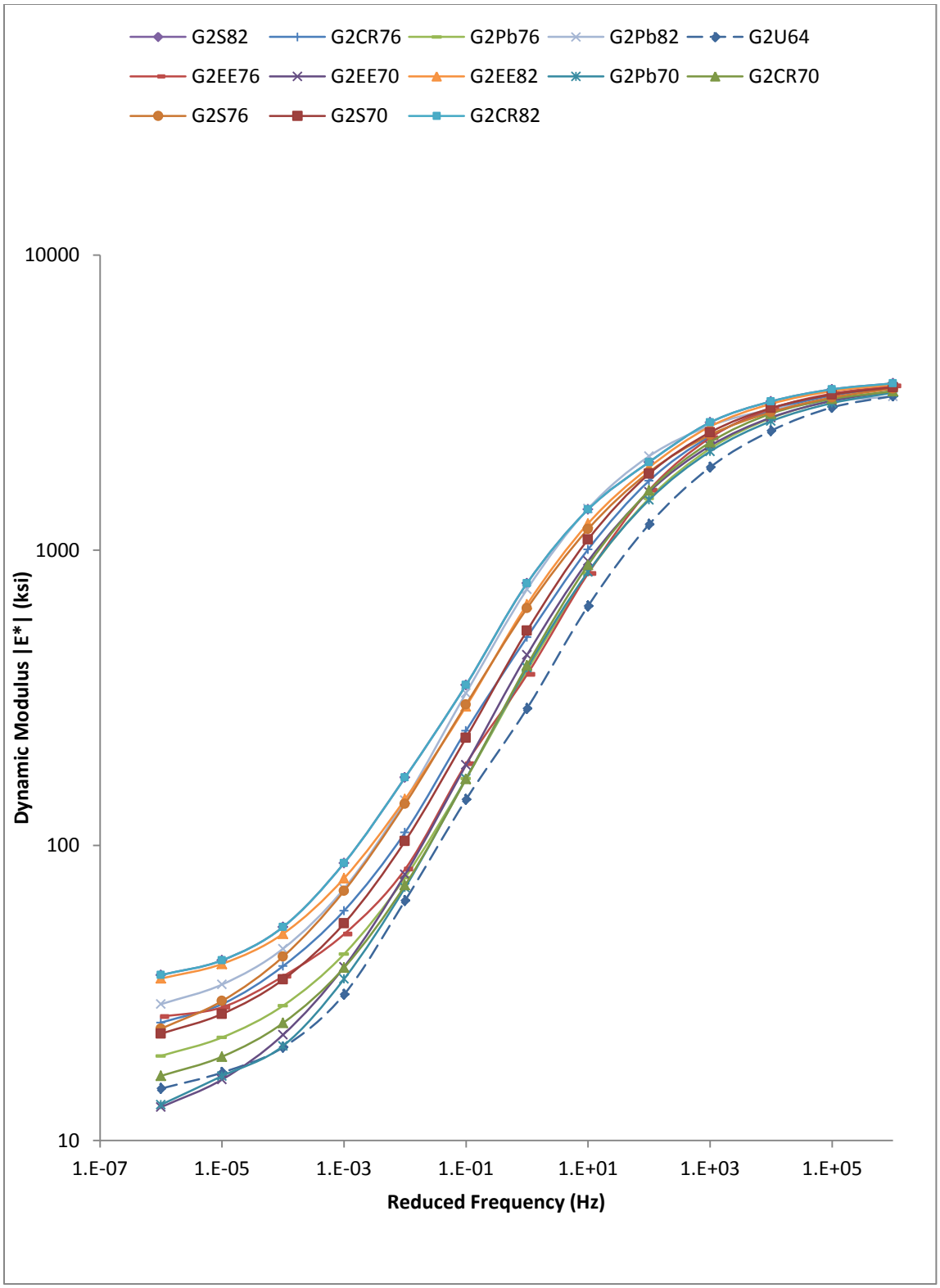

Figure 5.4Dynamic Modulus Master Curves for Mixes have gradation#2

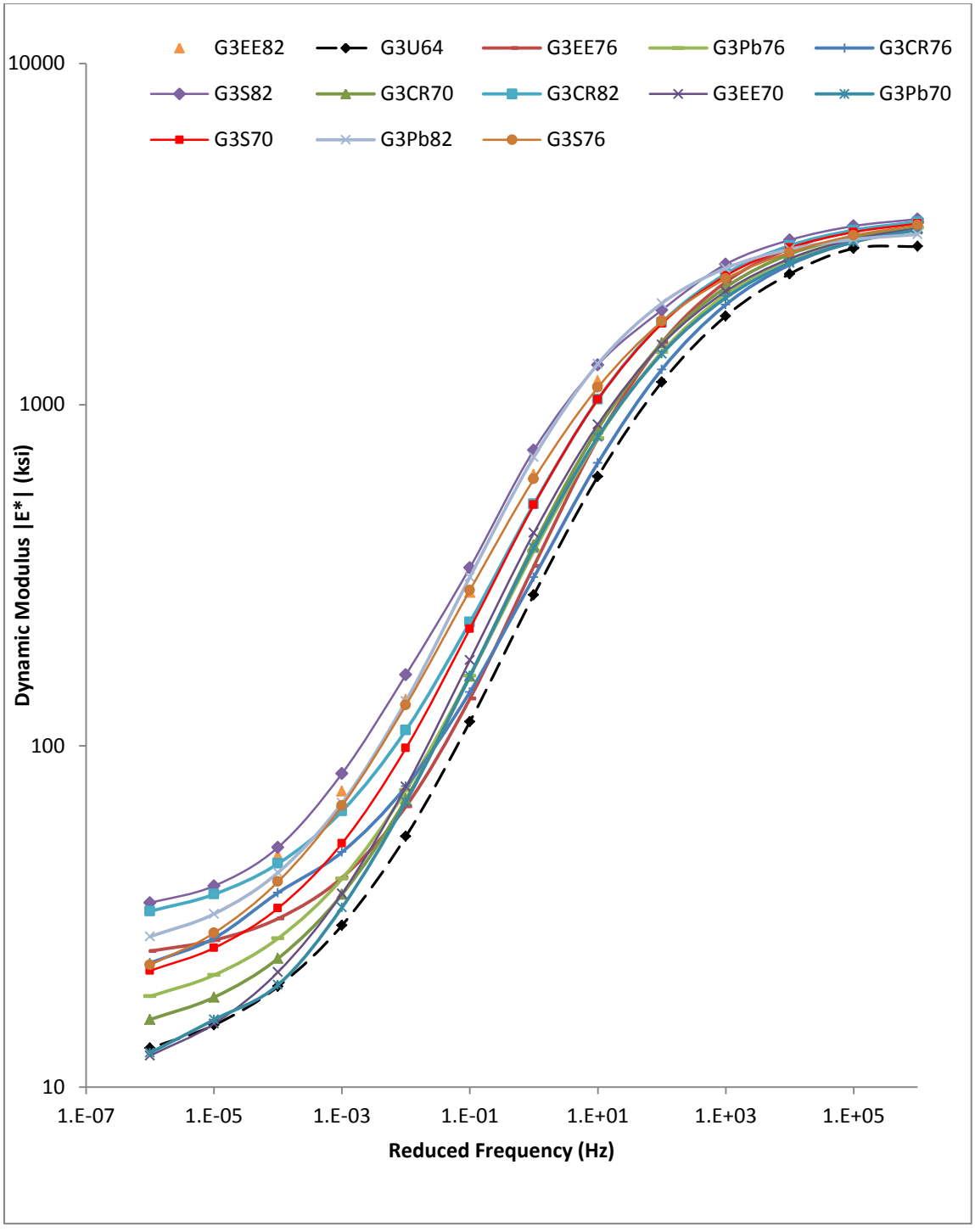

Figure 5.5Dynamic Modulus Master Curves for Mixes have gradation#3

In order to capture the difference between the three gradations mixes, comparison of their master curves' parameter are classified based on gradation level (i.e. G1, G2 and G3) as shown in Table 5.7.

Table 5.7Ranges of master curve parameters

Parameter	Gradation #1	Gradation #2	Gradation #3
δ	0.915 ~ 1.683	0.907 ~ 1.439	0.887 1.232
α+δ	3.7 ~ 3.8	3.5 ~3.6	3.4 ~3.5
β	-1.010 ~ -0.320	-0.794 ~ -0.110	-0.681 ~ -0.055
γ	0.573 ~ 0.803	0.583 ~ 0.728	0.612 ~ 0.933

The dynamic modulus |E*| and its master curve was selected as a material characterization input in the Mechanistic Empirical Pavement Design Guide (MEPDG) [NCHRP Project 1-37A]. The importance of data input is classified into three levels. Level-1 requires specific laboratory testing on asphalt concrete mixes. While information for Level-2 data can be estimated for locally predicted models along with lab measured binder properties. In Level -3, default values are used.

These parameters can be used as a Level-2 data input the current Mechanistic-Empirical Pavement Design of pavement structures, at which data are obtained for local material and for field quality control of the mixtures. So, the dynamic modulus master curve constructed from values obtained from the laboratory testing or from predictive equations is utilized in the MEPDG to account for temperature and rate of loading effects of asphalt mixtures at all analysis levels [AASHTO 2002].

Recent research work discussed the actual effect of these parameters and found that those parameters δ and α, depend on aggregate gradation and air void content, whereas β and γ depend on the characteristics of the asphalt binder and the magnitude of δ and α.

Parameter βdetermines the horizontal location of the transition zone and parameter γ determines the slope. The shift factors describe the temperature dependency of the modulus [Witczak et al 2002].It can be shown from Table 5.7 that samples of gradation#1 has higher range of δ (0.915 ~ 1.683) and α+ δ (3.7 ~ 3.8) when compared to the other two gradation mixes.

5.3.3. Prediction of Dynamic Modulus |E*|.

A correlation of the predicted and the measured values of the dynamic modulus were statistically evaluated. The correlation coefficient(r) which measures the prediction accuracy was used. A scatter-plot of laboratory measured dynamic moduli and the predicted values are presented in Figure 5.6.

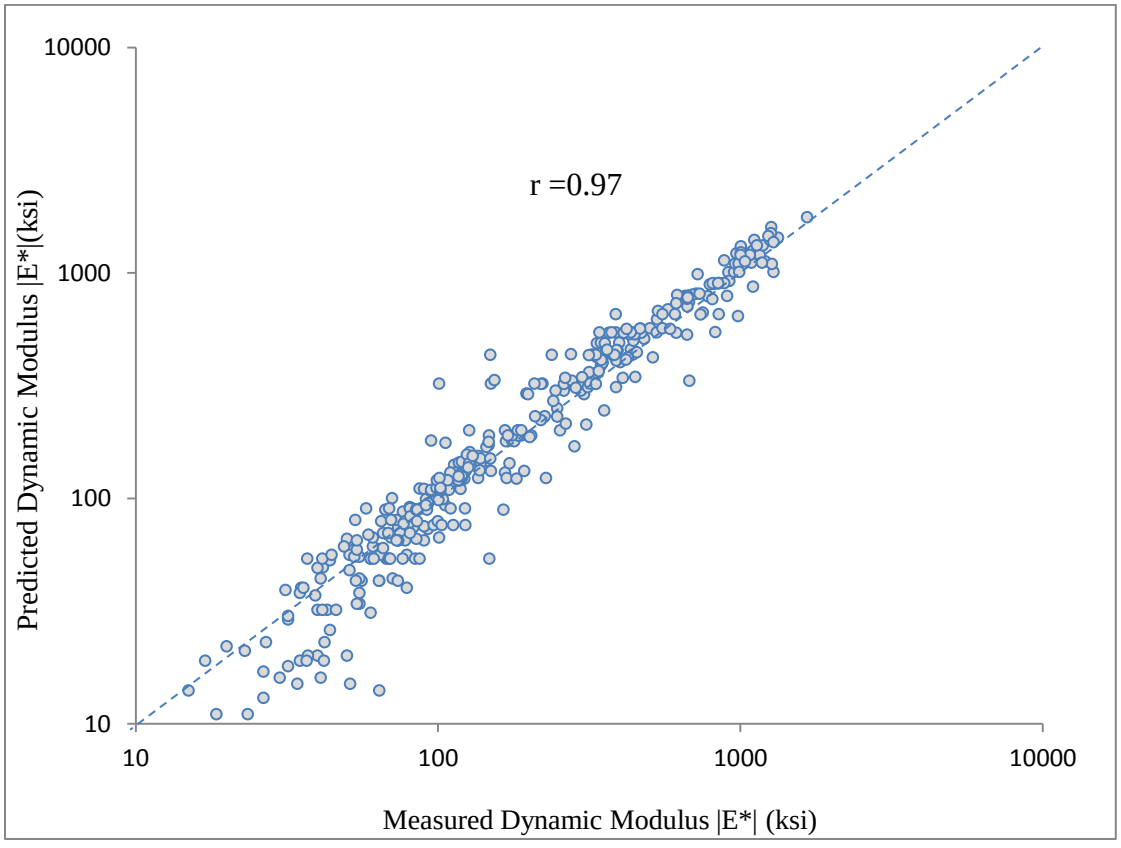

Figure 5.6Predictions vs. Measured values for all mixtures in log-log scale

It was observed that the coefficient of determination (R^2) was 0.952 which indicates to an excellent correlation between the measured and predicted values. It can be concluded from the slope of the regression line that the predicted values are 7% higher than the measured. Witczak model performed well in predicting the dynamic modulus |E*| of polymer modified asphalt mixtures tested in this study. It is important to mention that Dynamic modulus test requires skilled personnel to mix and compact the AMPT samples at correct optimum asphalt content and targeted voids, to assemble the compacted specimens with membrane to insure full confinement of the sample.

The outcome of this study is important in estimating |E*| values of local hot asphalt mixes and the resulting master curves could be used as level-2 input in MEPDG packages of pavement structural design by local agencies.

It can be found from previous discussion that better correlation for higher PG (i.e. 82 then 76 etc.) which can be explained by the significant effect of polymer modified asphalt on the mixes at higher contents which reach up to 6% for SBS, EE2and PB and 10% for CR. As a summary, Witczak prediction model can be used to estimate the dynamic modulus of polymer modified asphalt binders as a MEPDG level-2 data input in addition of using the master curves as level-1 provided that the same local material is used in the design.

5.4. Rutting Resistance of Asphalt Mixes using Asphalt Pavement Analyzer (APA)

Prediction of rutting performance of asphalt concrete has been a complicated task. In this research, a simple method of measuring rut depths of laboratory hot asphalt mixes using Asphalt Pavement Analyzer (APA) was carried out. In the APA, rutting resistance are evaluated by subjecting laboratory prepared specimens to three moving wheel and

measuring the permanent deformation in millimeters under applications of 8,000 wheels cycles.

The intention of using APA test method is to simulate field conditions pavement service temperature, wheel loads and wheel pressure. Series of rut-depth tests has been performed on modified and unmodified mixes and then ranked based on their rut potentials. Binders' properties (PG grade and Jnr), aggregate gradation (ρ_4 and ρ_{200}) in addition to mix properties (VMA and VFA) were studied to find out their effect on APA rut depths. Also, the correlation between mix rutting parameter $|E^*|_{54.4C,\ 5Hz}/\sin\phi$ and APA rut depths was examined for thirty nine mixes.

Six cylindrical samples of polymer modified asphalt concrete are compacted using the Superpave Gyratory Compactor, the final dimensions of the samples are 75 mm in height and 150mm in diameter and targeted air void of 7±1% which typically represents the field compacted pavement layers during its initial life. Compacted cylindrical samples were conditioned at testing temperature (i.e. 64°C) for10 hours before testing. A total of ninety specimens are prepared and tested for rut depth at 8000 loading cycles. Tables 5.8 to 5.10 summarize the results of rut depths of all tested samples. Figure 5.7 shows the results of rut depth at 8,000 load cycles for some mixes containing various modified and unmodified binders. Some modified binders showed rut depths of less than 1 mm. Only unmodified mixes showed more than 5 mm rut depths.

For the modified mixes, it can be shown that more than 60% of the final rutting occurs within 1,000 loading cycles. The comparative initial higher rate of rutting is attributed to the initial compaction or densification of the materials at that temperature and applied pressure. When the initial densification is completed, the rate of permanent deformation,

explained the slope of the curve, significantly decreases with the increase in loading cycles for each mixture.

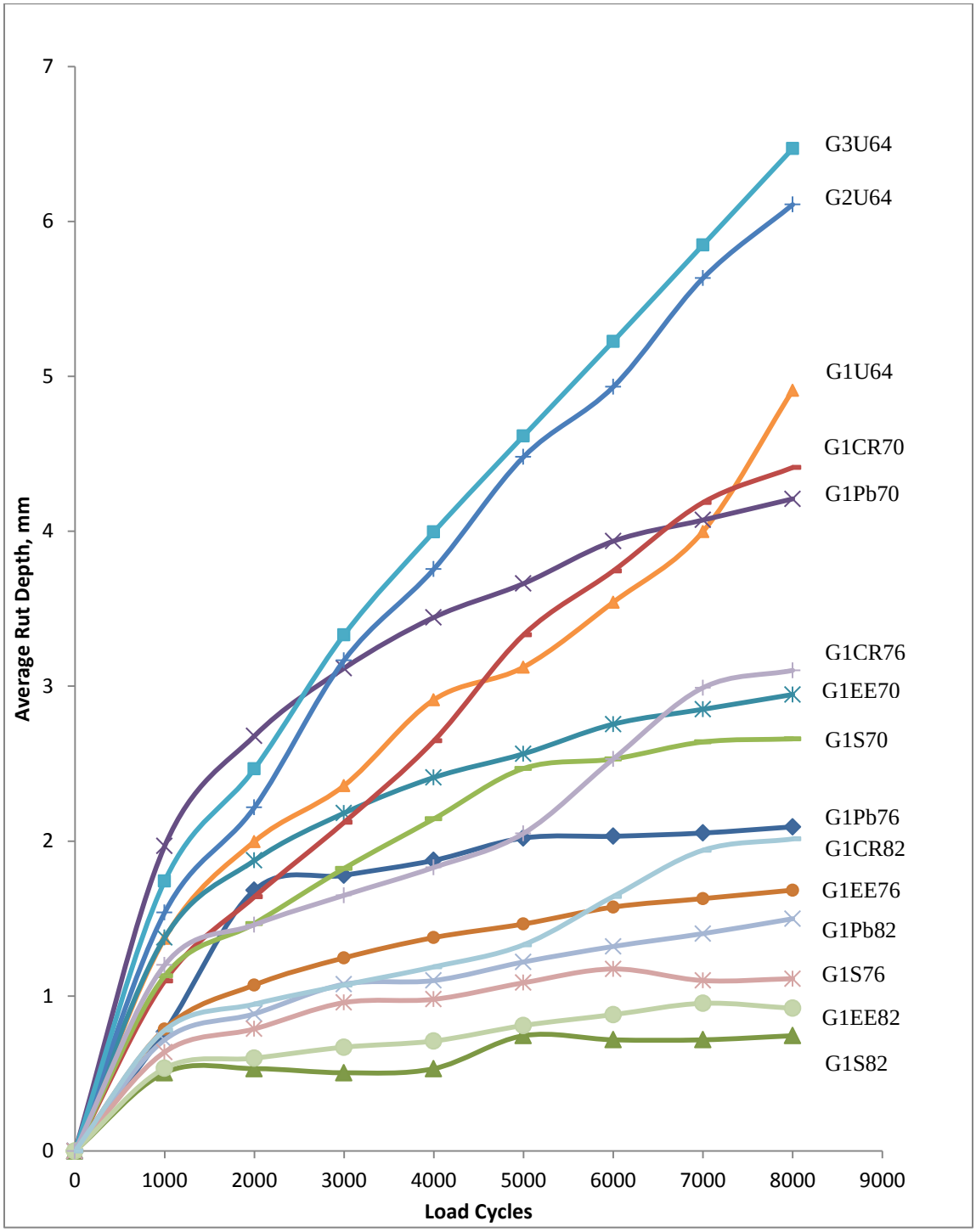

Figure 5.7Typical Rut Depth versus Load Cycle

The slope of rutting curves in the range of 2000 cycle to 8000 cycles is nearly equal far all mixes except for unmodified ones (PG 64-16). Therefore, it can be concluded that the major difference in final rut depth is due to the densification of materials and not by plastic flow at higher cycles. According to Superpave mix design, the plastic flow of asphalt pavement is likely to start once the air voids reach to approximately 2% [AASHTO R 35].

Table 5.8Rut Depths for gradation#1 mixes

AC	PG	Rut Depth (mm)				
		Wheel 1	Wheel 2	Wheel 3	Avg.	Stdv
G1U	PG 64	6.54	4.37	4.43	4.942	1.400
		4.48	6.71	3.12		
G1SBS	PG 70	2.02	2.89	2.23	2.993	0.802
		4.17	3.51	3.14		
	PG 76	1.18	1.53	1.47	1.674	0.597
		2.62	2.16	1.09		
	PG 82	0.34	0.77	0.70	0.702	0.251
		1.07	0.81	0.52		
G1CR	PG 70	3.58	5.28	2.95	4.022	0.809
		4.40	3.65	4.27		
	PG 76	2.36	4.87	1.78	3.563	1.420
		3.99	3.01	5.37		
	PG 82	1.70	0.32	1.78	1.823	1.249
		0.98	2.17	3.99		
G1EE	PG 70	3.05	4.08	2.98	3.176	0.686
		3.16	3.71	2.08		
	PG 76	2.16	1.35	1.55	1.419	0.431
		0.89	1.42	1.14		
	PG 82	0.94	1.66	1.41	1.01	0.429
		0.62	0.77	0.66		
G1Pb	PG 70	3.51	4.02	3.79	3.568	0.284
		3.48	3.36	3.26		
	PG 76	1.96	3.77	1.39	2.689	0.961
		2.92	2.39	3.72		
	PG 82	1.38	0.38	1.58	1.475	0.675
		1.37	1.67	2.48		

Table 5.9Rut Depths for gradation#2 mixes

Mix Code	PG	Rut Depth				
		Wheel 1	Wheel 2	Wheel 3	Avg.	Stdv
G2U	PG 64	6.54	7.37	4.43	6.107	1.035
		5.48	6.71	6.11		
G2SBS	PG 70	2.21	2.89	2.63	3.078	0.687
		3.89	3.91	2.94		
	PG 76	1.94	2.05	1.53	1.952	0.274
		2.31	1.77	2.11		
	PG 82	1.10	0.73	0.59	0.905	0.480
		0.33	0.97	1.71		
G2CR	PG 70	4.34	6.04	3.71	4.782	0.809
		5.16	4.41	5.03		
	PG 76	3.12	5.63	2.54	4.323	1.420
		4.75	3.77	6.13		
	PG 82	2.46	1.08	2.54	2.583	1.249
		1.74	2.93	4.75		
G2EE	PG 70	3.41	2.73	4.61	3.093	0.849
		2.54	3.05	2.22		
	PG 76	1.53	2.65	0.97	1.795	0.557
		1.83	1.74	2.05		
	PG 82	1.03	0.42	1.36	1.11	0.440
		1.74	1.14	0.95		
G2Pb	PG 70	3.88	4.39	4.16	3.938	0.284
		3.85	3.73	3.63		
	PG 76	2.33	4.14	1.76	3.059	0.961
		3.29	2.76	4.09		
	PG 82	1.75	0.75	1.95	1.845	0.675
		1.74	2.04	2.85		

Table 5.10Rut Depths for gradation#3 mixes

Mix	PG	Rut Depth				
		Position 1	Position 2	Position 3	Avg.	Stdv
G3U	PG 64	6.54	5.89	7.42	6.615	0.567
		7.02	6.71	6.11		
G3SBS	PG 70	3.12	2.13	2.97	2.761	0.513
		3.43	2.22	2.69		
	PG 76	1.28	1.04	1.34	1.683	0.593
		1.72	2.63	2.09		
	PG 82	0.62	0.94	1.07	0.984	0.253
		1.16	0.79	1.32		
G3CR	PG 70	4.83	3.57	4.62	4.092	0.652
		3.12	4.00	4.40		
	PG 76	1.11	3.03	2.77	2.653	0.833
		3.20	3.40	2.41		
	PG 82	3.36	1.12	1.35	1.614	1.056
		1.06	2.36	0.44		
G3EE	PG 70	4.10	5.13	4.03	4.226	0.686
		4.21	4.76	3.13		
	PG 76	3.21	2.40	2.60	2.469	0.431
		1.94	2.47	2.19		
	PG 82	0.99	1.71	1.46	1.21	0.361
		1.33	1.04	0.71		
G3Pb	PG 70	6.33	5.91	5.49	5.549	1.483
		5.24	2.94	7.38		
	PG 76	4.82	3.52	3.90	3.883	0.660
		2.94	4.39	3.72		
	PG 82	1.04	2.24	1.16	2.224	1.005
		3.33	3.36	2.21		

To properly analyze the results of rut depths, samples are grouped based on their PG grades and aggregate gradations. Figure 5.6showsa histogram comparison of all mixes based on PG and Gradations. No specific threshold rut depth value has been developed to classify an asphalt mix as poor or good, but a maximum of 14.0 mm rut depth is used. Currently, some agencies and department of transportation have considered a rut depth limit of 6.0 mm for asphalt mixes subjected to 0.3-3.0 millions ESALs [OHD L-43, 2002]a threshold between poor and good mixes.

All polymer modified mixes (36 mixes) are good in resisting rutting at service temperature of 64°C. On the hand, unmodified mixes of different aggregate structures have shown poor rutting resistance. It was evident that polymer modification has significant effect more on rutting and the Asphalt Pavement Analyzer (APA) can be used for screening of poor mixtures. That is, the APA can be used as proof tester for HMA mix.

Figure 5.8 shows the effect of asphalt grade on resulting rut depth. It is shown that polymer modification has significant effect in improving rutting resistance of the mix. This agrees with what is expected from the Superpave binder's specification point of view on using modification. Polymer type and content are affecting the stiffness of the overall mix, and hence reducing the densification and compaction of asphalt concrete mixes. The average rut depth of modified mixes was 5.89, 3.77, 2.6 and 1.46 mm for samples containing asphalt with PG 64, PG 70, PG 76 and PG 82, respectively.

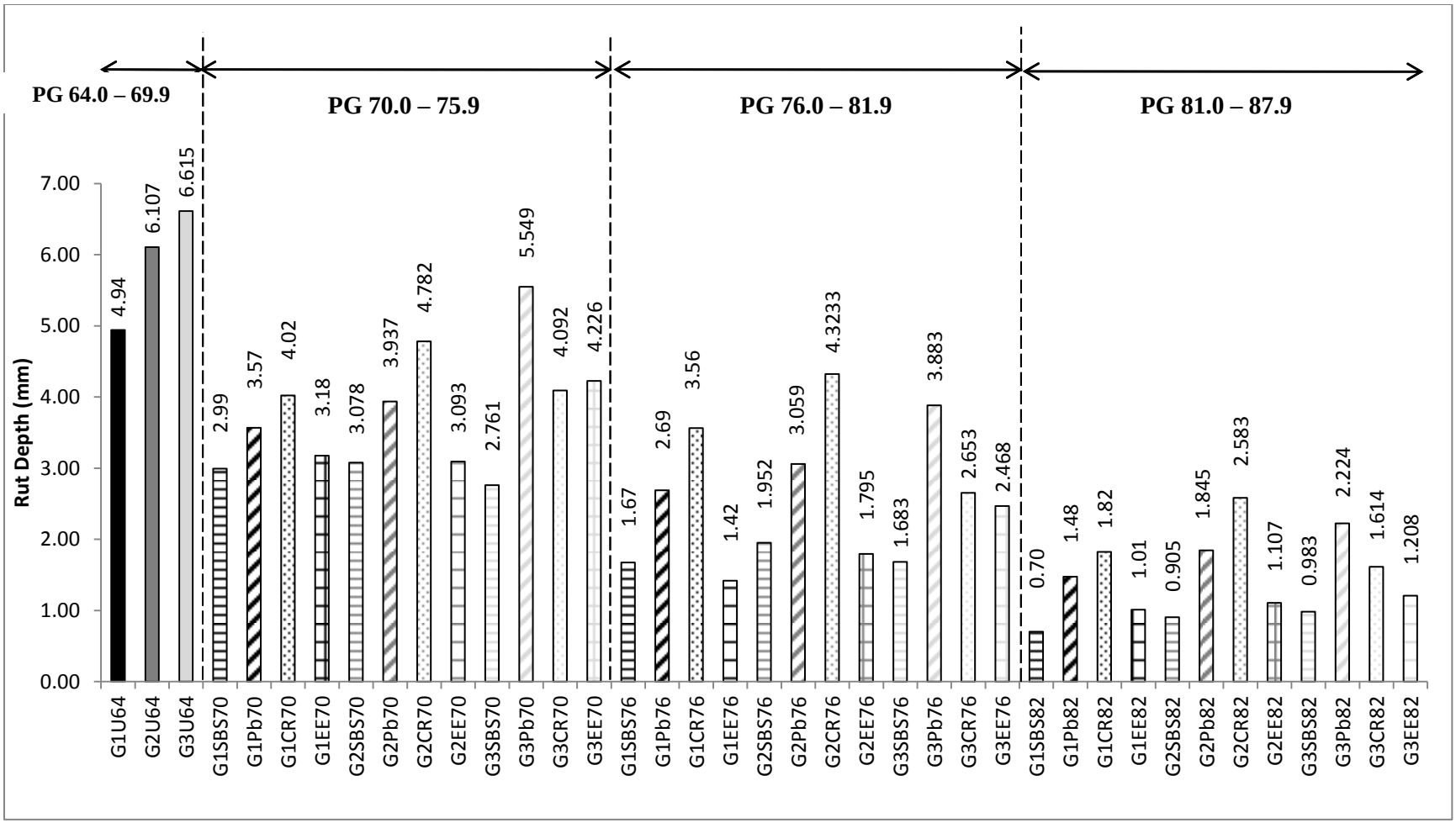

Figure 5.8Rut Depth results grouped based on PG grade of asphalt binders

The average rut depth was 2.54, 2.97 and 3.07 mm for mixes prepared from gradation#1, #2 and #3, respectively. Samples produced from G1 aggregate showed better rutting resistance than G2 and G3 mixes due to higher content of large aggregated and lower content of filler in the mix. In general, large aggregates tend to reduce particle movement within pavement layer and hence resist more loads. It is also contains more friction surfaces than small particles which enhance the shear resistance of asphalt mixes.

EE2 and SBS modified asphalt mixes showed lower rutting than PB and CR regardless of polymer content and aggregated gradation. The lowest rutting depths are shown for mixes contain 6% of SBS modified asphalt binders. The results are 0.7, 0.905 and 0.983 for gradation#1, #2 and #3, respectively. On the other hand, using PB with gradation#3 produces a weak mixes against rutting with rut depth of 5.5 mm.

5.4.1. Rut Depth Prediction model

Regression models are developed to predict Rut Depth (RD) from mix properties which include binders parameters (viscosity, effective asphalt content, actual PG temperature, $|G^*|_{64°C,\ 1.57Hz}/\sin\delta$ and Jnr), aggregate gradation (ρ4 and ρ200) and mix mechanical properties (Av, Pbe/f, $|E^*|_{54.4°C,\ 5Hz}/\sin\varphi$, VMA and VFA). A single independent variable, when used to predict rut potential, is shown to give poor prediction. For example, the amount of air void is likely to be the most important physical property of asphalt mixes that relates to rutting (Brown et al., 1989). Figures 5.9 and 5.10 show the correlation between rut depth and mix rutting parameter $|E^*|/\sin\varphi$. There is a negative relationship with good significance (R^2= 0.62) between the two parameters.

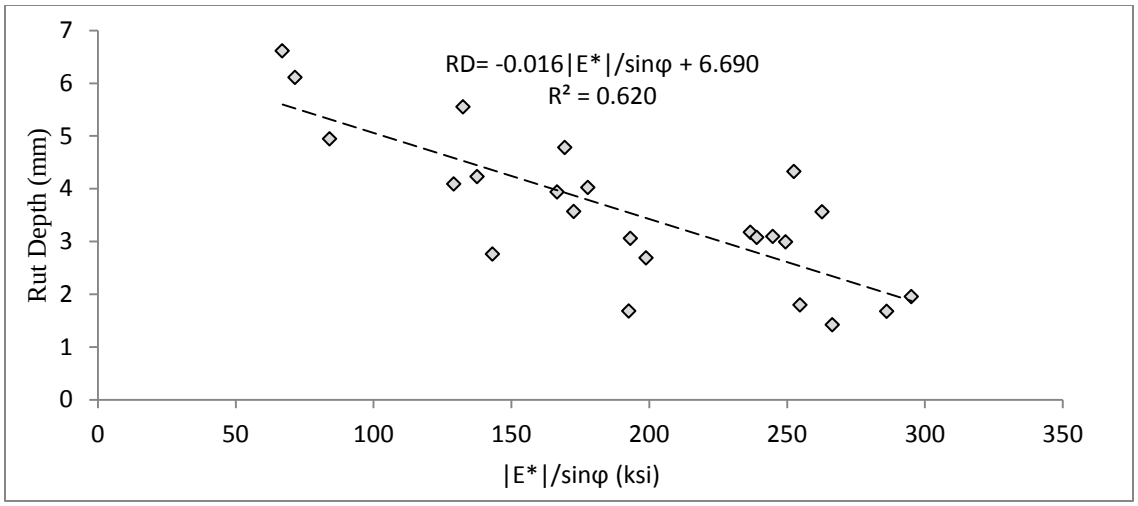

Figure 5.9Effect of Mix rutting parameter on Rut Depth

Figure 5.8 compares the rut depths results with binders' rutting parameter which has R^2 of 0.527.

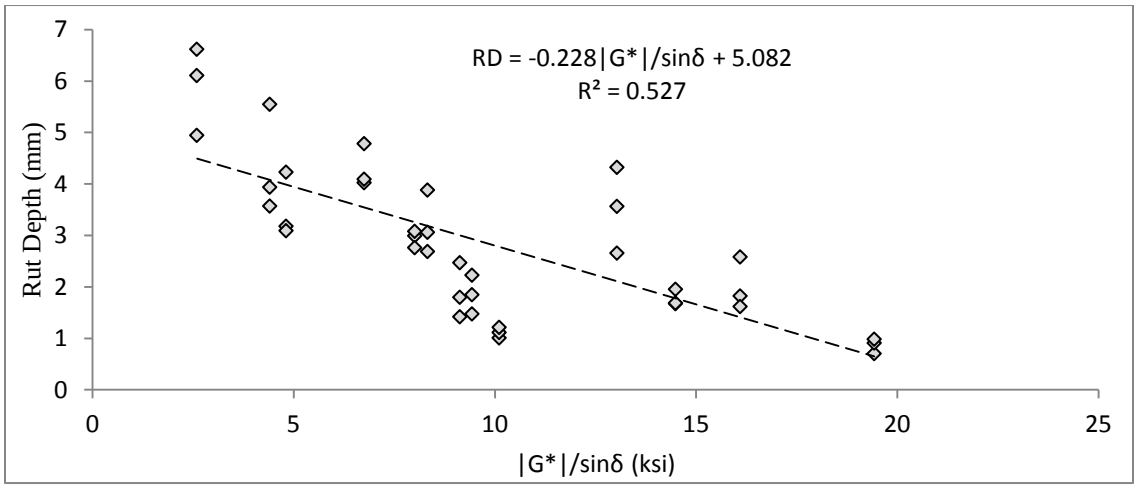

Figure 5.10Effect of Binder's rutting parameter on Rut Depth

The rut depths of polymer modified asphalt mixes generally decreases with increasing rut factor (|G*|/sinδ) and increasing of coarse aggregate content (ρ_4). The non-recoverable creep compliance (Jnr) was intended to explain the mechanism of reducing the rut depths for polymer modified asphalt mixes.

A total of 39 sets of data are used to develop a stepwise Linear Multiple Regression analysis. In this method (stepwise), the best correlated independent variable was first included in the model and the remaining variables are added according to their performance (R^2 and p-value) in the model. Minitab software package was used to perform this analysis.

Table 5.11Pearson correlation coefficients for Rut Depth prediction

	PG	%P	P	G*/sinδ	Av*	VMA	VFA	Pbe/filler	η	|E*|/sinφ
PCC	-0.881	-0.558	0.04	-0.426	0.00	-0.100	-0.056	-0.797	-0.57	-0.722
p-value	0.001	0.060	0.743	0.08	1.00	0.547	0.737	0.030	0.07	0.04

*constant variable

It was found that two parameters are better correlating with rut depth (RD); these two factors are actual performance temperature (PG) of the modified binders and the ratio between effective binder content and weight of material passing sieve no. 200 (Pb_e/f). Regression analysis is repeated on those two variables and a better model is generated in Equation 5.2.

$$RD = 36.6 - 0.316\ T_{PG} + 0.265\ \%P - 0.0375\ \rho4 - 0.0989\ VMA - 1.27\ Pbe/f \qquad (5.2)$$

Where:

RD: is rut depth in mm tested at 64°C and 8,000 cycles.

T_{PG}: is the actual service temperature at targeted PG grade, °C

%P: is percent of polymer from binders' weight.

VMA: is the Voids in Mineral Aggregates (%)

ρ4; is the content of coarse aggregate in the mix (%)

Pbe/f: is ratio between effective binder content and filler content

Statistical results of F-test are shown in Table 5.12.

Table 5.12ANOVA results of the developed model

Source	Df	SS	MS	F	P
Regression	5	72.75	14.55	40.48	0.00
Residual Error	33	11.862	0.359		
Total	38	84.61			

As shown from the ANOVA analysis of the generated model, the value of R^2 of 0.86means that about 86.0% of the variation in RD can be explained or accounted for by the estimated. Standard Error of Estimate S = 0.599 means that, on an average, the predicted values of the RD can vary by ±0.71 about the estimated regression equation for each value of independent variables during the sample period and by a much larger amount outside the sample period.

Each polymer has different physical properties that define its behavior when used in the modification of asphalt concrete mixes. Figure 5.11 shows a comparison between laboratories measured values of rut depth at 64°C and predicted values from Equation (5-2). Table 5.13 shows results of predicted and measured values of rut depths.

Table 5.13 Measured vs Predicted rut depths

Mix	Measured	Predicted	Mix	Measured	Predicted	Mix	Measured	Predicted
G1U64	4.94	5.75	G2U64	6.11	5.98	G3U64	6.62	6.04
G1S70	2.99	3.33	G2S70	3.08	3.55	G3S70	2.76	3.62
G1CR70	4.02	3.49	G2CR70	4.78	3.75	G3CR70	4.09	3.82
G1EE70	3.18	3.75	G2EE70	3.09	3.96	G3EE70	4.23	4.05
G1Pb70	3.57	4.38	G2Pb70	3.94	4.61	G3Pb70	5.55	4.68
G1S76	1.67	1.73	G2S76	1.95	1.96	G3S76	1.68	2.03
G1CR76	3.56	2.30	G2CR76	4.32	2.57	G3CR76	2.65	2.64
G1EE76	1.42	1.94	G2EE76	1.80	2.16	G3EE76	2.47	2.25
G1Pb76	2.69	2.42	G2Pb76	3.06	2.65	G3Pb76	3.88	2.72
G1S82	0.70	1.79	G2S82	0.91	1.71	G3S82	0.98	1.44
G1CR82	1.82	1.65	G2CR82	2.58	1.58	G3CR82	1.61	1.28
G1EE82	1.01	1.84	G2EE82	1.11	1.75	G3EE82	1.21	1.52
G1Pb82	1.48	1.99	G2Pb82	1.85	1.92	G3Pb82	2.22	1.69

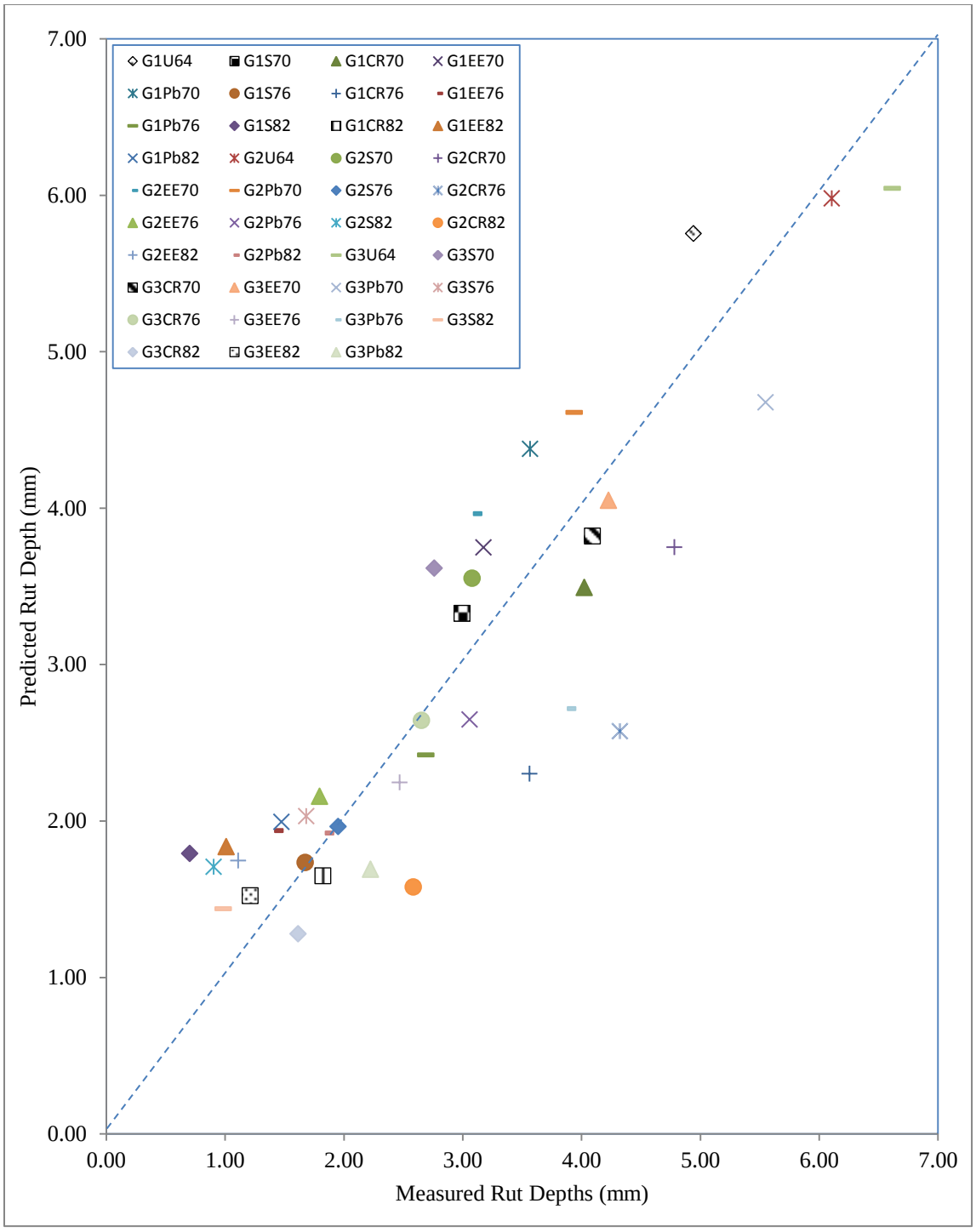

Figure 5.11Measured vs. Predicted RD results grouped based on Polymer type

Figure 5.11 shows the correlation between measured and predicted rut depths in millimeters. The resulted coefficient of correlation (r) of all samples is 0.885, which is statistically acceptable. Mixes that contains crumb rubber showed high scattered values when compared to other polymers used in this study. Measured values of rut depth for G2CR76 are 4.323 mm while predicted value is 2.57 mm which is approximately 60% higher. Similarly, for mixes that contain high content of polymers, G1Pb82 and G2EE82 have higher measured values than predicted.

5.5. Fatigue Characterization of Polymer Modified Asphalt Binders.

Flexural Fatigue test, AASHTO T-321 was used to test for fatigue properties of the prepared asphalt concrete beam samples. Samples were tested in a stress controlled mode to simulate asphalt pavement thick layer construction. Four samples were tested under different peak to peak stress (kPa). Corresponding stiffness (MPa), peak to peak strain $\times 10^{-6}$, peak to peak load (kN), deflection (mm), dissipated energy (MJ/m^3), and phase angle (°) were calculated by the software.

Beam's stiffness reduces rapidly at the beginning of the test then reaches a constant slope till failure which is defined as 40% of initial stiffness. Figure 5.12 shows typical trend for strain results of modified mix tested at peak to peak stress level of 500 kPa. Collected data were analyzed to determine relations between load repetition to failure (N*f*) and applied peak to peak strain (ε).

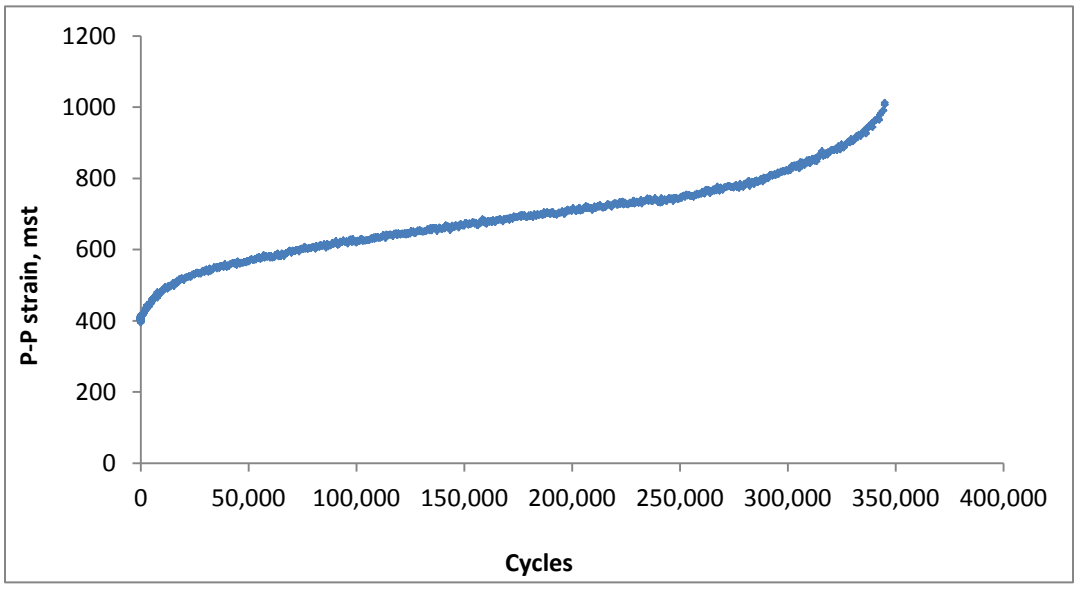

Figure 5.12Measured Strain vs. load cycles

The test was automatically terminated when the stiffness of the sample has reached 40% of its initial value. Figure 5.13 shows a typical result of SBS modified asphalt mix.

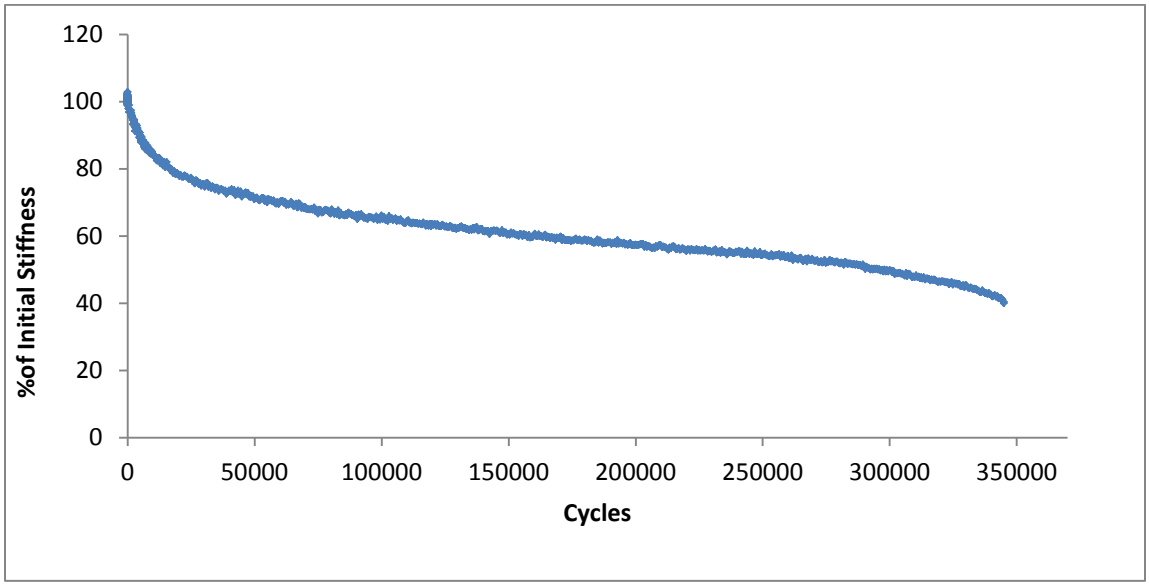

Figure 5.13Typical Fatigue life termination criteria based on stiffness.

It is shown that there is different permanent deformation response of concrete mix under repeated loadings before it reaches to failure. The relationship between fatigue life (N*f*) and applied stress (σ) was obtained for all prepared samples and a linear regression model was developed. Figure 5.14 shows the results of sample mixes prepared from gradation #1 and Table 5.14 shows the regression equations between N*f* and strain for samples contain gradation #1 aggregates. Appendix G contains the results of fatigue test for the other gradations

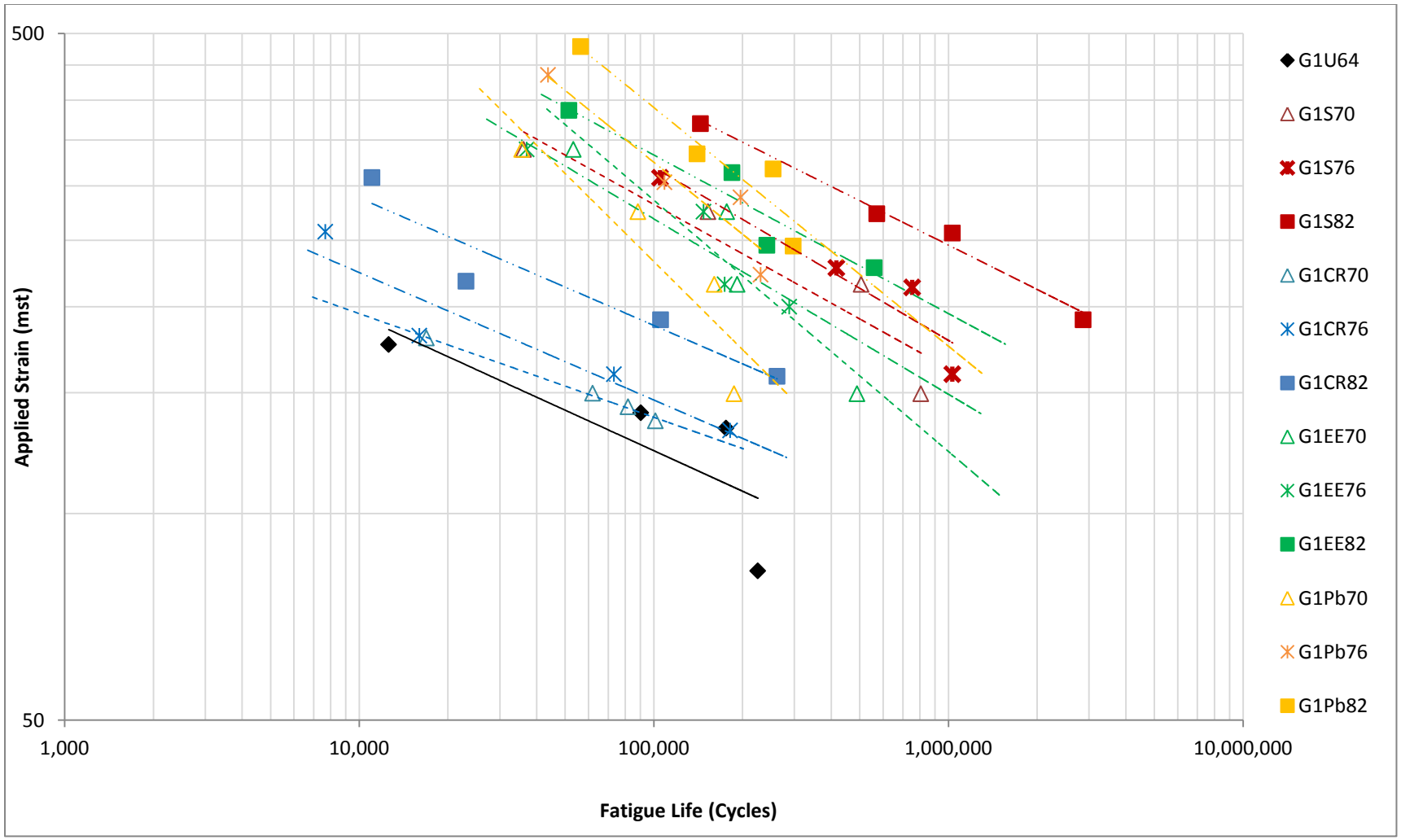

Figure 5.14 Fatigue Life vs. Applied stress for gradation

It was observed that polymer modified mixes showed better performance against fatigue compared to plain asphalt mixes under different levels of applied stress. SBS modified asphalt mixes have better fatigue resistance than other mixes followed by EE2 then CR then PB modified mixes at a given stress. Since most of fatigue properties of concrete mixes depend on binders' properties more than aggregate skeleton. At 300 mst, asphalt mixes modified with 4% of SBS, could resist fatigue up to 600,000 cycles, and while EE2 modified mixes would fail after 300,000 cycles. Fatigue results show that SBS modified asphalt mixes have higher stiffness than EE2, CR and PB modified mixes, respectively.

Table 5.14Results of Fatigue test for mixes contain gradation#1

Mix Code	Fatigue Equation	R^2
G1U64	$N_f = 7E+11(\varepsilon)^{-3.29}$	0.645
G1U70	$N_f = 1E+14(\varepsilon)^{-3.71}$	0.886
G1U76	$N_f = 9E+13(\varepsilon)^{-3.53}$	0.892
G1U82	$N_f = 1E+17(\varepsilon)^{-4.59}$	0.985
G1CR70	$N_f = 1E+19(\varepsilon)^{-6.59}$	0.995
G1CR76	$N_f = 3E+15(\varepsilon)^{-4.84}$	0.898
G1CR82	$N_f = 1E+16(\varepsilon)^{-4.84}$	0.898
G1EE70	$N_f = 1E+11(\varepsilon)^{-2.44}$	0.894
G1EE76	$N_f = 2E+13(\varepsilon)^{-3.41}$	0.871
G1EE82	$N_f = 8E+14(\varepsilon)^{-3.90}$	0.902
G1Pb70	$N_f = 4E+09(\varepsilon)^{-1.94}$	0.828
G1Pb76	$N_f = 3E+11(\varepsilon)^{-2.58}$	0.899
G1Pb82	$N_f = 5E+11(\varepsilon)^{-2.58}$	0.899

Fatigue equations listed in Table 5.14 are used to define the trend of fatigue response under different stress levels. The slope and location of the regression lines are defined

by the components of the equation (i.e. a and b). The higher the stress value, the lower the fatigue life obtained at same temperature and aggregate gradations. In order to simply the prediction of fatigue life (Nf) of polymer modified asphalt mixes tested at 20°C, a Multiple-linear regression model is created to estimate Nf values from mix properties as shown in Equation 5.3.

$$Nf = -27959664 + 91721\,T_{PG} - 206079\,\%P - 1630\,\varepsilon i + 172631 VMA + 152884\,\rho 4 + 2029661\,Pbe/f \quad (5.3)$$

Where:

N_f: is the fatigue life of asphalt pavement tested at 20°C

T_{PG}: is the actual service temperature at targeted PG grade, °C

%P: is percent of polymer from binders' weight.

εi: is the applied strain, mst.

VMA: is the Voids in Mineral Aggregates (%)

ρ4; is the content of coarse aggregate in the mix (%)

Pbe/f: is ratio between effective binder content and filler content

Table 5.15ANOVA results of developed regression model for Nf

Source	Df	SS	MS	F	P
Regression	6	3.55370E+12	5.92284E+11	2.74	0.031
Residual Error	29	6.26219E+12	2.15937E+11		
Total	35	9.81589E+12			

As shown from the ANOVA analysis of the generated model, the value of R^2 of 0.77 means that about 77.0% of the variation in N_f can be explained or accounted for by the estimated. Standard Error of Estimate S = 0.91 means that, on an average, the predicted

values of the N_f can vary by ±0.91 about the estimated regression equation for each value of independent variables during the sample period and by a much larger amount outside the sample period.

Fatigue tests were conducted on laboratory prepared mixes to develop fatigue life models to characterize the behavior of different polymer modified asphalt concrete mixes that represent typical wearing courses of local pavements. Tests were carried out at intermediate temperature of 20°C under different strain levels. The analysis of variance showed that the impacts of strain amplitude, binders' actual PG temperature (T_{PG}), Polymer content (%P), voids in mineral aggregates (VMA), percent of course aggregate (ρ4) and effective binder content to filler ratio have a significant effect on fatigue behavior.

CHAPTER 6

CONCLUSIONS AND RECOMMENDATIONS

6.1. Introduction

The performance of polymer modified asphalt concrete mixes were evaluated in terms of the engineering properties related to the asphalt binder and aggregate blends. The effect of polymer type and content on Superpave performance grading (PG^{+}) of local asphalt binders has been studied in this research. Styrene-Butadiene-Styrene (SBS), Crumb Rubber (CR), Polybilt (Pb) in addition to Eastman (EE2) were selected. Superpave mix design was used to prepare asphalt concrete mixes from different polymer type and content. Three different dense-graded aggregate blends of wearing courses with different aggregate gradations of 12.5 mm nominal maximum aggregate sizes (NMAS) were used in the design of thirty nine different concrete mixes.

6.2. Conclusions

The following conclusions were drawn from this research:

Ras-Tannura modified asphalt binders have shown higher PG actual temperatures at high service temperatures than Riyadh asphalts. Adding 2% of SBS, EE2 and Pb and 5%of CR polymer to Riyadh or Ras-Tannura asphalt binders can improve rutting resistance of asphalt pavements servicing at 70°C. While adding 4% of SBS, EE2 and Pb are required to improve rutting resistance at 76°C. Highly modified asphalt binders (6% and 10%) are used at specific locations at which low speed and extremely heavy

vehicles exist. Regression equation that predicts the Jnr values as a function of PG temperature and polymer content for each type of polymer modified asphalt binders was developed and discussed.

Cost analysis of using polymer in the modification of asphalt binders indicated that minimum polymer content is required in case of SBS. However, crumb rubber modified asphalt binders at any performance grade showed better cost effectiveness than other polymer type.

It is found that adding 5.8% of SBS to Ras-Tannura asphalt binders can improve rutting resistance of asphalt pavements servicing at 76°C and under extremely heavy traffic (PG 7(E)). While adding 5.2% of SBS or 9.5% of CR or 5.2% of EE2 or6.7% of Pb to improve rutting resistance at 76°servicing under very heavy traffic loads. For lower levels of highways, including collectors and local roads, PG 76(H) and PG 76(S) can be achieved by adding 3.5% of SBS or 7.0% of CR or 5.3% of EE2 or 5.9% of PB. This minimum amount of polymers content is required to improve the asphalt binder at the targeted temperature with less significant effect on Jnr values.

Similarly, 4.9% of SBS polymer is required to fulfill the highest PG+ grade at 70°C (i.e. PG 70(E)). For PG 70(V), 3.9% of SBS or 6.8% of CR or 5.1% of EE2 or 5.8% can be used and for PG 70(S-H), 2% or 5.0% or 3.3% or 3.9% of SBS, CR, EE2, PB should be used. For asphalt binders at which the improvement in PG temperature is not required (i.e. PG 64), a minimum content of polymers are required to reduce the non-recoverable strains and hence resist higher levels of traffic loads. A PG 64(E) grade of asphalt

binders can be obtained by adding 3% of SBS or 5.0% of CR or 2.2% of EE2 or 2.3% of PB.

PG 64(S) is the grade of neat (unmodified) asphalt binders obtained from asphalt refineries, this is applicable for both Riyadh and Ras-Tannura asphalts. It was also concluded that only SBS polymers can be used for grades PG 70(E) and PG 76(E). The elastomeric properties of SBS polymers can reduce the non-recoverable creep compliance to a value lesser than 0.5 kPa^{-1}.

The values of non-recoverable compliance (Jnr) of polymer modified asphalt binders are significantly affected by Temperature in a non-linear form. A mathematical equation that predicts Jnr from Temperature and polymer content [$(Jnr = C + a (T_{PG})^n – Di (\%P)$] can be used to predict the performance of local asphalts. This equation can be used to predict the traffic level at which an asphalt pavement can resist at targeted PG service temperature.

Mixes contain higher contents of coarse aggregates showed higher values of $|E^*|/\sin\phi$ at same PG grade of asphalt binders, polymer type and polymer content. The highest value of rutting parameter was shown for 6% SBS modified asphalt mix prepared from coarser gradation (i.e. G1) this value reaches 363.3 ksi.

Unmodified wearing courses showed a rut depth of around 6mm after 8,000 load cycles, while highly polymer modified mixes can reduce rutting to less than 1mm. The slope of the permanent deformation curves of unmodified mixes was 3-4 times higher than the slope of modified mixes. A multiple linear regression equation that predicts rut depth at 64°C and 8,000 loads cycles was developed as a function of mix properties that include, actual PG temperature, polymer content, voids in mineral aggregates effective polymer

content and filler content. A correlation between laboratory measured and predicted rut depth values was developed.

Fatigue life of asphalt pavements and modulus characteristics play an important role in pavement design. Ultimately they govern the required thickness of asphalt to structurally support heavy vehicles. Asphalt‘s fatigue behavior is influenced by numerous factors and therefore can be difficult to characterize. Fatigue tests were conducted on laboratory prepared mixes to develop fatigue life models to characterize the behavior of different polymer modified asphalt concrete mixes that represent typical wearing courses of local pavements. Tests were carried out at intermediate temperature of 20°Cunder different strain levels. The analysis of variance showed that the impacts of strain amplitude, binders’ actual PG temperature (T_{PG}), Polymer content (%P), voids in mineral aggregates (VMA), percent of course aggregate (ρ4) and effective binder content to filler ratio have a significant effect on fatigue behavior. The developed model give the pavement engineer the ability to undergo a more accurate assessment of fatigue damage than at present for different polymer modified asphalt concrete mixes. The research shows that with such characterization for the given pavement‘s design life, thinner and less expensive roads can be constructed in Saudi Arabia.

6.3. Recommendations

This research work has generated mathematical equations that predict dynamic moduli, rutting resistance and fatigue life for wearing coarse pavements recommended by ministry of transportation in the kingdom of Saudi Arabia using local materials. From the outcome of performance grading of asphalt binders, a catalog of polymer content and its relative cost is available for pavement practitioners for four different polymer types

included in this study. It is also recommended that local design engineers and practitioners use rutting and fatigue prediction equations developed in this study to predict the performance of wearing coarse layers produced from lime stone aggregates and the four polymer modified asphalt binders.

Further work can be conducted on different aggregate sizes to represent base courses. Furthermore, different aggregate type (Basalt or/and Granite) can be included in a future study. Due to differences in polymer types and cost, hybrid combination of polymers can be used to improve the performance of asphalt binders. The suitable polymers ratio that gives the best binders' performance against rutting and fatigue in a cost effective way can be studied.

References

Delgadillo, R., & Bahia, H. U. (2010). The relationship between nonlinearity of asphalt binders and asphalt mixture permanent deformation. Road Materials and Pavement Design, 11(3), 653-680.

Wahhab, H. A. A., Al-Dubabe, I. A., Asi, I. M., & Ali, M. F. (1998). Performance-based characterization of Arab asphalt. Building and environment, 33(6), 375-383.

Wong, W. G., Han, H., He, G., Wang, K. C., & Lu, W. (2004). Rutting response of hot-mix asphalt to generalized dynamic shear moduli of asphalt binder. Construction and Building Materials, 18(6), 399-408.

Isacsson, U., & Zeng, H. (1998). Cracking of asphalt at low temperature as related to bitumen rheology. Journal of materials science, 33(8), 2165-2170.

Airey, G. D. (2003). Rheological properties of styrene butadiene styrene polymer modified road bitumens. Fuel, 82(14), 1709-1719.

Paje, S. E., Luong, J., Vázquez, V. F., Bueno, M., & Miro, R. (2013). Road pavement rehabilitation using a binder with a high content of crumb rubber: Influence on noise reduction. Construction and building materials, 47, 789-798.

Lee, S. J., Akisetty, C. K., & Amirkhanian, S. N. (2008). The effect of crumb rubber modifier (CRM) on the performance properties of rubberized binders in HMA pavements. Construction and Building Materials, 22(7), 1368-1376.

Jeong, K. D., Lee, S. J., Amirkhanian, S. N., & Kim, K. W. (2010). Interaction effects of crumb rubber modified asphalt binders. Construction and Building Materials, 24(5), 824-831.

Cong, P., Xun, P., Xing, M., & Chen, S. (2013). Investigation of asphalt binder containing various crumb rubbers and asphalts. Construction and Building Materials, 40, 632-641.

Presti, D. L. (2013). Recycled tyre rubber modified bitumens for road asphalt mixtures: a literature review. Construction and Building Materials, 49, 863-881.

Nejad, F. M., Aghajani, P., Modarres, A., & Firoozifar, H. (2012). Investigating the properties of crumb rubber modified bitumen using classic and SHRP testing methods. Construction and Building Materials, 26(1), 481-489.

Wasage, T. L. J., Stastna, J., & Zanzotto, L. (2011). Rheological analysis of multi-stress creep recovery (MSCR) test. International Journal of Pavement Engineering, 12(6), 561-568.

Clopotel, C. S., & Bahia, H. U. (2012). Importance of elastic recovery in the DSR for binders and mastics. Engineering Journal (Eng. J.), 16(4), 99-106.

American Association of State Highway and Transportation Officials (AASHTO). 2009."*Multiple Stress Creep Recovery (MSCR) Test of Asphalt Binder Using a Dynamic Shear Rheometer (DSR)*", AASHTODesignation TP 70-11.

American Association of State Highway and Transportation Officials (AASHTO). 2009."*Performance-Graded Asphalt Binder Using Multiple Stress Creep Recovery (MSCR) Test*", AASHTODesignation MP 19-10.

American Association of State Highway and Transportation Officials (AASHTO). 2015."*Determining the Dynamic Modulus and Flow Number for Asphalt Mixtures Using the Asphalt Mixture Performance Tester (AMPT)*", AASHTODesignation **TP 79-15**.

American Association of State Highway and Transportation Officials (AASHTO). 2015."*Determining Rutting Susceptibility of Hot Mix Asphalt (HMA) Using the Asphalt Pavement Analyzer (APA)*", AASHTODesignation **T 340-10**.

Airey G. (2003). "Rheological properties of styrene butadiene styrene polymer modified road bitumen's". *Fuel*, 82, 1709–19.

Al-Abdul Wahhab, H.I., I.M. Asi, I.A. Al-Dubabe and M.F. Ali (1997). Development of Performance-Based Bitumen Specifications for the Gulf Countries, Construction and Building Materials Journal, 11(1), 15-22.

Alexander Bernier, Adam Zofka , Iliya Yut (2012) "Laboratory evaluation of rutting susceptibility of polymer-modified asphalt mixtures containing recycled pavements." Construction and Building Materials. 31(1), 58–66.

Baha Vural Kök , Hakan Çolak (2011). " Laboratory comparison of the crumb-rubber and SBS modified bitumen and hot mix asphalt." Construction and Building Materials. 25(8), 3204–3212.

Diaz, Luis G.; Archilla, Adrián R. (2013). " From Testing to Design: An Easy Way to Use and Interpret the Results from the Asphalt Mixture Performance Tester (AMPT) ." International Journal of Pavement Research & Technology., 6(5), 527–545.

F. Moreno-Navarro, M. Sol-Snchez, M.C. Rubio-Gmez, M. Segarra-Martnez. (2014) "The use of additives for the improvement of the mechanical behavior of high modulus asphalt mixes." Construction and Building Materials. 70(1), 65-70.

Fan Bai, Xinhua Yang , Guowei Zeng (2014) , " Creep and recovery behavior characterization of asphalt mixture in compression," Construction and Building Materials, 54(1). 504- 511.

Halit Özen. (2011) "Rutting evaluation of hydrated lime and SBS modified asphalt mixtures for laboratory and field compacted samples". Construction and Building Materials. 25(2), 756–765.

Kalhan Mitra, Animesh Das, Sumit Basu. (2012) "Mechanical behavior of asphalt mix: An experimental and numerical study". Construction and Building Materials. 27(1), 545–552.

Lubinda F. Walubita, Allex E. Alvarez , Geoffrey S. Simate (2011). " Evaluating and comparing different methods and models for generating relaxation modulus master-curves for asphalt mixes." Construction and Building Materials. 25(5), 2619–2626.

Maninder Singh , Praveen Kumar, Mannan Rai Maurya.(2013) "Strength characteristics of SBS modified asphalt mixes with various aggregates." Construction and Building Materials. 41(1), 815-823.

Nuha S. Mashaan, Asim Hassan Ali, Mohamed Rehan Karim and Mahrez Abdelaziz. (2011). "Effect of blending time and crumb rubber content onproperties of crumb rubber modified asphalt binder". International Journal of the Physical Sciences. 6(9), 2189-2193.

S. Anjan kumar and A. Veeraragavan (2011). " Dynamic mechanical characterization of asphalt concrete mixes with modified asphalt binders." Materials Science and Engineering A., 528(21), 6445–6454.

Taner Alatas, Mehmet Yılmaz, Baha Vural Kok, and Aykut fatih Koral;(2012) , " Comparison of permanent deformation and fatigue resistance of hot mix asphalts prepared with the same performance grade binders," Construction and Building Materials, 30(1) , 66- 72.

W.G. Wonga , Haifeng Hana, Guiping Hea, Kelvin C.P. Wangb, Weimin Luc.(2004) "Rutting response of hot-mix asphalt to generalized dynamic shear moduli of asphalt binder". Construction and Building Materials. 18(6), 399-408.

Wasage, T.L.J., Stastna J. and Zanzotto L. (2011). “Rheological analysis of multistress creep and recovery (MSCR) test”, Internation Journal of Pavement Engineering. 12(6), 561-568.

Yanqing Zhao, Jimin Tang and Hui Liu;(2012), " Construction of triaxial dynamic modulus master curve for asphalt mixtures," Construction and Building Materials, 37(1), 21- 26.

Zhu, H., Sun, L., Yang, J., Chen, Z., and Gu, W. (2011). ”Developing Master Curves and Predicting Dynamic Modulus of Polymer-Modified Asphalt Mixtures.” J. Mater. Civ. Eng., 23(2), 131–137.

AASHTO Standard Method TP 70-11: Multiple Stress Creep Recovery (MSCR) Test of Asphalt Binder Using a Dynamic Shear Rheometer (DSR).

AASHTO Standard Method MP 19-10: Performance-Graded Asphalt Binder Using Multiple Stress Creep Recovery (MSCR) Test.

AASHTO Standard Method TP 79-15: Determining the Dynamic Modulus and Flow Number for Asphalt Mixtures Using the Asphalt Mixture Performance Tester (AMPT).

Al-Abdul Wahhab, H.I., F.M. Ali, I.M. Asi and I.A. Al Dhubeeb. 1994. Adaptation of SHRP Performance Based Asphalt Specification to the Gulf Countries, Final Report, KACST.

Al-Abdul Wahhab, H.I., I.A. Al-Dubabe, I.M. Asi and M.F. Ali .1997.. Performance-Based Characterization of Arab Asphalt, Building and Environment Journal, 32(2), 1-9.

Al-Abdul Wahhab, H.I., I.A. Mahmoud and M.G. Baig. 2002. Performance Modification of Saudi Asphalt Binder Using SABIC Polymer, Sixth Saudi Engineering Conference, KFUPM, Dhahran.

Al-Abdul Wahhab, H.I., I.M. Asi, F.M. Ali and I.A. Al-Dubabe. 1999. Prediction of Asphalt Rheological Properties Using HP-GPC, Journal of Materials in Civil Engineering, 11(1), 6-14.

Al-Abdul Wahhab, H.I., I.M. Asi, I.A. Al-Dubabe and M.F. Ali. 1997. Development of Performance-Based Bitumen Specifications for the Gulf Countries, Construction and Building Materials Journal, 11(1), 15-22.

Al-Abdul Wahhab, H.I., M.F. Ali, I.M. Asi and I.A. Al-Dubabe 1996. HP-GPC Characterization of Asphalt and Modified Asphalts from Gulf Countries and Their Relation to Performance Based Properties, Proceedings of the 212th

National Meeting of American Chemical Society, Symposium on Modified Asphalt, 1296-1301.

Al-Dubabe, I.A., H.I. Al-Abdul Wahhab, I.M. Asi and M.F. Ali. 1998. Polymer Modification of Arab Asphalt, ASCE Material Journal, 10(3), 161-167.

Ali, M., H. Al-Abdul Wahhab, I. Asi and I. Al-Dubabe. 1999. Characterization of Polymer Modified Gulf Asphalts, Petroleum Science and Technology, 17(2), 125-146.

Ali, N., S. Zahran, J. Trogdon and A. Bergan. 1994. A Mechanistic Evaluation of Modified Asphalt Paving Mixtures, Canadian Journal of Civil Engineering, 21, 954 p.

Asi, I.M., H.I. Al-Abdul Wahhab, I.A. Al-Dubabe and M.F. Ali. 1997. Performance Modeling of Arabian Asphalt Using HP-GPC, Materials Engineering and Performance Journal, 6(4), 503-510.

Alatas, T., Yılmaz,M., Kok,V., Koral F. 2012.Comparison of permanent deformation and fatigue resistance of hot mix asphalts prepared with the same performance grade binders. Construction and Building Materials, 30(1), 66- 72.

Bai, F., Yang, X., Zeng G. 2014.Creep and recovery behavior characterization of asphalt mixture in compression. Construction and Building Materials, 54(1). 504- 511.

Bai, F., Yang, X., Zeng, G. 2016. A stochastic viscoelastic–viscoplastic constitutive model and its application to crumb rubber modified asphalt mixtures. Construction and Building Materials, 89(3), 802–809.

Bernier, A., Zofka, A. , Yut, I. 2012.Laboratory evaluation of rutting susceptibility of polymer-modified asphalt mixtures containing recycled pavements. Construction and Building Materials, 31(1), 58–66.

Cong, P., Xun, P., Xing, M., Chen, Sh. 2013. Investigation of asphalt binder containing various crumb rubbers and asphalts. Construction and Building Materials, 40(3), 632–641.

Diaz, G., Archilla, R. 2013. From Testing to Design: An Easy Way to Use and Interpret the Results from the Asphalt Mixture Performance Tester (AMPT) .International Journal of Pavement Research & Technology, 6(5), 527–545.

Isacsson, U., Zeng, H. 1998.Cracking of Asphalt at Low Temperature as Related to Bitumen Rheology, Journal of Materials and Structures, 33(8), 2165-2170.

Jeong, K., Lee, S., Amirkhanian, S., Kim K. 2010.Interaction effects of crumb rubber modified asphalt binders. Construction and Building Materials, 24(5), 824–831.

Kök, B., Çolak, V. 2011. Laboratory comparison of the crumb-rubber and SBS modified bitumen and hot mix asphalt. Construction and Building Materials, 25(8), 3204–3212.

Kumar, S., Veeraragavan, A. 2011. Dynamic mechanical characterization of asphalt concrete mixes with modified asphalt binders. Materials Science and Engineering: A, 528(21), 6445–6454.

Lee, S., Akisetty, Ch., Amirkhanian, S. 2008.The effect of crumb rubber modifier (CRM) on the performance properties of rubberized binders in HMA pavements. Construction and Building Materials, 22(7), 1368–1376.

Lu, X., Isacsson, U. 1997. Rheological Characterization of SBS Copolymer Modified Bitumens, Construction and Building Materials, 11(1), 23-32.

Lu, X., Isacsson, U., Ekblad, J. 1998. Low Temperature Properties of Styrene-Butadiene-Styrene Polymer Modified Bitumen, Construction and Building Materials, 12, 405-414.

Lu, X., Isacsson, U. 2001.Effect of Binder Rheology on the Low-Temperature Cracking of Asphalt Mixtures, Road Materials and Pavement Design, 2(1), 29-47.

Moreno-Navarro, F., Sol-Snchez, M., Rubio-Gmez, M., Segarra-Martnez, M. 2014.The use of additives for the improvement of the mechanical behavior of high modulus asphalt mixes.Construction and Building Materials, 70(1), 65-70.

NationalCooperativeHighwayResearchProgram, NCHRP, report 513. 2003. Simple Performance Tester forSuperpave Mix Design:First-Article Developmentand Evaluation.

Nejad, M., Aghajani, P., Modarres, A., Firoozifar, H. 2012.Investigating the properties of crumb rubber modified bitumen using classicand SHRP testing methods. Construction and Building Materials, 26(1), 481–489.

Özen, H. 2012.Rutting evaluation of hydrated lime and SBS modified asphalt mixtures for laboratory and field compacted samples. Construction and Building Materials, 25(2), 756–765.

Paje, E., Luong, J., Vázquez, F., Bueno, M., Miró, R. 2013.Road pavement rehabilitation using a binder with a high contentof crumb rubber: Influence on noise reduction. Construction and Building Materials, 47(3), 789–798.

Presti, D. 2013.Recycled Tyre Rubber Modified Bitumens for road asphalt mixtures: A literature review. Construction and Building Materials, 49(3), 863–881.

Shen, J., Amirkhanian, S., Xiao, F., Tang, B. 2008. Surface area of crumb rubber modifier and its influence on high-temperature viscosity of CRM binders. International Journal of Pavement Engineering, 10(5), 375-381.

Singh, M., Kumar, P., Maurya, R. 2013.Strength characteristics of SBS modified asphalt mixes with various aggregates." Construction and Building Materials, 41(1), 815-823.

Wonga, G., Hana, H., Hea,G., Wang,P., Lu, W. 2004.Rutting response of hot-mix asphalt to generalized dynamic shear moduli of asphalt binder. Construction and Building Materials, 18(6), 399-408.

Walubita, L., Alvarez, A., Simate, G. 2011.Evaluating and comparing different methods and models for generating relaxation modulus master-curves for asphalt mixes. Construction and Building Materials. 25(5), 2619–2626.

Wanga,H., Danga, Z., Lib, L., Youc, Z.2013. Analysis on fatigue crack growth laws for crumb rubber modified (CRM) asphalt mixture. Construction and Building Materials, 47(2), 1342–1349.

Xiang, L. , Cheng, J., Kang, Sh.2015. Thermal oxidative aging mechanism of crumb rubber/SBS composite modified asphalt. Construction and Building Materials, 75(1), 169–175.

Xiao, F., Amirkhanian, S. 2014.Special issue on utilization of crumb rubber in asphalt mixtures. Construction and Building Materials, 67(B), 1–216.

Zhao,Y., Tang, J., Liu, H. 2012. Construction of triaxial dynamic modulus master curve for asphalt mixtures. Construction and Building Materials, 37(1), 21- 26.

Zhu, H., Sun, L., Yang, J., Chen, Z., and Gu, W. 2011. Developing Master Curves and Predicting Dynamic Modulus of Polymer-Modified Asphalt Mixtures. Journal of Materials in Civil Engineering, 23(2), 131–137.

AASHTO T 340-10 (2015). Determining Rutting Susceptibility of Hot Mix Asphalt (HMA) Using the Asphalt Pavement Analyzer (APA).

Kandhal, P. S., & Cooley, L. A. (2003). Accelerated laboratory rutting tests: Evaluation of the asphalt pavement analyzer (No. 508). Transportation Research Board.

Skok, E. L., Johnson, E. N., & Turk, A. (2002). Asphalt Pavement Analyzer (APA) Evaluation.

Stuart, K. D., & Izzo, R. P. (1995). CORRELATION OF SUPERPAVE G*/SIN DELTA WITH RUTTING SUSCEPTIBILITY FROM LABORATORY MIXTURE TESTS (WITH DISCUSSION AND CLOSURE). Transportation Research Record, (1492).

Lai, J. S. (1989). Development of a laboratory rutting-resistance testing method for asphalt mixes. Final report, January 1988-August 1989(No. PB-90-231192/XAB). Georgia Inst. of Tech., Atlanta, GA (USA). School of Civil Engineering.

Brovelli, C., Crispino, M., Pais, J., & Pereira, P. (2015). Using polymers to improve the rutting resistance of asphalt concrete. Construction and Building Materials, 77, 117-123.

Fontes, L. P., Triches, G., Pais, J. C., & Pereira, P. A. (2010). Evaluating permanent deformation in asphalt rubber mixtures. Construction and Building Materials, 24(7), 1193-1200.

Tangella, S. R., Craus, J., Deacon, J. A., & Monismith, C. L. (1990). Summary report on fatigue response of asphalt mixtures (No. SHRP-A-312).

Wahhab, H. I. A. A. (2012). Effect of Modifiers and Additives on Fatigue Behavior of Asphalt Concrete Mixes in the Gulf. International Journal of Pavement Research and Technology, 5(5), 326-332.

Adhikari, S., Shen, S., & You, Z. (2009). Evaluation of fatigue models of hot-mix asphalt through laboratory testing. Transportation Research Record: Journal of the Transportation Research Board, (2127), 36-42.

Witczak, M. A., Mamlouk, M. W., Kaloush, M. S., & Kaloush, K. E. (2006). Validation of initial and failure stiffness definitions in flexure fatigue test for hot mix asphalt. Journal of Testing and Evaluation, 35(1), 95-102.

Shen, S., & Carpenter, S. (2007). Development of an asphalt fatigue model based on energy principles. Asphalt Paving Technology-Proceedings, 76, 525.

Shell Pavement Design Manual: Asphalt Pavements and Overlays for Road Traffic. Shell International Petroleum Co., Ltd., London, 1978.

Thickness Design Manual. Research Report 82-2. Asphalt Institute, Lexington, Ky., 1982.

Adhikari, S., Shen, S., & You, Z. (2009). Evaluation of fatigue models of hot-mix asphalt through laboratory testing. Transportation Research Record: Journal of the Transportation Research Board, (2127), 36-42.

Hartman, A. M., & Gilchrist, M. D. (2004). Evaluating four-point bend fatigue of asphalt mix using image analysis. Journal of materials in civil engineering, 16(1), 60-68.

Pais, J., & Minhoto, M. (2010). The prediction of fatigue life of asphalt mixtures using four-point bending tests. In 24th ARRB Conference–Building on 50 years of road and transport research. ARRB Group Ltd and Authors 2010.

Kutay, M. E., Gibson, N. H., & Youtcheff, J. (2008). Conventional and viscoelastic continuum damage (VECD)-based fatigue analysis of polymer modified asphalt pavements (with discussion). Journal of the Association of Asphalt Paving Technologists, 77.

Khattak, M., & Baladi, G. (2001). Fatigue and permanent deformation models for polymer-modified asphalt mixtures. Transportation Research Record: Journal of the Transportation Research Board, (1767), 135-145.

Delgadillo, R. and Bahia, H.U. "The relationship between non linearity of asphalt binders and asphalt mixtures permanent deformation". Road Materials and PavementDesign, vol. 3, 653–680, 2010

Becker Y, Me´ndez MP, Rodrı´guez Y. Polymer modified asphalt.Vis Technol 2001;9(1):39–50.

H.I. Al-Abdul Wahhab*1, I.M. Asi1, S.A. Ali2, S. Al-Swailmi3 and A. Al-Nour4 Pavement Stripping in Saudi Arabia: Predictionand PreventionThe Journal of Engineering Research 1 (2004) 29-38

AASHTO T 321: Determining the Fatigue Life of Compacted Hot-Mix Asphalt (HMA) Subjected to Repeated Flexural Bending.

Witczak, M.W., Kaloush, K., Pellinen, T., and El-Basyouny, M., Von Quintus, H.Simple Performance Test for Superpave Mix Design. National Cooperative HighwayResearch Program (NCHRP) Report 465. Transportation Research Board, NationalResearch Council, Washington, D.C., 2002.

Guide for Mechanistic-Empirical Design of New and Rehabilitated Pavement Structures. National Cooperative Highway Research Program (NCHRP) Report 1-37A, Transportation Research Board, National Research Council, Washington, D.C., 2004.

Pellinen, T.K., Witczak, M.W. "Stress Dependent Master Curve Construction forDynamic (Complex) Modulus (with Discussion)." Journal of the Association of AsphaltPaving Technologists, Vol. 71, 2002, pp. 281-309.

Christensen Jr., D.W., Pellinen, T., and Bonaquist, R.F. “Hirsch Model for Estimatingthe Modulus of Asphalt Concrete.” Journal of the Association of Asphalt PavingTechnologists, Vol.72, 2003, pp. 97-121.

Kaloush, K.E., and Witczak, M.W. “Tertiary Flow Characteristics of Asphalt Mixtures(with Discussion and Closure).” Journal of Association of Asphalt Paving Technologists,Vol.71, 2002, pp. 248-280.

Pellinen, T.K., and Witczak, M.W. “Use of Stiffness of Hot-Mix Asphalt As A SimplePerformance Test.” In Transportation Research Record 1789. Transportation ResearchBoard, National Research Council, Washington, D.C., 2002, pp.80-90.

“AASHTO Interim Guide for Design of Pavement Structures.” American Association ofState Highway and Transportation Officials, Washington, D.C., 1972.AASHTO Road Test, History and Description of Project. Highway Research Board(HRB) Special Report 61A, 1961

Huang, Y., Bird, R. N., & Heidrich, O. (2007). A review of the use of recycled solid waste materials in asphalt pavements. Resources, Conservation and Recycling, 52(1), 58-73.

Azizian, M. F., Nelson, P. O., Thayumanavan, P., & Williamson, K. J. (2003). Environmental impact of highway construction and repair materials on surface and ground waters: Case study: crumb rubber asphalt concrete. Waste management, 23(8), 719-728.

APPENDICES

Appendix A

A-1: Rutting Parameter |G|/sinδ of CR Modified Ras-Tannura Asphalt Binders*

A-2: Rutting Parameter |G|/sinδ of CR Modified Riyadh Asphalt Binders*

Table A- 1.1.

Rutting Parameter |G|/sinδ of CR Modified Ras-Tannura Asphalt Binders*

%P	Testing	Un-aged		Aged		PG Grade
	Temperature, ℃	|G*|/sinδ (kPa)	PG Temperature	|G*|/sinδ (kPa)	PG Temperature	
0%	64	1.012	65.3	2.598	64.1	PG 64
	70	0.485		1.191		
5%	64	2.981	73.1	6.751	74.0	PG 70
	70	1.463		3.385		
	76	0.885		1.763		
	82	0.633		0.966		
7.5%	64	3.87	82.6	13.041	79.2	PG 76
	70	2.034		6.357		
	76	1.43		3.16		
	82	0.643		1.606		
10%	64	5.832	83.1	16.1	83.6	PG 82
	70	3.321		8.005		
	76	1.923		5.12		
	82	0.984		2.631		

Table A- 1.2.

Rutting Parameter |G|/sinδ of EE Modified Ras-Tannura Asphalt Binders*

%P	Testing	Un-aged		Aged		PG Grade
	Temperature, °C	|G*|/sinδ (kPa)	PG Temperature	|G*|/sinδ (kPa)	PG Temperature	
0%	64	1.012	65.3	2.598	64.1	PG 64
	70	0.485		1.191		
2%	64	3.187	78.3	4.816	70.1	PG 70
	70	1.6815		2.234		
	76	1.059		1.325		
	82	0.7592		1.12		
4%	64	5.2115	84.7	9.135	76.1	PG 76
	70	3.0905		4.488		
	76	1.9995		2.225		
	82	1.2315		1.153		
6%	64	8.026	89.1	10.112	82.5	PG 82
	70	4.7895		6.022		
	76	3.205		3.737		
	82	1.7888		2.29		

Table A- 1.3.

Rutting Parameter |G|/sinδ of Pb Modified Ras-Tannura Asphalt Binders*

%P	Testing	Un-aged		Aged		PG Grade
	Temperature, °C	|G*|/sinδ (kPa)	PG Temperature	|G*|/sinδ (kPa)	PG Temperature	
0%	64	1.012	65.3	2.598	64.1	PG 64
	70	0.485		1.191		
2%	64	3.54	78.9	4.41	75.3	PG 70
	70	1.803		2.211		
	76	1.312		1.046		
	82	0.812		0.773		
4%	64	4.3	83.7	8.332	79.0	PG 76
	70	2.54		5.775		
	76	1.76		3.487		
	82	1.12		1.377		
6%	64	6.98	88.5	9.431	82.2	PG 82
	70	4.01		7.5		
	76	2.95		6.133		
	82	1.63		2.264		

Table A-2.1

Rutting Parameter |G|/sinδ of SBS Modified Riyadh Asphalt Binders*

%P	Testing	Un-aged		Aged		PG Grade
	Temperature, ℃	|G*|/sinδ	PG	|G*|/sinδ	PG	
		(kPa)	Temperature	(kPa)	Temperature	
0%	64	1.004	64.09	2.39	64.10	PG 64
	70	0.532		1.11		
2%	64	2.89	75.81	6.92	73.02	PG 70
	70	1.68		3.32		
	76	0.98		1.65		
	82	0.672		0.83		
4%	64	5.72	82.65	13.21	78.76	PG 76
	70	3.21		6.43		
	76	2.09		3.84		
	82	1.12		2.09		
6%	64	8.23	87.43	16.43	82.13	PG 82
	70	4.93		9.43		
	76	3.01		5.21		
	82	1.54		2.22		

Table A-2.2

Rutting Parameter |G|/sinδ of CR Modified Riyadh Asphalt Binders*

%P	Testing	Un-aged		Aged		PG Grade
	Temperature, ℃	|G*|/sinδ	PG	|G*|/sinδ	PG	
		(kPa)	Temperature	(kPa)	Temperature	
0%	64	1.004	64.09	2.39	64.10	PG 64
	70	0.532		1.11		
5%	64	2.64	72.6	5.43	71.9	PG 70
	70	1.21		3.09		
	76	0.76		1.54		
	82	0.53		0.87		
7.5%	64	3.23	79.4	8.43	77.8	PG 76
	70	1.83		5.07		
	76	1.32		2.78		
	82	0.54		1.43		
10%	64	5.12	84.97	12.21	82.5	PG 82
	70	2.98		6.32		
	76	1.64		3.98		
	82	1.39		2.53		

Table A-2.3

Rutting Parameter |G|/sinδ of EE2 Modified Riyadh Asphalt Binders*

%P	Testing	Un-aged		Aged		PG Grade
	Temperature, ℃	|G*|/sinδ	PG	|G*|/sinδ	PG	
		(kPa)	Temperature	(kPa)	Temperature	
0%	64	1.004	65.3	2.39	64.1	PG 64
	70	0.532		1.11		
2%	64	2.9	73.7	4.23	72.3	PG 70
	70	1.22		2.98		
	76	0.88		1.72		
	82	0.43		0.89		
4%	64	4.73	83.5	8.04	80.1	PG 76
	70	3.98		4.12		
	76	1.65		2.92		
	82	1.1		1.54		
6%	64	7.77	89.1	12.32	82.4	PG 82
	70	4.12		5.73		
	76	2.87		3.88		
	82	1.54		2.43		

Table A-2.4

Rutting Parameter |G|/sinδ of Pb Modified Riyadh Asphalt Binders*

%P	Testing	Un-aged		Aged		PG Grade
	Temperature, ℃	|G*|/sinδ	PG	|G*|/sinδ	PG	
		(kPa)	Temperature	(kPa)	Temperature	
0%	64	1.004	64.09	2.39	64.10	PG 64
	70	0.532		1.11		
2%	64	2.8674	71.8	3.4839	70.6	PG 70
	70	1.46043		2.24		
	76	0.76272		1.2		
	82	0.65772		0.89		
4%	64	3.483	80.3	6.58228	79	PG 76
	70	2.0574		4.56225		
	76	1.4256		2.75473		
	82	0.9072		1.08783		
6%	64	5.6538	83.7	7.45049	82.2	PG 82
	70	3.2481		4.2028		
	76	2.3895		2.5359		
	82	1.3203		1.1297		

Appendix B

MSCR recovery and Non-recoverable Compliance

Table B-1.1
MSCR results for SBS modified Ras-Tannura Asphalts

Polymer type	%P	T, °C	MSCR Recovery (%)		Diff. (%)	Jnr (1/kPa)		Diff (%)
			0.1	3.2		0.1	3.2	
Unmodified	0%	64	4.2	1.5	64.3	3.240	3.810	15.0
		58	10.0	3.6	64.0	1.290	1.480	12.8
SBS	2%	70	19.0	8.1	57.3	1.593	2.036	21.8
		64	28.4	18.7	34.0	0.635	0.875	18.1
		58	39.3	34.0	13.4	0.237	0.268	11.2
	4%	76	30.7	16.3	47.1	1.196	1.703	29.8
		70	42.1	29.2	30.8	0.499	0.685	27.2
		64	53.6	46.6	13.1	0.199	0.241	17.7
		58	66.1	62.2	5.8	0.069	0.079	12.9
	6%	76	68.3	54.0	20.9	0.218	0.363	39.9
		70	75.4	67.7	10.3	0.088	0.128	31.6
		64	83.8	78.0	6.9	0.030	0.043	32.0
		58	91.3	85.0	6.9	0.010	0.015	32.4

Table B-1.2
MSCR results for SBS modified Riyadh Asphalts

Polymer type	%P	T, °C	MSCR Recovery (%)		Diff. (%)	Jnr (1/kPa)		Diff (%)
			0.1	3.2		0.1	3.2	
Unmodified	0%	64	2.7	1.0	63.7	4.277	5.715	25.2
		58	7.6	2.3	69.4	1.703	2.220	23.3
Riyadh-SBS	2%	70	14.8	7.6	48.7	2.103	3.054	31.1
		64	22.1	16.3	26.4	0.838	1.313	36.1
		58	30.6	20.9	18.5	0.313	0.402	22.2
	4%	76	24.0	10.4	56.6	1.579	2.555	38.2
		70	32.9	21.6	34.3	0.659	1.028	35.9
		64	41.8	34.4	17.6	0.263	0.362	27.3
		58	51.6	46.1	10.7	0.091	0.119	23.1
	6%	76	62.8	47.3	24.7	0.288	0.545	47.2
		70	70.2	63.2	10.0	0.116	0.192	39.5
		64	78.4	66.7	14.9	0.040	0.065	38.6
		58	82.2	71.4	13.2	0.013	0.023	41.3

Table B-2.1
MSCR results for CR modified Ras-Tannura Asphalts

Polymer type	%P	T, °C	MSCR Recovery (%)		Diff (%)	Jnr (1/kPa)		Diff (%)
			0.1	3.2		0.1	3.2	
Unmodified	0%	64	4.2	1.5	64.286	3.24	3.81	14.961
		58	9.99	3.6	63.964	1.29	1.48	12.838
CR	5%	70	45.235	5.291	88.303	0.574	1.247	53.953
	5%	64	47.548	16.24	65.845	0.268	0.468	42.764
	5%	58	52.252	31.048	40.581	0.098	0.158	37.961
	7.5%	76	15.316	1.81	88.183	2.102	2.83	25.719
	7.5%	70	22.736	8.857	61.045	0.906	1.163	22.094
	7.5%	64	34.264	23.32	31.94	0.346	0.419	17.456
	7.5%	58	46.918	40.802	13.035	0.118	0.135	12.591
	10%	76	23.592	2.604	88.963	2.243	3.548	36.801
	10%	70	30.252	9.776	67.684	0.979	1.471	33.435
	10%	64	47.299	22.51	52.409	0.329	0.35	40.197
	10%	58	57.184	39.817	30.371	0.122	0.182	33.234

Table B-2.2
MSCR results for CR modified Riyadh Asphalts

Polymer type	%P	T, °C	MSCR Recovery (%)		Diff (%)	Jnr (1/kPa)		Diff (%)
			0.1	3.2		0.1	3.2	
Unmodified	0%	64	2.70	0.98	63.7	4.277	5.715	25.2
		58	7.64	2.34	69.4	1.703	2.220	23.3
CR	2%	70	35.28	3.92	88.9	0.758	1.871	59.5
		64	37.09	12.02	67.6	0.354	0.702	49.6
		58	40.76	22.98	43.6	0.129	0.237	45.4
	4%	76	11.95	1.34	88.8	2.775	4.245	34.6
		70	17.73	6.55	63.0	1.196	1.745	31.4
		64	26.73	17.26	35.4	0.457	0.629	27.3
		58	36.60	30.19	17.5	0.156	0.203	23.1
	6%	76	18.40	1.93	89.5	2.961	5.322	44.4
		70	23.60	7.23	69.3	1.292	2.207	41.4
		64	36.89	16.66	54.8	0.434	0.525	17.3
		58	44.60	29.46	33.9	0.161	0.273	41.0

Table B-3.1
MSCR results for EE modified Ras-Tannura Asphalts

Polymer type	%P	T, °C	MSCR Recovery (%)		Diff (%)	Jnr (1/kPa)		Diff (%)
			0.1	3.2		0.1	3.2	
Unmodified	0%	64	4.2	1.5	64.286	3.24	3.81	14.961
		58	9.99	3.6	63.964	1.29	1.48	12.838
EE2	2%	70	12.998	3.7	71.534	3.314	3.043	34.282
		64	15.908	3.109	80.455	1.65	1.96	24.836
		58	23.258	12.001	48.403	0.657	0.825	20.408
	4%	76	28.39	7.44	73.793	1.616	3.482	53.576
		70	23.678	5.987	74.715	0.988	1.634	39.518
		64	29.033	6.624	77.186	0.446	0.675	33.927
		58	37.42	18.392	50.85	0.178	0.249	28.644
	6%	76	48.72	3.554	92.705	1.839	6.628	72.257
		70	70.961	5.624	92.074	0.206	1.206	82.9
		64	72.954	25.761	63.697	0.053	0.27	80.281
		58	78.839	52.38	28.201	0.03	0.064	53.102

Table B-3.2
MSCR results for EE2 modified Riyadh Asphalts

Polymer type	%P	T, °C	MSCR Recovery (%)		Diff (%)	Jnr (1/kPa)		Diff (%)
			0.1	3.2		0.1	3.2	
Unmodified	0%	64	2.70	0.98	63.7	4.277	5.715	25.2
		58	7.64	2.34	69.4	1.703	2.220	23.3
EE2	2%	70	10.14	2.74	73.0	4.374	5.340	18.1
		64	12.41	2.30	81.5	2.178	2.940	25.9
		58	18.14	8.88	51.0	0.867	1.238	29.9
	4%	76	22.14	5.51	75.1	2.133	5.223	59.2
		70	18.47	4.43	76.0	1.304	2.451	46.8
		64	22.65	4.90	78.4	0.589	1.013	41.9
		58	29.19	13.61	53.4	0.235	0.374	37.1
	6%	76	38.00	2.63	93.1	2.427	9.942	75.6
		70	55.35	4.16	92.5	0.272	1.809	85.0
		64	56.90	19.06	66.5	0.070	0.405	82.7
		58	61.49	38.76	37.0	0.040	0.096	58.8

Table B-4.1
MSCR results for PB modified Ras-Tannura Asphalts

Polymer type	%P	T, °C	MSCR Recovery (%)		Diff (%)	Jnr (1/kPa)		Diff (%)
			0.1	3.2		0.1	3.2	
Unmodified	0%	64	4.2	1.5	64.286	3.24	3.81	14.961
		58	9.99	3.6	63.964	1.29	1.48	12.838
Pb	2%	70	9.806	3.76	61.656	1.861	2.445	23.895
	2%	64	17.607	1.712	90.275	0.787	1.048	24.908
	2%	58	23.302	9.937	57.354	0.31	0.386	19.837
	4%	76	12.753	4.867	61.836	1.348	4.132	67.375
	4%	70	31.318	6.118	80.465	1.032	1.843	44.011
	4%	64	35.462	12.776	63.973	0.483	0.74	34.798
	4%	58	86.558	17.83	79.401	0.189	0.253	25.078
	6%	76	40.94	1.56	96.19	1.286	7.026	81.697
	6%	70	53.87	4.9	90.904	0.501	2.222	77.474
	6%	64	69.66	6.165	91.15	0.164	1.344	87.798
	6%	58	72.54	12.66	82.548	0.103	0.76	86.447

Table B-4.2
MSCR results for PB modified Riyadh Asphalts

Polymer type	%P	T, °C	MSCR Recovery (%)		Diff (%)	Jnr (1/kPa)		Diff (%)
			0.1	3.2		0.1	3.2	
Unmodified	0%	64	2.70	0.98	63.7	4.277	5.715	25.2
		58	7.64	2.34	69.4	1.703	2.220	23.3
Pb	2%	70	7.65	2.78	63.6	2.457	5.340	54.0
		64	13.73	1.27	90.8	1.039	6.340	83.6
		58	18.18	7.35	59.5	0.409	7.340	94.4
	4%	76	9.95	3.60	63.8	1.779	8.340	78.7
		70	24.43	4.53	81.5	1.362	9.340	85.4
		64	27.66	9.45	65.8	0.638	10.340	93.8
		58	67.52	13.19	80.5	0.249	11.340	97.8
	6%	76	31.93	1.15	96.4	1.698	12.340	86.2
		70	42.02	3.63	91.4	0.661	13.340	95.0
		64	54.33	4.56	91.6	0.216	14.340	98.5
		58	56.58	9.37	83.4	0.136	15.340	99.1

Appendix C

MSCR Recovery Rates and Recoverable Compliances

Table C- 1.

MSCR recovery rates and recoverable compliances (CR modified asphalts)

P	PG	Stress (kPa)	Temp. (^{0}C)	Jnr (1/kPa)	%R	RR_{NI}	RR_{NSS}	$\%R_{NI}$	$\%R_{NSS}$	$\dot{J}r_{NI}$	$\dot{J}r_{NSS}$
CR	**PG 70**	0.1	58	0.0031	52.0300	0.0045	0.0005	21.7000	2.2400	0.0447	0.0046
		0.1	64	0.0084	47.3600	0.0089	0.0010	18.1900	2.0200	0.0894	0.0099
		0.1	70	0.0181	45.2000	0.0181	0.0026	16.4400	2.3700	0.1806	0.0260
		0.1	76	0.8432	40.0000	0.0426	0.0075	14.0000	3.2900	0.4260	0.0749
		3.2	58	0.1579	31.0500	0.1189	0.0058	16.2300	0.8000	1.1894	0.0585
		3.2	64	0.4684	16.2400	0.1668	0.0081	9.3200	0.4500	1.6677	0.0809
		3.2	70	1.2474	5.2900	0.1724	0.0074	4.0900	0.1800	1.7244	0.0742
		3.2	76	2.8926	0.6400	0.1645	0.0070	1.7700	0.0700	1.6450	0.0699
	PG 76	0.1	58	0.0037	46.7100	0.0053	0.0003	23.8500	1.2700	0.0532	0.0028
		0.1	64	0.0109	34.1100	0.0098	0.0004	18.4600	0.8100	0.0977	0.0043
		0.1	70	0.0285	22.6400	0.0162	0.0005	13.8000	0.4000	0.1624	0.0047
		0.1	76	2.1023	15.3200	0.0258	0.0008	10.3900	0.3300	0.2580	0.0082
		3.2	58	0.1350	40.8000	0.1599	0.0062	21.9100	0.8600	1.5987	0.0624
		3.2	64	0.4195	23.3200	0.2458	0.0066	14.0400	0.3800	2.4580	0.0662
		3.2	70	1.1627	8.8600	0.2782	0.0044	6.8200	0.1100	2.7822	0.0443
		3.2	76	2.8302	1.8100	0.2569	0.0028	2.7900	0.0300	2.5688	0.0284
	PG 82	0.1	58	0.0039	56.9100	0.0073	0.0006	25.6200	2.1400	0.0731	0.0061
		0.1	64	0.0104	47.1100	0.0132	0.0132	21.1300	1.8200	0.1324	0.0114
		0.1	70	0.0308	30.1300	0.0212	0.0015	15.0600	1.0600	0.2124	0.0149
		0.1	76	2.2425	23.5900	0.0352	0.0025	12.0100	0.8400	0.3525	0.0246
		3.2	58	0.1823	39.8200	0.2074	0.2074	21.3900	0.8800	2.0738	0.0854
		3.2	64	0.5501	22.5100	0.2969	0.2969	13.0800	0.4600	2.9693	0.1049
		3.2	70	1.4713	9.7800	0.3456	0.0108	6.6200	0.2100	3.4555	0.1082
		3.2	76	3.5484	2.6000	0.3488	0.0080	2.9900	0.0700	3.4882	0.0805

Table C- 2.

MSCR recovery rates and recoverable compliances (EE2 modified asphalts)

P	PG	Stress (kPa)	Temp. (^{0}C)	Jnr (1/kPa)	%R	RR_{NI}	RR_{NSS}	$\%R_{NI}$	$\%R_{NSS}$	$\dot{J}r_{NI}$	$\dot{J}r_{NSS}$
EE2	**PG 70**	0.1	58	0.0206	23.1800	0.0111	0.0005	12.8900	0.5700	0.1107	0.0049
		0.1	64	0.0518	15.8500	0.0186	0.0008	9.4600	0.4200	0.1863	0.0082
		0.1	70	0.1040	12.9600	0.0321	0.0011	8.3900	0.2900	0.3206	0.0110
		3.2	58	0.8253	12.0000	0.2456	0.0060	8.1800	0.2000	2.4558	0.0605
		3.2	64	2.1957	5.4000	0.2574	0.0037	3.5500	0.0500	2.5740	0.0374
		3.2	70	5.0430	0.5000	0.2532	0.0028	0.2000	0.0200	2.5320	0.0281
	PG 76	0.1	58	0.0056	37.2700	0.0049	0.0004	17.0900	1.3600	0.0488	0.0039
		0.1	64	0.0140	28.9400	0.0085	0.0007	13.4500	1.1300	0.0848	0.0071
		0.1	70	0.0893	17.5400	0.0342	0.0016	9.8900	0.4600	0.3416	0.0159
		0.1	76	1.3798	17.0900	0.0670	0.0069	6.6300	2.2800	0.6695	0.0688
		3.2	58	0.2493	18.3900	0.1064	0.0038	10.8900	0.3900	1.0641	0.0384
		3.2	64	0.6752	6.6200	0.1200	0.0031	5.1900	0.1300	1.2001	0.0307
		3.2	70	3.5463	3.2000	0.2087	0.0044	1.8400	0.0400	2.0870	0.0439
		3.2	76	6.2517	0.9100	0.2517	0.0065	1.2800	0.0300	2.5172	0.0646
	PG 82	0.1	58	0.0010	78.4700	0.0043	0.0002	38.3300	1.3800	0.0428	0.0015
		0.1	64	0.0017	72.5400	0.0086	0.0086	34.1300	2.7300	0.0863	0.0069
		0.1	70	0.0065	70.6300	0.0218	0.0018	30.0900	2.5000	0.2182	0.0183
		0.1	76	1.8388	48.7200	0.0724	0.0071	20.3300	2.0000	0.7237	0.0710
		3.2	58	0.0642	52.4000	0.1060	0.0065	24.5700	1.5100	1.0597	0.0650
		3.2	64	0.2705	25.7600	0.1551	0.0082	13.3600	0.7100	1.5508	0.0819
		3.2	70	1.2060	5.6200	0.1785	0.0061	4.3700	0.1500	1.7852	0.0607
		3.2	76	6.6281	0.5100	0.3031	0.0093	1.4400	0.0400	3.0310	0.0927

Table C- 3.

MSCR recovery rates and recoverable compliances (PB modified asphalts)

P	PG	Stress (kPa)	Temp. (^{0}C)	Jnr (1/kPa)	%R	RR_{NI}	RR_{NSS}	$\%R_{NI}$	$\%R_{NSS}$	$\dot{J}r_{NI}$	$\dot{J}r_{NSS}$
Pb	PG 70	0.1	58	0.045	0.050	0.056	0.061	0.066	0.071	0.076	0.080
		0.1	64	0.095	0.106	0.117	0.128	0.139	0.150	0.160	0.171
		0.1	70	0.410	0.461	0.512	0.563	0.614	0.666	0.717	0.768
		3.2	58	1.516	1.696	1.875	2.055	2.236	2.417	2.597	2.779
		3.2	64	3.325	5.300	4.156	4.571	4.988	5.405	5.823	6.240
		3.2	70	0.410	0.600	0.512	0.001	0.310	0.500	0.717	0.002
	PG 76	0.1	58	0.035	0.039	0.042	0.046	0.050	0.053	0.057	0.060
		0.1	64	0.074	31.210	0.090	0.098	0.106	0.114	0.121	0.129
		0.1	70	0.136	30.000	0.164	0.178	0.192	0.206	0.218	0.231
		3.2	58	1.144	1.273	1.402	1.532	1.661	1.791	1.921	2.052
		3.2	64	2.584	2.901	3.218	3.537	4.010	4.178	4.500	4.821
		3.2	70	5.185	5.859	6.539	7.223	0.430	8.598	9.289	9.982
	PG 82	0.1	58	0.001	78.470	0.004	0.000	38.332	1.376	0.043	0.002
		0.1	64	0.002	69.300	0.009	0.009	34.130	2.735	0.086	0.007
		0.1	70	0.410	0.461	0.512	0.563	0.614	0.666	0.717	0.768
		3.2	58	0.064	52.400	0.106	0.007	24.573	1.505	1.060	0.065
		3.2	64	0.270	26.100	0.155	0.008	16.800	0.707	1.551	0.082
		3.2	70	0.410	0.461	0.512	0.563	0.614	0.666	0.717	0.000

APPENDIX – D

Job Mix Formula of Polymer Modified Asphalt Concretes

Table D-1

Volumetric parameters of designed samples using gradation #1

AC Mix	OAC (%)	G_{sb}	Av (%)	G_{mb}	VMA (%)	VFA (%)
G1U64	4.8	2.61	4.0	2.331	14.80	72.97
G1S70	4.8	2.61	4.0	2.341	14.52	72.46
G1S76	4.9	2.61	4.0	2.352	14.21	71.85
G1S82	5.0	2.61	4.0	2.357	14.21	71.85
G1EE70	4.7	2.61	4.0	2.342	14.49	72.39
G1EE76	4.8	2.61	4.0	2.346	14.43	72.28
G1EE82	4.9	2.61	4.0	2.351	14.34	72.10
G1CR70	5.2	2.61	4.0	2.313	15.99	74.98
G1CR76	5.4	2.61	4.0	2.344	15.04	73.41
G1CR82	5.6	2.61	4.0	2.381	13.88	71.19
G1Pb70	4.7	2.61	4.0	2.342	14.49	72.39
G1Pb76	4.8	2.61	4.0	2.345	14.47	72.35
G1Pb82	4.9	2.61	4.0	2.349	14.41	72.24

Table D-2

Volumetric parameters of designed samples using gradation #2

AC Mix	OAC (%)	G_{sb}	Av (%)	G_{mb}	VMA (%)	VFA (%)
G2U64	5.0	2.63	4.0	2.344	15.06	73.45
G2S70	5.0	2.63	4.0	2.349	14.88	73.12
G2S76	5.1	2.63	4.0	2.351	14.90	73.15
G2S82	5.2	2.63	4.0	2.353	14.92	73.18
G2EE70	5.0	2.63	4.0	2.342	15.14	73.57
G2EE76	5.1	2.63	4.0	2.346	15.08	73.48
G2EE82	5.2	2.63	4.0	2.351	14.99	73.31
G2CR70	5.2	2.63	4.0	2.313	16.63	75.94
G2CR76	5.3	2.63	4.0	2.344	15.60	74.36
G2CR82	5.4	2.63	4.0	2.381	14.36	72.14
G2Pb70	4.7	2.63	4.0	2.342	15.14	73.57
G2Pb76	4.8	2.63	4.0	2.345	15.12	73.54
G2Pb82	4.9	2.63	4.0	2.349	15.06	73.44

Table D-3

Volumetric parameters of designed samples using gradation #3

AC Mix	OAC (%)	G_{sb}	Av (%)	G_{mb}	VMA (%)	VFA (%)
G3U64	5.2	2.63	4.0	2.441	12.31	67.50
G3S70	5.2	2.63	4.0	2.398	13.85	71.13
G3S76	5.3	2.63	4.0	2.399	13.91	71.24
G3S82	5.3	2.63	4.0	2.401	14.02	71.46
G3EE70	4.7	2.63	4.0	2.366	14.91	73.18
G3EE76	4.8	2.63	4.0	2.37	14.86	73.08
G3EE82	4.9	2.63	4.0	2.356	15.45	74.11
G3CR70	5.3	2.63	4.0	2.36	15.66	74.46
G3CR76	5.5	2.63	4.0	2.364	15.70	74.52
G3CR82	5.7	2.63	4.0	2.40	14.60	72.60
G3Pb70	4.8	2.63	4.0	2.441	12.31	67.50
G3Pb76	4.8	2.63	4.0	2.444	11.53	65.32
G3Pb82	4.8	2.63	4.0	2.446	11.46	65.10

APPENDIX – E

Performance Grading of Polymer Modified Asphalt Binders

Table C.1.

PG and PG+ grading of CR Modified Asphalt Binders

Polymer	% P	T_{PG}, °C	**(PG)** (AASHTO M320)	Performance Grade Plus (PG^{+}) at 3.2 kPa stress and PG temperature (AASHTO TP70)			
				Testing Temperature, °C	Percent Recovery, %	Non-recoverable compliance (Jnr), 1/kPa	(PG+)
CR	5	73.96	PG 70	70	5.3	1.25	70 (H)
				64	16.2	0.47	64 (V)
				58	31.0	0.16	58 (E)
	7.5	79.2	PG 76	76	1.8	1.83	76 (H)
				70	8.9	0.96	70 (V)
				64	23.3	0.42	64 (E)
	10	83.6	PG 82	82	0.71	4.88	82(S)
				76	2.6	3.50	76 (S)
				70	9.8	1.47	70 (H)

Table C.2.

PG and PG+ grading of EE2 Modified Asphalt Binders

Polymer	%P	T_{PG}, °C	**Performance Grade (PG)** (AASHTO M320)	Performance Grade Plus (PG^{+}) at 3.2 kPa stress and PG temperature (AASHTO TP70)			
				Testing Temperature, °C	Percent Recovery, %	Non-recoverable compliance (Jnr), 1/kPa	Performance Grade (PG)
EE2	2	70.1	PG 70	70	0.41	5.04	70 (S)
				64	3.1	2.20	64 (S)
				58	12.0	0.83	58 (V)
	4	76.1	PG 76	76	1.0	3.5	76 (S)
				70	2.94	1.6	70 (H)
				64	6.6	0.68	64 (V)
	6	82.5	PG 82	82	1.9	10.0	82 (S)
				76	2.83	6.6	76 (S)
				70	5.8	2.51	70 (S)

Table C.3.

PG and PG+ grading of PB Modified Asphalt Binders

Polymer	%P	T_{PG}, °C	**Performance Grade (PG)** (AASHTO M320)	Performance Grade Plus (PG^{+}) at 3.2 kPa stress and PG temperature (AASHTO TP70)			
				Testing T, °C	R, %	Jnr, 1/kPa	Performance Grade (PG)
Pb	2	75.3	PG 70	70	1.34	2.45	70 (S)
				64	1.71	1.05	64 (H)
				58	9.9	0.39	58 (E)
	4	78.97	PG 76	76	1.2	4.13	76 (S)
				70	3.7	1.8	70 (H)
				64	5.8	0.74	64 (V)
	6	83.4	PG 82	76	2.3	6.74	76 (S)
				70	10.1	0.89	70 (V)
				64	16.76	0.497	64 (E)

APPENDIX – F

Results of Dynamic Modulus and Phase angle for Modified Mixes

Table F.1.1
Dynamic Modulus |E*| (MPa) and Phase angle, δ (degrees), test results for G1U64 at 25°C

	10Hz		5Hz		1Hz		0.1Hz	
Sample	|E*| (MPa)	δ (deg.)	|E*| (MPa)	δ (deg.)	|E*| (MPa)	δ (deg.)	|E*| (MPa)	δ (deg.)
S1	3662.1	24.9	3000.0	27.3	1710.3	32.4	758.6	32.8
S2	4869.0	23.1	3813.8	25.3	2455.2	30.2	1096.6	32.6
S3	3744.8	25.6	3013.8	28.5	1613.8	33.5	696.6	33.1
Average	4092.0	24.5	3275.9	27.0	1926.4	32.0	850.6	32.8
StDv	674.2	1.3	465.9	1.6	460.4	1.7	215.3	0.3

Table F.1.2
Dynamic Modulus |E*| (MPa) and Phase angle, δ (degrees), test results for G1U64 at 37.8°C

	10Hz		5Hz		1Hz		0.1Hz	
Sample	|E*| (MPa)	δ (deg.)	|E*| (MPa)	δ (deg.)	|E*| (MPa)	δ (deg.)	|E*| (MPa)	δ (deg.)
S1	1158.6	32.8	827.6	33.1	448.3	31.2	220.7	23.8
S2	1351.7	31.6	1213.8	32.3	620.7	30.6	324.1	25.5
S3	1075.9	34.1	806.9	34.4	358.6	31.8	206.9	23.5
Average	1195.4	32.8	949.4	33.3	475.9	31.2	250.6	24.3
StDv	141.56	1.3	229.2	1.1	133.2	0.6	64.1	1.1

Table F.1.3
Dynamic Modulus |E*| (MPa) and Phase angle, δ (degrees), test results for G1U64 at 54.4°C

	10Hz		5Hz		1Hz		0.1Hz	
Sample	|E*| (MPa)	δ (deg.)	|E*| (MPa)	δ (deg.)	|E*| (MPa)	δ (deg.)	|E*| (MPa)	δ (deg.)
S1	275.9	27.8	220.7	26.6	158.6	21.1	117.2	14.9
S2	455.2	31.6	1213.8	29.5	220.7	24.6	144.8	17.2
S3	262.1	28.4	806.9	27.6	144.8	21.5	110.3	15.8
Average	331.0	29.3	747.1	27.9	174.7	22.4	124.1	16.0
StDv	107.7	2.0	499.2	1.5	40.4	1.9	18.2	1.2

Table F.2.1
Dynamic Modulus |E*| (MPa) and Phase angle, δ (degrees), test results for G1S70 at 25°C

	10Hz		5Hz		1Hz		0.1Hz	
Sample	|E*| (MPa)	δ (deg.)	|E*| (MPa)	δ (deg.)	|E*| (MPa)	δ (deg.)	|E*| (MPa)	δ (deg.)
S1	4703.4	23.8	3951.7	26.7	2427.6	31.5	1034.5	31.2
S2	5089.7	24.1	4365.5	26.5	2489.7	31.2	917.2	32.5
S3	4765.5	24.2	4062.1	26.4	2117.2	31.8	869.0	30.7
Average	4852.9	24.0	4126.4	26.5	2344.8	31.5	940.2	31.5
StDv	207.39	0.21	214.27	0.15	199.52	0.30	85.12	0.93

Table F.2.2
Dynamic Modulus |E*| (MPa) and Phase angle, δ (degrees), test results for G1S70 at 37.8°C

	10Hz		5Hz		1Hz		0.1Hz	
Sample	|E*| (MPa)	δ (deg.)	|E*| (MPa)	δ (deg.)	|E*| (MPa)	δ (deg.)	|E*| (MPa)	δ (deg.)
S1	1682.8	30.5	1186.2	32.5	620.7	30.3	324.1	22.5
S2	1537.9	31.3	1144.8	33.1	579.3	31.6	303.4	21.0
S3	1593.1	29.7	1200.0	32.5	634.5	29.6	351.7	20.8
Average	1604.6	30.5	1177.0	32.7	611.5	30.5	326.4	21.4
StDv	73.09	0.80	28.71	0.35	28.71	1.01	24.22	0.93

Table F.2.3
Dynamic Modulus |E*| (MPa) and Phase angle, δ (degrees), test results for G1S70 at 54.4°C

	10Hz		5Hz		1Hz		0.1Hz	
Sample	|E*| (MPa)	δ (deg.)	|E*| (MPa)	δ (deg.)	|E*| (MPa)	δ (deg.)	|E*| (MPa)	δ (deg.)
S1	413.8	31.3	358.6	25.7	248.3	19.4	179.3	14.1
S2	503.4	29.5	400.0	24.5	303.4	18.1	241.4	12.7
S3	420.7	29	344.8	23.1	248.3	17.2	213.8	19.3
Average	446.0	29.9	367.8	24.4	266.7	18.2	211.5	15.4
StDv	49.89	1.21	28.71	1.30	31.85	1.11	31.10	3.48

Table F.3.1
Dynamic Modulus |E*| (MPa) and Phase angle, δ (degrees), test results for G1CR70 at 25°C

	10Hz		5Hz		1Hz		0.1Hz	
Sample	|E*| (MPa)	δ (deg.)	|E*| (MPa)	δ (deg.)	|E*| (MPa)	δ (deg.)	|E*| (MPa)	δ (deg.)
S1	5103.4	22.7	4262.1	25.1	2206.9	30.4	1110.3	30.5
S2	5441.4	21.5	4386.2	24.7	2537.9	28.9	1220.7	30.1
S3	4675.9	23.6	4137.9	25.7	2062.1	30.1	937.9	29.9
Average	5073.6	22.6	4262.1	25.2	2269.0	29.8	1089.7	30.2
StDv	383.63	1.05	124.14	0.50	243.93	0.79	142.51	0.31

Table F.3.2
Dynamic Modulus |E*| (MPa) and Phase angle, δ (degrees), test results for G1CR70 at 37.8°C

	10Hz		5Hz		1Hz		0.1Hz	
Sample	|E*| (MPa)	δ (deg.)	|E*| (MPa)	δ (deg.)	|E*| (MPa)	δ (deg.)	|E*| (MPa)	δ (deg.)
S1	1806.9	31.5	1496.6	32.1	717.2	29.9	365.5	22.2
S2	2075.9	30.9	1537.9	31.9	862.1	30.4	400.0	21.9
S3	1889.7	31	1379.3	30.8	793.1	30.8	379.3	21.7
Average	1924.1	31.1	1471.3	31.6	790.8	30.4	381.6	21.9
StDv	137.76	0.32	82.28	0.70	72.44	0.45	17.36	0.25

Table F.3.3
Dynamic Modulus |E*| (MPa) and Phase angle, δ (degrees), test results for G1CR70 at 54.4°C

	10Hz		5Hz		1Hz		0.1Hz	
Sample	|E*| (MPa)	δ (deg.)	|E*| (MPa)	δ (deg.)	|E*| (MPa)	δ (deg.)	|E*| (MPa)	δ (deg.)
S1	475.9	28.4	386.2	25.8	255.2	19.8	186.2	14.1
S2	531.0	26.9	413.8	24.1	275.9	18.4	248.3	12.4
S3	482.8	27.8	393.1	25.8	227.6	20.1	144.8	11.3
Average	496.6	27.7	397.7	25.2	252.9	19.4	193.1	12.6
StDv	30.06	0.75	14.36	0.98	24.22	0.91	52.07	1.41

Table F.4.1
Dynamic Modulus |E*| (MPa) and Phase angle, δ (degrees), test results for G1EE70 at 25°C

	10Hz		5Hz		1Hz		0.1Hz	
Sample	|E*| (MPa)	δ (deg.)	|E*| (MPa)	δ (deg.)	|E*| (MPa)	δ (deg.)	|E*| (MPa)	δ (deg.)
S1	4358.6	20.7	3751.7	25.6	2110.3	27.4	841.4	28.5
S2	3682.8	23.5	3462.1	24.9	1813.8	30.1	1241.4	28.9
S3	4075.9	22.7	3600.0	25.1	1979.3	30.6	931.0	29.4
Average	4039.1	22.3	3604.6	25.2	1967.8	29.4	1004.6	28.9
StDv	339.43	1.44	144.88	0.36	148.61	1.72	209.90	0.45

Table F.4.2
Dynamic Modulus |E*| (MPa) and Phase angle, δ (degrees), test results for G1EE70 at 37.8°C

	10Hz		5Hz		1Hz		0.1Hz	
Sample	|E*| (MPa)	δ (deg.)	|E*| (MPa)	δ (deg.)	|E*| (MPa)	δ (deg.)	|E*| (MPa)	δ (deg.)
S1	1524.1	33.2	1096.6	33.5	682.8	30.2	317.2	21.1
S2	1655.2	32.6	1220.7	32.9	586.2	29.5	496.6	20.4
S3	1620.7	32.1	1131.0	33.1	544.8	28.7	337.9	18.9
Average	1600.0	32.6	1149.4	33.2	604.6	29.5	383.9	20.1
StDv	67.92	0.55	64.08	0.31	70.78	0.75	98.10	1.12

Table F.4.3
Dynamic Modulus |E*| (MPa) and Phase angle, δ (degrees), test results for G1EE70 at 54.4°C

	10Hz		5Hz		1Hz		0.1Hz	
Sample	|E*| (MPa)	δ (deg.)	|E*| (MPa)	δ (deg.)	|E*| (MPa)	δ (deg.)	|E*| (MPa)	δ (deg.)
S1	413.8	25.3	351.7	22.6	275.9	15.6	241.4	10.4
S2	434.5	25.1	372.4	21.6	275.9	17.3	275.9	10.8
S3	420.7	26.7	365.5	23.4	262.1	18.8	262.1	12.6
Average	423.0	25.7	363.2	22.5	271.3	17.2	259.8	11.3
StDv	10.53	0.87	10.53	0.90	7.96	1.60	17.36	1.17

Table F.5.1
Dynamic Modulus |E*| (MPa) and Phase angle, δ (degrees), test results for G1PB70 at 25°C

	10Hz		5Hz		1Hz		0.1Hz	
Sample	|E*| (MPa)	δ (deg.)	|E*| (MPa)	δ (deg.)	|E*| (MPa)	δ (deg.)	|E*| (MPa)	δ (deg.)
S1	4206.9	21.2	3255.2	22.5	1869.0	27.8	855.2	26.4
S2	3986.2	22.9	3179.3	25.7	1779.3	30.1	793.1	25.3
S3	4600.0	22.6	3448.3	24.1	1951.7	26.7	917.2	26.6
Average	4264.4	22.2	3294.3	24.1	1866.7	28.2	855.2	26.1
StDv	310.91	0.91	138.68	1.60	86.23	1.73	62.07	0.70

Table F.5.2
Dynamic Modulus |E*| (MPa) and Phase angle, δ(degrees), test results for G1PB70 at 37.8°C

	10Hz		5Hz		1Hz		0.1Hz	
Sample	|E*| (MPa)	δ (deg.)	|E*| (MPa)	δ (deg.)	|E*| (MPa)	δ (deg.)	|E*| (MPa)	δ (deg.)
S1	1606.9	30.5	1269.0	31.6	751.7	28.6	386.2	25.6
S2	1517.2	31.5	1172.4	32.5	627.6	29.3	351.7	27.5
S3	1482.8	32.1	1241.4	33	682.8	29.1	365.5	26.9
Average	1535.6	31.4	1227.6	32.4	687.4	29.0	367.8	26.7
StDv	64.08	0.81	49.73	0.71	62.20	0.36	17.36	0.97

Table F.5.3
Dynamic Modulus |E*| (MPa) and Phase angle, δ(degrees), test results for G1PB70 at 54.4°C

	10Hz		5Hz		1Hz		0.1Hz	
Sample	|E*| (MPa)	δ (deg.)	|E*| (MPa)	δ (deg.)	|E*| (MPa)	δ (deg.)	|E*| (MPa)	δ (deg.)
S1	462.1	25.7	372.4	22.7	296.6	17.1	220.7	15.2
S2	420.7	24.4	351.7	21.4	310.3	15.9	234.5	13.4
S3	406.9	26.9	331.0	23.6	275.9	17.2	200.0	15.1
Average	429.9	25.7	351.7	22.6	294.3	16.7	218.4	14.6
StDv	28.71	1.25	20.69	1.11	17.36	0.72	17.36	1.01

Table F.6.1
Dynamic Modulus |E*| (MPa) and Phase angle, δ (degrees), test results for G1S76 at 25°C

	10Hz		5Hz		1Hz		0.1Hz	
Sample	|E*| (MPa)	δ (deg.)	|E*| (MPa)	δ (deg.)	|E*| (MPa)	δ (deg.)	|E*| (MPa)	δ (deg.)
S1	7586.2	18.4	6303.4	20.7	4234.5	26.1	2103.4	30.2
S2	7082.8	18.9	6075.9	21.3	4124.1	26.8	1958.6	30.1
S3	6765.5	18.7	5606.9	21.5	3944.8	26.4	1896.6	31.0
Average	7144.8	18.7	5995.4	21.2	4101.1	26.4	1986.2	30.4
StDv	413.85	0.25	355.18	0.42	146.19	0.35	106.17	0.49

Table F.6.2
Dynamic Modulus |E*| (MPa) and Phase angle, δ (degrees), test results for G1S76 at 37.8°C

	10Hz		5Hz		1Hz		0.1Hz	
Sample	|E*| (MPa)	δ (deg.)	|E*| (MPa)	δ (deg.)	|E*| (MPa)	δ (deg.)	|E*| (MPa)	δ (deg.)
S1	3048.3	27.1	2393.1	28.7	1303.4	30.5	641.4	26.8
S2	2579.3	30.2	2055.2	31.7	1131.0	35.7	544.8	31.2
S3	2751.7	28.7	2117.2	30.7	1172.4	31.3	489.7	27.2
Average	2793.1	28.7	2188.5	30.4	1202.3	32.5	558.6	28.4
StDv	237.21	1.55	179.88	1.53	90.01	2.80	76.80	2.43

Table F.6.3
Dynamic Modulus |E*| (MPa) and Phase angle, δ (degrees), test results for G1S76 at 54.4°C

	10Hz		5Hz		1Hz		0.1Hz	
Sample	|E*| (MPa)	δ (deg.)	|E*| (MPa)	δ (deg.)	|E*| (MPa)	δ (deg.)	|E*| (MPa)	δ (deg.)
S1	731.0	29.7	634.5	27.9	379.3	24.6	241.4	18.1
S2	703.4	30.4	579.3	28.5	358.6	24.1	262.1	17.3
S3	655.2	30.2	510.3	28.4	337.9	24.6	213.8	17.2
Average	696.6	30.1	574.7	28.3	358.6	24.4	239.1	17.5
StDv	38.40	0.36	62.20	0.32	20.69	0.29	24.22	0.49

Table F.7.1
Dynamic Modulus |E*| (MPa) and Phase angle, δ (degrees), test results for G1CR76 at 25°C

	10Hz		5Hz		1Hz		0.1Hz	
Sample	|E*| (MPa)	δ (deg.)	|E*| (MPa)	δ (deg.)	|E*| (MPa)	δ (deg.)	|E*| (MPa)	δ (deg.)
S1	7379.3	23.8	5800.0	25.6	3937.9	29.6	1731.0	30.1
S2	7869.0	23.1	6089.7	25.1	4275.9	30.1	1841.4	30.9
S3	6889.7	22.4	5586.2	24.9	3751.7	28.8	1593.1	29.1
Average	7379.3	23.1	5825.3	25.2	3988.5	29.5	1721.8	30.0
StDv	489.66	0.70	252.67	0.36	265.70	0.66	124.39	0.90

Table F.7.2
Dynamic Modulus |E*| (MPa) and Phase angle, δ (degrees), test results for G1CR76 at 37.8°C

	10Hz		5Hz		1Hz		0.1Hz	
Sample	|E*| (MPa)	δ (deg.)	|E*| (MPa)	δ (deg.)	|E*| (MPa)	δ (deg.)	|E*| (MPa)	δ (deg.)
S1	4165.5	32.8	2627.6	33.6	1048.3	34.9	455.2	33.7
S2	3724.1	32.6	2524.1	33.9	1013.8	33.8	372.4	33.1
S3	4344.8	30.9	2758.6	32.1	1165.5	33.2	482.8	32.6
Average	4078.2	32.1	2636.8	33.2	1075.9	34.0	436.8	33.1
StDv	319.43	1.04	117.51	0.96	79.53	0.86	57.43	0.55

Table F.7.3
Dynamic Modulus |E*| (MPa) and Phase angle, δ (degrees), test results for G1CR76 at 54.4°C

	10Hz		5Hz		1Hz		0.1Hz	
Sample	|E*| (MPa)	δ (deg.)	|E*| (MPa)	δ (deg.)	|E*| (MPa)	δ (deg.)	|E*| (MPa)	δ (deg.)
S1	586.2	38.4	427.6	36.1	200.0	34.6	82.8	27.1
S2	634.5	37.8	400.0	36.9	206.9	33.7	69.0	25.3
S3	682.8	37.5	489.7	36.3	248.3	34.1	131.0	27.9
Average	634.5	37.9	439.1	36.4	218.4	34.1	94.3	26.8
StDv	48.28	0.46	45.92	0.42	26.11	0.45	32.59	1.33

Table F.8.1
Dynamic Modulus |E*| (MPa) and Phase angle, δ (degrees), test results for G1EE76 at 25°C

	10Hz		5Hz		1Hz		0.1Hz	
Sample	|E*| (MPa)	δ (deg.)	|E*| (MPa)	δ (deg.)	|E*| (MPa)	δ (deg.)	|E*| (MPa)	δ (deg.)
S1	5537.9	20.7	4627.6	23.6	2889.7	28.3	1365.5	30.9
S2	5427.6	22.3	4593.1	24.2	2655.2	29.0	1151.7	32.1
S3	5627.6	21.4	4834.5	24.1	2848.3	30.1	1344.8	33.4
Average	5531.0	21.5	4685.1	24.0	2797.7	29.1	1287.4	32.1
StDv	100.18	0.80	130.55	0.32	125.16	0.91	117.92	1.25

Table F.8.2
Dynamic Modulus |E*| (MPa) and Phase angle, δ (degrees), test results for G1EE76 at 37.8°C

	10Hz		5Hz		1Hz		0.1Hz	
Sample	|E*| (MPa)	δ (deg.)	|E*| (MPa)	δ (deg.)	|E*| (MPa)	δ (deg.)	|E*| (MPa)	δ (deg.)
S1	1986.2	30.2	1524.1	31.7	820.7	32.7	351.7	29.1
S2	1903.4	30.4	1358.6	31.2	710.3	32.4	296.6	27.3
S3	1937.9	30.1	1406.9	32	758.6	32.1	324.1	26.5
Average	1942.5	30.2	1429.9	31.6	763.2	32.4	324.1	27.6
StDv	41.57	0.15	85.12	0.40	55.32	0.30	27.59	1.33

Table F.8.3
Dynamic Modulus |E*| (MPa) and Phase angle, δ (degrees), test results for G1EE76 at 54.4°C

	10Hz		5Hz		1Hz		0.1Hz	
Sample	|E*| (MPa)	δ (deg.)	|E*| (MPa)	δ (deg.)	|E*| (MPa)	δ (deg.)	|E*| (MPa)	δ (deg.)
S1	524.1	34.5	386.2	32.6	206.9	29.6	137.9	20.5
S2	420.7	34.1	331.0	32	186.2	28.1	124.1	19.5
S3	510.3	32.1	351.7	29.6	248.3	27.4	158.6	18.8
Average	485.1	33.6	356.3	31.4	213.8	28.4	140.2	19.6
StDv	56.17	1.29	27.87	1.59	31.60	1.12	17.36	0.85

Table F.9.1
Dynamic Modulus |E*| (MPa) and Phase angle, δ (degrees), test results for G1PB76 at 25°C

	10Hz		5Hz		1Hz		0.1Hz	
Sample	|E*| (MPa)	δ (deg.)	|E*| (MPa)	δ (deg.)	|E*| (MPa)	δ (deg.)	|E*| (MPa)	δ (deg.)
S1	5032.9	22.5	4118.7	23.5	2521.3	28.7	1138.7	30.4
S2	5228.5	27.2	4500.4	30.1	2694.5	32.4	1148.4	30.6
S3	4975.1	26.4	4170.0	28.0	2514.8	33.1	1113.1	31.1
Average	5078.9	25.4	4263.0	27.2	2576.9	31.4	1133.4	30.7
StDv	132.81	2.51	207.16	3.37	101.91	2.36	18.24	0.36

Table F.9.2
Dynamic Modulus |E*| (MPa) and Phase angle, δ (degrees), test results for G1PB76 at 37.8°C

	10Hz		5Hz		1Hz		0.1Hz	
Sample	|E*| (MPa)	δ (deg.)	|E*| (MPa)	δ (deg.)	|E*| (MPa)	δ (deg.)	|E*| (MPa)	δ (deg.)
S1	1748.2	28.0	1632.7	31.0	680.0	30.5	311.1	24.2
S2	1767.4	32.0	1292.7	33.7	654.4	32.6	298.3	24.5
S3	1575.0	31.7	1154.8	40.1	628.7	32.7	291.9	24.8
Average	1696.9	30.6	1360.1	34.9	654.4	31.9	300.5	24.5
StDv	106.00	2.23	245.99	4.67	25.66	1.24	9.80	0.30

Table F.9.3
Dynamic Modulus |E*| (MPa) and Phase angle, δ (degrees), test results for G1PB76 at 54.4°C

	10Hz		5Hz		1Hz		0.1Hz	
Sample	|E*| (MPa)	δ (deg.)	|E*| (MPa)	δ (deg.)	|E*| (MPa)	δ (deg.)	|E*| (MPa)	δ (deg.)
S1	449.8	31.1	344.8	29.4	203.9	26.2	124.1	18.1
S2	406.9	29.2	335.8	27.1	200.9	20.5	117.2	12.5
S3	410.8	31.5	296.9	29.9	186.2	22.4	137.9	13.8
Average	422.5	30.6	325.8	28.8	197.0	23.0	126.4	14.8
StDv	23.71	1.23	25.50	1.49	9.47	2.90	10.53	2.93

Table F.10.1
Dynamic Modulus |E*| (MPa) and Phase angle, δ (degrees), test results for G1S82 at 25°C

	10Hz		5Hz		1Hz		0.1Hz	
Sample	|E*| (MPa)	δ (deg.)	|E*| (MPa)	δ (deg.)	|E*| (MPa)	δ (deg.)	|E*| (MPa)	δ (deg.)
S1	8206.9	20.9	6820.7	23.2	4896.6	26.7	2351.7	30.1
S2	8282.8	21.1	6944.8	22.4	4951.7	25.9	2448.3	28.4
S3	7951.7	20.3	6765.5	22.1	4779.3	25.3	2358.6	30.7
Average	8147.1	20.8	6843.7	22.6	4875.9	26.0	2386.2	29.7
StDv	173.42	0.42	91.84	0.57	88.05	0.70	53.86	1.19

Table F.10.2
Dynamic Modulus |E*| (MPa) and Phase angle, δ (degrees), test results for G1S82 at 37.8°C

	10Hz		5Hz		1Hz		0.1Hz	
Sample	|E*| (MPa)	δ (deg.)	|E*| (MPa)	δ (deg.)	|E*| (MPa)	δ (deg.)	|E*| (MPa)	δ (deg.)
S1	4034.5	30.2	2627.6	31.2	1310.3	33.4	517.2	33.5
S2	3910.3	30.6	2689.7	31.7	1393.1	33.7	482.8	33.8
S3	3827.6	29.4	2496.6	30.9	1731.0	34.1	551.7	33.2
Average	3924.1	30.1	2604.6	31.3	1478.2	33.7	517.2	33.5
StDv	104.14	0.61	98.58	0.40	222.87	0.35	34.48	0.30

Table F.10.3
Dynamic Modulus |E*| (MPa) and Phase angle, δ (degrees), test results for G1S82 at 54.5°C

	10Hz		5Hz		1Hz		0.1Hz	
Sample	|E*| (MPa)	δ (deg.)	|E*| (MPa)	δ (deg.)	|E*| (MPa)	δ (deg.)	|E*| (MPa)	δ (deg.)
S1	793.1	38.3	544.8	37.7	213.8	36.6	82.8	32.7
S2	869.0	37.5	586.2	36.9	248.3	35.4	117.2	31.4
S3	896.6	37.3	620.7	36.4	275.9	34.9	131.0	30.1
Average	852.9	37.7	583.9	37.0	246.0	35.6	110.3	31.4
StDv	53.57	0.53	37.98	0.66	31.10	0.87	24.87	1.30

Table F.11.1
Dynamic Modulus |E*| (MPa) and Phase angle, δ (degrees), test results for G1CR82 at 25°C

	10Hz		5Hz		1Hz		0.1Hz	
Sample	|E*| (MPa)	δ (deg.)	|E*| (MPa)	δ (deg.)	|E*| (MPa)	δ (deg.)	|E*| (MPa)	δ (deg.)
S1	6172.4	20.5	5131.0	22.9	3165.5	28.5	1400.0	31.6
S2	7724.1	19.4	6779.3	21.5	4069.0	26.3	1917.2	30.6
S3	6158.6	20.3	5227.6	22.8	3110.3	28.9	1448.3	32.5
Average	6685.1	20.1	5712.6	22.4	3448.3	27.9	1588.5	31.6
StDv	899.9	0.6	925.0	0.8	538.2	1.4	285.7	1.0

Table F.11.2
Dynamic Modulus |E*| (MPa) and Phase angle, δ (degrees), test results for G1CR82 at 37.8°C

	10Hz		5Hz		1Hz		0.1Hz	
Sample	|E*| (MPa)	δ (deg.)	|E*| (MPa)	δ (deg.)	|E*| (MPa)	δ (deg.)	|E*| (MPa)	δ (deg.)
S1	2200.0	29.7	1689.7	30.8	937.9	30.6	427.6	25.4
S2	3131.0	28.6	2317.2	30.1	1275.9	31.3	600.0	27.4
S3	2179.3	30.5	1917.2	31.8	937.9	31.6	400.0	27.7
Average	2503.4	29.6	1974.7	30.9	1050.6	31.2	475.9	26.8
StDv	543.6	1.0	317.7	0.9	195.1	0.5	108.4	1.3

Table F.11.3
Dynamic Modulus |E*| (MPa) and Phase angle, δ (degrees), test results for G1CR82 at 54.4°C

54.4	10Hz		5Hz		1Hz		0.1Hz	
Sample	|E*| (MPa)	δ (deg.)	|E*| (MPa)	δ (deg.)	|E*| (MPa)	δ (deg.)	|E*| (MPa)	δ (deg.)
S1	731.0	30.5	565.5	29.2	337.9	25.7	200.0	19.3
S2	1006.9	31.4	724.1	30.3	489.7	26.4	310.3	18.9
S3	682.8	31.1	531.0	30.1	303.4	25.9	200.0	19
Average	806.9	31.0	606.9	29.9	377.0	26.0	236.8	19.1
StDv	174.9	0.5	103.0	0.6	99.1	0.4	63.7	0.2

Table F.12.1
Dynamic Modulus |E*| (MPa) and Phase angle, δ (degrees), test results for G1EE82 at 25°C

25	10Hz		5Hz		1Hz		0.1Hz	
Sample	|E*| (MPa)	δ (deg.)	|E*| (MPa)	δ (deg.)	|E*| (MPa)	δ (deg.)	|E*| (MPa)	δ (deg.)
S1	6896.6	22.8	5862.1	24.4	3800.0	28.3	1758.621	31.8
S2	8096.6	21.4	6144.8	23	4620.7	26.7	2193.103	30.4
S3	7572.4	20.8	6041.4	21.9	4241.4	25.2	2482.759	29
Average	7521.8	21.7	6016.1	23.1	4220.7	26.7	2144.8	30.4
StDv	601.60	1.03	143.07	1.25	410.74	1.55	364.47	1.40

Table F.12.2
Dynamic Modulus |E*| (MPa) and Phase angle, δ (degrees), test results for G1EE82 at 37.8°C

37.8	10Hz		5Hz		1Hz		0.1Hz	
Sample	|E*| (MPa)	δ (deg.)	|E*| (MPa)	δ (deg.)	|E*| (MPa)	δ (deg.)	|E*| (MPa)	δ (deg.)
S1	2979.3	30.8	2324.1	31.5	1220.7	33.2	413.79	33.1
S2	3179.3	29.4	2455.2	30.5	1365.5	32.5	524.14	32.6
S3	3455.2	28.1	3248.3	29.6	1448.3	32.6	551.72	34.9
Average	3204.6	29.4	2675.9	30.5	1344.8	32.8	496.6	33.5
StDv	238.94	1.35	500.04	0.95	115.20	0.38	72.99	1.21

Table F.12.3
Dynamic Modulus |E*| (MPa) and Phase angle, δ (degrees), test results for G1EE82 at 54.4°C

54.4	10Hz		5Hz		1Hz		0.1Hz	
Sample	|E*| (MPa)	δ (deg.)	|E*| (MPa)	δ (deg.)	|E*| (MPa)	δ (deg.)	|E*| (MPa)	δ (deg.)
S1	620.7	37.1	455.2	36.4	179.3	33.6	96.6	27.4
S2	751.7	36.5	551.7	36.1	269.0	34.5	117.2	29.4
S3	965.5	36.1	710.3	35.9	331.0	34.7	131.0	28.3
Average	779.3	36.6	572.4	36.1	259.8	34.3	114.9	28.4
StDv	174.06	0.50	128.84	0.25	76.28	0.59	17.36	1.00

Table F.13.1
Dynamic Modulus |E*| (MPa) and Phase angle, δ (degrees), test results for G1PB82 at 25°C

	10Hz		5Hz		1Hz		0.1Hz	
Sample	|E*| (MPa)	δ (deg.)	|E*| (MPa)	δ (deg.)	|E*| (MPa)	δ (deg.)	|E*| (MPa)	δ (deg.)
S1	5282.8	22.8	4227.6	25.3	2531.0	30.4	1082.8	32.6
S2	5813.8	21.2	5082.8	23.5	3137.9	29.1	1317.2	31.2
S3	5069.0	22.3	4131.0	24.1	2558.6	29.9	1048.3	31.1
Average	5388.5	22.1	4480.5	24.3	2742.5	29.8	1149.4	31.6
StDv	383.51	0.82	523.84	0.92	342.71	0.66	146.35	0.84

Table F.13.2
Dynamic Modulus |E*| (MPa) and Phase angle, δ (degrees), test results for G1PB82 at 37.8°C

	10Hz		5Hz		1Hz		0.1Hz	
Sample	|E*| (MPa)	δ (deg.)	|E*| (MPa)	δ (deg.)	|E*| (MPa)	δ (deg.)	|E*| (MPa)	δ (deg.)
S1	1772.4	31.4	1986.2	32.5	641.4	31.4	317.2	26.6
S2	1896.6	30.7	1420.7	32	696.6	31.6	344.8	27.1
S3	1448.3	30.7	1075.9	31.4	593.1	30.8	303.4	25.6
Average	1705.7	30.9	1494.3	32.0	643.7	31.3	321.8	26.4
StDv	231.45	0.40	459.61	0.55	51.76	0.42	21.07	0.76

Table F.13.3
Dynamic Modulus |E*| (MPa) and Phase angle, δ (degrees), test results for G1PB82 at 54.4°C

	10Hz		5Hz		1Hz		0.1Hz	
Sample	|E*| (MPa)	δ (deg.)	|E*| (MPa)	δ (deg.)	|E*| (MPa)	δ (deg.)	|E*| (MPa)	δ (deg.)
S1	510.3	31.8	406.9	28.9	262.1	25.4	158.6	16.9
S2	537.9	31.2	441.4	29.6	275.9	25.8	172.4	17.1
S3	434.5	29.6	331.0	28.1	213.8	24.1	137.9	15.8
Average	494.3	30.9	393.1	28.9	250.6	25.1	156.3	16.6
StDv	53.57	1.14	56.45	0.75	32.59	0.89	17.36	0.70

Table F.14.1
Dynamic Modulus |E*| (MPa) and Phase angle, δ (degrees), test results for G2U64 at 25°C

	10Hz		5Hz		1Hz		0.1Hz	
Sample	|E*| (MPa)	δ (deg.)	|E*| (MPa)	δ (deg.)	|E*| (MPa)	δ (deg.)	|E*| (MPa)	δ (deg.)
S1	5841.4	22.8	4986.2	24.6	2965.5	30.1	1558.6	35.6
S2	6137.9	22.4	5131.0	23.9	3082.8	29.6	1379.3	31.9
S3	5262.1	21.6	4848.3	23.1	2758.6	28.8	1310.3	31.6
Average	5747.1	22.3	4988.5	23.9	2935.6	29.5	1416.1	33.0
StDv	445.47	0.61	141.39	0.75	164.12	0.66	128.16	2.23

Table F.14.2
Dynamic Modulus |E*| (MPa) and Phase angle, δ (degrees), test results for G2U64 at 37.8°C

	10Hz		5Hz		1Hz		0.1Hz	
Sample	|E*| (MPa)	δ (deg.)	|E*| (MPa)	δ (deg.)	|E*| (MPa)	δ (deg.)	|E*| (MPa)	δ (deg.)
S1	2317.2	31.5	1903.4	31.1	1034.5	33.5	593.1	36.1
S2	2724.1	28.1	2110.3	28.5	1179.3	31.7	531.0	27.3
S3	2248.3	28.5	1924.1	28.1	986.2	29.9	544.8	20.1
Average	2429.9	29.4	1979.3	29.2	1066.7	31.7	556.3	27.8
StDv	257.15	1.86	113.95	1.63	100.49	1.80	32.59	8.01

Table F.14.3
Dynamic Modulus |E*| (MPa) and Phase angle, δ (degrees), test results for G2U64 at 54.4°C

	10Hz		5Hz		1Hz		0.1Hz	
Sample	|E*| (MPa)	δ (deg.)	|E*| (MPa)	δ (deg.)	|E*| (MPa)	δ (deg.)	|E*| (MPa)	δ (deg.)
S1	731.0	32.7	586.2	31.5	372.4	28.9	365.5	23.7
S2	903.4	30.1	758.6	30.0	510.3	28.3	262.1	22.5
S3	751.7	29.1	572.4	27.3	413.8	26.1	303.4	26.1
Average	795.4	30.6	639.1	29.6	432.2	27.8	310.3	24.1
StDv	94.14	1.86	103.75	2.13	70.78	1.47	52.07	1.83

Table F.15.1
Dynamic Modulus |E*| (MPa) and Phase angle, δ (degrees), test results for G2S70 at 25°C

	10Hz		5Hz		1Hz		0.1Hz	
Sample	|E*| (MPa)	δ (deg.)	|E*| (MPa)	δ (deg.)	|E*| (MPa)	δ (deg.)	|E*| (MPa)	δ (deg.)
S1	6200.0	20.0	5227.6	23.6	3331.0	27.1	1606.9	29.5
S2	6420.7	21.6	5675.9	22.9	3434.5	29.5	1503.4	32.4
S3	6731.0	19.6	5965.5	24.1	3482.8	30.2	1958.6	29.6
Average	6450.6	20.4	5623.0	23.5	3416.1	28.9	1689.7	30.5
StDv	266.78	1.06	371.80	0.60	77.52	1.63	238.60	1.65

Table F.15.2
Dynamic Modulus |E*| (MPa) and Phase angle, δ (degrees), test results for G2S70 at 37.8°C

	10Hz		5Hz		1Hz		0.1Hz	
Sample	|E*| (MPa)	δ (deg.)	|E*| (MPa)	δ (deg.)	|E*| (MPa)	δ (deg.)	|E*| (MPa)	δ (deg.)
S1	2986.2	27.2	2206.9	28.3	1248.3	30.1	606.9	25.8
S2	2717.2	28.4	2310.3	29.4	1310.3	29.4	558.6	25.7
S3	3544.8	26.7	2793.1	28.1	1496.6	30.1	758.6	26.4
Average	3082.8	27.4	2436.8	28.6	1351.7	29.9	641.4	26.0
StDv	422.16	0.87	312.89	0.70	129.21	0.40	104.36	0.38

Table F.15.3
Dynamic Modulus |E*| (MPa) and Phase angle, δ (degrees), test results for G2S70 at 54.4°C

	10Hz		5Hz		1Hz		0.1Hz	
Sample	|E*| (MPa)	δ (deg.)	|E*| (MPa)	δ (deg.)	|E*| (MPa)	δ (deg.)	|E*| (MPa)	δ (deg.)
S1	855.2	28.6	648.3	29.3	455.2	25.2	248.3	20.3
S2	1124.1	27.4	889.7	27.4	503.4	24.7	379.3	17.5
S3	1089.7	28.4	806.9	28.3	420.7	24.3	324.1	18.2
Average	1023.0	28.1	781.6	28.3	459.8	24.7	317.2	18.7
StDv	146.35	0.64	122.66	0.95	41.57	0.45	65.79	1.46

Table F.16.1
Dynamic Modulus |E*| (MPa) and Phase angle, δ (degrees), test results for G2CR70 at 25°C

	10Hz		5Hz		1Hz		0.1Hz	
Sample	|E*| (MPa)	δ (deg.)	|E*| (MPa)	δ (deg.)	|E*| (MPa)	δ (deg.)	|E*| (MPa)	δ (deg.)
S1	6710.3	22.4	5689.7	25.3	3248.3	31.0	1531.0	29.2
S2	7186.2	30.3	6165.5	24.9	3455.2	31.2	1731.0	30.1
S3	8558.6	22.5	6289.7	25.3	3937.9	30.5	1937.9	31.2
Average	7485.1	25.1	6048.3	25.2	3547.1	30.9	1733.3	30.2
StDv	959.70	4.53	316.72	0.23	353.90	0.36	203.46	1.00

Table F.16.1
Dynamic Modulus |E*| (MPa) and Phase angle, δ (degrees), test results for G2CR70 at 37.8°C

	10Hz		5Hz		1Hz		0.1Hz	
Sample	|E*| (MPa)	δ (deg.)	|E*| (MPa)	δ (deg.)	|E*| (MPa)	δ (deg.)	|E*| (MPa)	δ (deg.)
S1	2448.3	31.6	1917.2	31.3	1137.9	28.5	558.6	24.8
S2	2655.2	28.5	2131.0	28.9	1262.1	30.4	586.2	23.5
S3	2869.0	30.1	2310.3	29.1	1386.2	29.1	737.9	23.5
Average	2657.5	30.1	2119.5	29.8	1262.1	29.3	627.6	23.9
StDv	210.35	1.55	196.80	1.33	124.14	0.97	96.55	0.75

Table F.16.1
Dynamic Modulus |E*| (MPa) and Phase angle, δ (degrees), test results for G2CR70 at 54.4°C

	10Hz		5Hz		1Hz		0.1Hz	
Sample	|E*| (MPa)	δ (deg.)	|E*| (MPa)	δ (deg.)	|E*| (MPa)	δ (deg.)	|E*| (MPa)	δ (deg.)
S1	813.8	27.1	655.2	25.2	462.1	22.1	337.9	16.9
S2	827.6	28.6	696.6	26.3	441.4	21.6	365.5	15.1
S3	1241.4	27.1	972.4	25.4	620.7	22.4	455.2	12.8
Average	960.9	27.6	774.7	25.6	508.0	22.0	386.2	14.9
StDv	242.98	0.87	172.46	0.59	98.10	0.40	61.30	2.06

Table F.17.1
Dynamic Modulus |E*| (MPa) and Phase angle, δ (degrees), test results for G2EE70 at 25°C

	10Hz		5Hz		1Hz		0.1Hz	
Sample	|E*| (MPa)	δ (deg.)	|E*| (MPa)	δ (deg.)	|E*| (MPa)	δ (deg.)	|E*| (MPa)	δ (deg.)
S1	5475.9	22.6	4531.0	24.7	3469.0	27.3	1827.6	29.3
S2	5400.0	22.9	4269.0	25.3	3186.2	30.1	1351.7	30.1
S3	6020.7	21.1	5400.0	23.7	2986.2	27.4	1793.1	28.4
Average	5632.2	22.2	4733.3	24.6	3213.8	28.3	1657.5	29.3
StDv	338.59	0.96	592.03	0.81	242.56	1.59	265.35	0.85

Table F.17.2
Dynamic Modulus |E*| (MPa) and Phase angle, δ (degrees), test results for G2EE70 at 37.8°C

	10Hz		5Hz		1Hz		0.1Hz	
Sample	|E*| (MPa)	δ (deg.)	|E*| (MPa)	δ (deg.)	|E*| (MPa)	δ (deg.)	|E*| (MPa)	δ (deg.)
S1	2413.8	27.1	1951.7	28.5	1165.5	30.1	655.2	24.9
S2	2206.9	29.1	1813.8	29.3	1055.2	28.5	579.3	23.1
S3	2062.1	27.3	1648.3	27.5	986.2	29.3	482.8	24.1
Average	2227.6	27.8	1804.6	28.4	1069.0	29.3	572.4	24.0
StDv	176.77	1.10	151.93	0.90	90.45	0.80	86.41	0.90

Table F.17.3
Dynamic Modulus |E*| (MPa) and Phase angle, δ (degrees), test results for G2EE70 at 54.4°C

	10Hz		5Hz		1Hz		0.1Hz	
Sample	|E*| (MPa)	δ (deg.)	|E*| (MPa)	δ (deg.)	|E*| (MPa)	δ (deg.)	|E*| (MPa)	δ (deg.)
S1	806.9	27.5	655.2	28.4	510.3	30.0	413.8	24.7
S2	648.3	24.1	551.7	29.4	420.7	29.1	220.7	22.5
S3	751.7	25.9	600.0	27.4	358.6	29.4	324.1	25.1
Average	735.6	25.8	602.3	28.4	429.9	29.5	319.5	24.1
StDv	80.53	1.70	51.76	1.00	76.28	0.46	96.63	1.40

Table F.18.1
Dynamic Modulus |E*| (MPa) and Phase angle, δ (degrees), test results for G2PB70 at 25°C

	10Hz		5Hz		1Hz		0.1Hz	
Sample	|E*| (MPa)	δ (deg.)	|E*| (MPa)	δ (deg.)	|E*| (MPa)	δ (deg.)	|E*| (MPa)	δ (deg.)
S1	7517.2	22.7	6351.7	24.1	3979.3	28	1800.0	32.1
S2	7703.4	21.7	6482.8	23.4	4186.2	26.9	2034.5	30.6
S3	8827.6	22.4	6786.2	23.8	4372.4	27.3	2075.9	30.4
Average	8016.1	22.3	6540.2	23.8	4179.3	27.4	1970.1	31.0
StDv	708.91	0.51	222.87	0.35	196.64	0.56	148.77	0.93

Table F.18.2
Dynamic Modulus |E*| (MPa) and Phase angle, δ (degrees), test results for G2PB70 at 37.8°C

	10Hz		5Hz		1Hz		0.1Hz	
Sample	|E*| (MPa)	δ (deg.)	|E*| (MPa)	δ (deg.)	|E*| (MPa)	δ (deg.)	|E*| (MPa)	δ (deg.)
S1	3062.1	32.1	2420.7	33.1	1213.8	35.2	455.2	35.2
S2	2889.7	30.9	2324.1	31.8	1296.6	33.5	482.8	32.8
S3	3172.4	30.6	2565.5	31.4	1441.4	33	579.3	32.3
Average	3041.4	31.2	2436.8	32.1	1317.2	33.9	505.7	33.4
StDv	142.51	0.79	121.49	0.89	115.20	1.15	65.18	1.55

Table F.18.3
Dynamic Modulus |E*| (MPa) and Phase angle, δ (degrees), test results for G2PB70 at 54.4°C

	10Hz		5Hz		1Hz		0.1Hz	
Sample	|E*| (MPa)	δ (deg.)	|E*| (MPa)	δ (deg.)	|E*| (MPa)	δ (deg.)	|E*| (MPa)	δ (deg.)
S1	572.4	38.3	420.7	37.5	186.2	32.9	103.4	29
S2	717.2	37	503.4	36.2	269.0	32.5	110.3	29
S3	827.6	36.4	606.9	35.6	275.9	31.6	131.0	28.1
Average	705.7	37.2	510.3	36.4	243.7	32.3	114.9	28.7
StDv	127.97	0.97	93.29	0.97	49.89	0.67	14.36	0.52

Table F.19.1
Dynamic Modulus |E*| (MPa) and Phase angle, δ (degrees), test results for G2S76 at 25°C

	10Hz		5Hz		1Hz		0.1Hz	
Sample	|E*| (MPa)	δ (deg.)	|E*| (MPa)	δ (deg.)	|E*| (MPa)	δ (deg.)	|E*| (MPa)	δ (deg.)
S1	6241.4	18.9	5193.1	21.6	3324.1	26.4	1800.0	28.3
S2	6020.7	20.2	5062.1	22.5	3075.9	25.1	1710.3	29.5
S3	6075.9	19.5	5351.7	20.8	3255.2	27.0	1662.1	28.4
Average	6112.6	19.5	5202.3	21.6	3218.4	26.2	1724.1	28.7
StDv	114.85	0.65	145.05	0.85	128.16	0.97	69.99	0.67

Table F.19.2
Dynamic Modulus |E*| (MPa) and Phase angle, δ (degrees), test results for G2S76 at 37.8°C

	10Hz		5Hz		1Hz		0.1Hz	
Sample	|E*| (MPa)	δ (deg.)	|E*| (MPa)	δ (deg.)	|E*| (MPa)	δ (deg.)	|E*| (MPa)	δ (deg.)
S1	2689.7	26.4	2186.2	27.3	1275.9	30.5	620.7	27.4
S2	2937.9	25.9	2420.7	27.9	1372.4	29.1	758.6	28.3
S3	2737.9	27.6	2372.4	25.3	1089.7	28.7	579.3	25.1
Average	2788.5	26.6	2326.4	26.8	1246.0	29.4	652.9	26.9
StDv	131.64	0.87	123.82	1.36	143.73	0.95	93.89	1.65

Table F.19.3
Dynamic Modulus |E*| (MPa) and Phase angle, δ (degrees), test results for G2S76 at 54.4°C

	10Hz		5Hz		1Hz		0.1Hz	
Sample	|E*| (MPa)	δ (deg.)	|E*| (MPa)	δ (deg.)	|E*| (MPa)	δ (deg.)	|E*| (MPa)	δ (deg.)
S1	937.9	26.7	696.6	24.8	489.7	23.4	351.7	15.3
S2	896.6	25.1	682.8	25.1	475.9	22.9	324.1	12.9
S3	813.8	26.1	820.7	23.7	503.4	21.4	379.3	14.7
Average	882.8	26.0	733.3	24.5	489.7	22.6	351.7	14.3
StDv	63.21	0.81	75.97	0.74	13.79	1.04	27.59	1.25

Table F.20.1
Dynamic Modulus |E*| (MPa) and Phase angle, δ (degrees), test results for G2CR76 at 25°C

	10Hz		5Hz		1Hz		0.1Hz	
Sample	|E*| (MPa)	δ (deg.)	|E*| (MPa)	δ (deg.)	|E*| (MPa)	δ (deg.)	|E*| (MPa)	δ (deg.)
S1	8896.6	14.8	8013.8	18.4	5710.3	22.3	3227.6	26.3
S2	7379.3	15.3	6627.6	14.9	4944.8	22.6	2675.9	25.6
S3	7675.9	16.9	6806.9	17.3	5110.3	20.1	2551.7	27.7
Average	7983.9	15.7	7149.4	16.9	5255.2	21.7	2818.4	26.5
StDv	804.16	1.10	753.91	1.79	402.78	1.37	359.77	1.07

Table F.20.2
Dynamic Modulus |E*| (MPa) and Phase angle, δ (degrees), test results for G2CR76 at 37.8°C

	10Hz		5Hz		1Hz		0.1Hz	
Sample	|E*| (MPa)	δ (deg.)	|E*| (MPa)	δ (deg.)	|E*| (MPa)	δ (deg.)	|E*| (MPa)	δ (deg.)
S1	3551.7	24.5	2682.8	26.4	1751.7	28.3	848.3	26.7
S2	2779.3	24.7	2420.7	26.3	1241.4	28.9	662.1	25.4
S3	3082.8	27.3	2606.9	28.5	1172.4	30.1	565.5	25.9
Average	3137.9	25.5	2570.1	27.1	1388.5	29.1	692.0	26.0
StDv	389.15	1.56	134.85	1.24	316.44	0.92	143.73	0.66

Table F.20.3
Dynamic Modulus |E*| (MPa) and Phase angle, δ (degrees), test results for G2CR76 at 54.4°C

	10Hz		5Hz		1Hz		0.1Hz	
Sample	|E*| (MPa)	δ (deg.)	|E*| (MPa)	δ (deg.)	|E*| (MPa)	δ (deg.)	|E*| (MPa)	δ (deg.)
S1	1275.9	27.4	1020.7	27.8	544.8	26.3	344.8	20.2
S2	924.1	28.6	731.0	28.1	413.8	25.4	303.4	17.3
S3	875.9	28.4	682.8	27.6	372.4	23.8	262.1	17.3
Average	1025.3	28.1	811.5	27.8	443.7	25.2	303.4	18.3
StDv	218.34	0.64	182.77	0.25	90.01	1.27	41.38	1.67

Table F.21.1
Dynamic Modulus |E*| (MPa) and Phase angle, δ (degrees), test results for G2EE76 at 25°C

	10Hz		5Hz		1Hz		0.1Hz	
Sample	|E*| (MPa)	δ (deg.)	|E*| (MPa)	δ (deg.)	|E*| (MPa)	δ (deg.)	|E*| (MPa)	δ (deg.)
S1	8206.9	20.1	6820.7	21.9	4682.8	25.1	2469.0	30.1
S2	8724.1	18.4	7496.6	20.8	5213.8	23.8	2758.6	26.9
S3	8972.4	18.5	7682.8	19.3	5469.0	23.5	2841.4	29.1
Average	8634.5	19.0	7333.3	20.7	5121.8	24.1	2689.7	28.7
StDv	390.55	0.95	453.62	1.31	401.09	0.85	195.55	1.64

Table F.21.4
Dynamic Modulus |E*| (MPa) and Phase angle, δ (degrees), test results for G2EE76 at 37.8°C

	10Hz		5Hz		1Hz		0.1Hz	
Sample	|E*| (MPa)	δ (deg.)	|E*| (MPa)	δ (deg.)	|E*| (MPa)	δ (deg.)	|E*| (MPa)	δ (deg.)
S1	3089.7	30.3	2537.9	31.5	1448.3	34.8	544.8	34.6
S2	3158.6	30.2	2627.6	31.2	1482.8	33.9	620.7	34.1
S3	3048.3	27.9	2710.3	29.5	1379.3	31.3	593.1	31.5
Average	3098.9	29.5	2625.3	30.7	1436.8	33.3	586.2	33.4
StDv	55.74	1.36	86.23	1.08	52.67	1.82	38.40	1.66

Table F.21.3
Dynamic Modulus |E*| (MPa) and Phase angle, δ (degrees), test results for G2EE76 at 54.4°C

	10Hz		5Hz		1Hz		0.1Hz	
Sample	|E*| (MPa)	δ (deg.)	|E*| (MPa)	δ (deg.)	|E*| (MPa)	δ (deg.)	|E*| (MPa)	δ (deg.)
S1	1027.6	28.4	800.0	27.4	482.8	23.6	303.4	16.3
S2	1165.5	27.9	937.9	28.1	558.6	24.8	337.9	17.3
S3	937.9	26.3	731.0	25.9	475.9	22.5	310.3	15.0
Average	1043.7	27.5	823.0	27.1	505.7	23.6	317.2	16.2
StDv	114.64	1.10	105.35	1.12	45.92	1.15	18.25	1.15

Table F.22.1
Dynamic Modulus |E*| (MPa) and Phase angle, δ (degrees), test results for G2PB76 at 25°C

	10Hz		5Hz		1Hz		0.1Hz	
Sample	|E*| (MPa)	δ (deg.)	|E*| (MPa)	δ (deg.)	|E*| (MPa)	δ (deg.)	|E*| (MPa)	δ (deg.)
S1	6586.2	24.8	4931.0	27.3	2765.5	31.7	1234.5	32.6
S2	5627.6	24.1	4627.6	28.4	2413.8	32.5	1048.3	31.6
S3	6786.2	25.3	5386.2	27.3	3262.1	33.1	1234.5	31.4
Average	6333.3	24.7	4981.6	27.7	2813.8	32.4	1172.4	31.9
StDv	619.32	0.60	381.83	0.64	426.19	0.70	107.51	0.64

Table F.22.2
Dynamic Modulus |E*| (MPa) and Phase angle, δ (degrees), test results for G2PB76 at 37.8°C

	10Hz		5Hz		1Hz		0.1Hz	
Sample	|E*| (MPa)	δ (deg.)	|E*| (MPa)	δ (deg.)	|E*| (MPa)	δ (deg.)	|E*| (MPa)	δ (deg.)
S1	2675.9	32.1	2048.3	31.9	1000.0	31.8	482.8	24.4
S2	1917.2	31.4	1510.3	31.1	779.3	29.4	434.5	22.5
S3	2489.7	30.7	1793.1	30.3	972.4	30.4	496.6	22.3
Average	2360.9	31.4	1783.9	31.1	917.2	30.5	471.3	23.1
StDv	395.36	0.70	269.08	0.80	120.25	1.21	32.59	1.16

Table F.22.3
Dynamic Modulus |E*| (MPa) and Phase angle, δ (degrees), test results for G2PB76 at 54.4°C

	10Hz		5Hz		1Hz		0.1Hz	
Sample	|E*| (MPa)	δ (deg.)	|E*| (MPa)	δ (deg.)	|E*| (MPa)	δ (deg.)	|E*| (MPa)	δ (deg.)
S1	689.7	27.6	510.3	25.8	344.8	21.6	220.7	14.8
S2	634.5	25.9	482.8	23.5	296.6	19.4	317.2	12.8
S3	572.4	27.7	420.7	25.8	275.9	21.7	206.9	15.3
Average	632.2	27.1	471.3	25.0	305.7	20.9	248.3	14.3
StDv	58.65	1.01	45.92	1.33	35.39	1.30	60.12	1.32

Table F.23.1
Dynamic Modulus |E*| (MPa) and Phase angle, δ (degrees), test results for G2S82 at 25°C

	10Hz		5Hz		1Hz		0.1Hz	
Sample	|E*| (MPa)	δ (deg.)	|E*| (MPa)	δ (deg.)	|E*| (MPa)	δ (deg.)	|E*| (MPa)	δ (deg.)
S1	8344.8	15.3	7600.0	19.4	4675.9	26.3	2310.3	30.2
S2	9503.4	17.3	8324.1	20.1	4765.5	25.9	3979.3	29.5
S3	9027.6	16.3	8269.0	18.3	4710.3	24.8	2593.1	28.5
Average	8958.6	16.3	8064.4	19.3	4717.2	25.7	2960.9	29.4
StDv	582.38	1.00	403.10	0.91	45.22	0.78	893.21	0.85

Table F.23.2
Dynamic Modulus |E*| (MPa) and Phase angle, δ (degrees), test results for G2S82 at 37.8°C

	10Hz		5Hz		1Hz		0.1Hz	
Sample	|E*| (MPa)	δ (deg.)	|E*| (MPa)	δ (deg.)	|E*| (MPa)	δ (deg.)	|E*| (MPa)	δ (deg.)
S1	2820.7	29.3	2137.9	30.4	1151.7	30.5	537.9	24.8
S2	3524.1	27.6	2558.6	26.5	1482.8	27.4	1110.3	28.4
S3	3289.7	27.3	2475.9	29.3	1372.4	31.1	758.6	27.5
Average	3211.5	28.1	2390.8	28.7	1335.6	29.7	802.3	26.9
StDv	358.18	1.08	222.87	2.01	168.55	1.99	288.70	1.87

Table F.23.3
Dynamic Modulus |E*| (MPa) and Phase angle, δ (degrees), test results for G2S82 at 54.4°C

	10Hz		5Hz		1Hz		0.1Hz	
Sample	|E*| (MPa)	δ (deg.)	|E*| (MPa)	δ (deg.)	|E*| (MPa)	δ (deg.)	|E*| (MPa)	δ (deg.)
S1	875.9	30.4	669.0	28.5	413.8	23.7	275.9	16.4
S2	1303.4	28.9	1400.0	28.3	813.8	27.4	455.2	17.8
S3	972.4	27.5	710.3	27.9	482.8	24.5	344.8	18.3
Average	1050.6	28.9	926.4	28.2	570.1	25.2	358.6	17.5
StDv	224.25	1.45	410.64	0.31	213.83	1.95	90.45	0.98

Table F.24.1
Dynamic Modulus |E*| (MPa) and Phase angle, δ (degrees), test results for G2CR82 at 25°C

	10Hz		5Hz		1Hz		0.1Hz	
Sample	|E*| (MPa)	δ (deg.)	|E*| (MPa)	δ (deg.)	|E*| (MPa)	δ (deg.)	|E*| (MPa)	δ (deg.)
S1	7013.8	20.1	6634.5	22.4	5400.0	28.3	1875.9	32.4
S2	7731.0	17.4	6241.4	20.4	4165.5	26.3	2213.8	31.5
S3	8303.4	18.4	6896.6	21.3	4565.5	25.3	2186.2	29.7
Average	7682.8	18.6	6590.8	21.4	4710.3	26.6	2092.0	31.2
StDv	646.18	1.37	329.76	1.00	629.86	1.53	187.65	1.37

Table F.24.1
Dynamic Modulus |E*| (MPa) and Phase angle, δ (degrees), test results for G2CR82 at 37.8°C

	10Hz		5Hz		1Hz		0.1Hz	
Sample	|E*| (MPa)	δ (deg.)	|E*| (MPa)	δ (deg.)	|E*| (MPa)	δ (deg.)	|E*| (MPa)	δ (deg.)
S1	2082.8	31.5	1544.8	34.2	820.7	31.2	386.2	27.3
S2	2489.7	29.4	2048.3	29.3	1103.4	33.2	620.7	26.3
S3	2565.5	28.4	2006.9	29.6	1062.1	29.7	572.4	25.7
Average	2379.3	29.8	1866.7	31.0	995.4	31.4	526.4	26.4
StDv	259.61	1.58	279.49	2.75	152.71	1.76	123.82	0.81

Table F.24.3
Dynamic Modulus |E*| (MPa) and Phase angle, δ (degrees), test results for G2CR82 at 54.4°C

	10Hz		5Hz		1Hz		0.1Hz	
Sample	|E*| (MPa)	δ (deg.)	|E*| (MPa)	δ (deg.)	|E*| (MPa)	δ (deg.)	|E*| (MPa)	δ (deg.)
S1	78	30.4	60	28.4	43	21.7	37	14.7
S2	91	28.5	79	27.7	56	22.9	39	16.2
S3	111	27.8	81	26	54	21.3	44	14.9
Average	93.3	28.9	73.3	27.4	51.0	22.0	40.0	15.3
StDv	16.62	1.35	11.59	1.23	7.00	0.83	3.61	0.81

Table F.25.1
Dynamic Modulus |E*| (MPa) and Phase angle, δ (degrees), test results for G2EE82 at 25°C

	10Hz		5Hz		1Hz		0.1Hz	
Sample	|E*| (MPa)	δ (deg.)	|E*| (MPa)	δ (deg.)	|E*| (MPa)	δ (deg.)	|E*| (MPa)	δ (deg.)
S1	9193.1	17.9	7110.3	21.3	4669.0	26.8	2324.1	30.5
S2	9744.8	17.6	7544.8	19.4	6137.9	24.1	3151.7	28.5
S3	9600.0	18.1	7310.3	20.4	5062.1	25.7	2551.7	28.4
Average	9512.6	17.9	7321.8	20.4	5289.7	25.5	2675.9	29.1
StDv	286.05	0.25	217.47	0.95	760.47	1.36	427.53	1.18

Table F.25.2
Dynamic Modulus |E*| (MPa) and Phase angle, δ (degrees), test results for G2EE82 at 37.8°C

	10Hz		5Hz		1Hz		0.1Hz	
Sample	|E*| (MPa)	δ (deg.)	|E*| (MPa)	δ (deg.)	|E*| (MPa)	δ (deg.)	|E*| (MPa)	δ (deg.)
S1	3055.2	29.7	2117.2	31.7	1151.7	34.3	558.6	25.9
S2	3255.2	28.3	2455.2	29.4	1310.3	32.7	627.6	25.4
S3	3144.8	29.3	2524.1	28.1	1393.1	31.2	689.7	26.1
Average	3151.7	29.1	2365.5	29.7	1285.1	32.7	625.3	25.8
StDv	100.18	0.72	217.76	1.82	122.66	1.55	65.55	0.36

Table F.25.3
Dynamic Modulus |E*| (MPa) and Phase angle, δ (degrees), test results for G2EE82 at 54.4°C

	10Hz		5Hz		1Hz		0.1Hz	
Sample	|E*| (MPa)	δ (deg.)	|E*| (MPa)	δ (deg.)	|E*| (MPa)	δ (deg.)	|E*| (MPa)	δ (deg.)
S1	813.8	28.3	620.7	26.4	406.9	22.5	282.8	15.4
S2	1041.4	27.6	869.0	26.5	565.5	22.4	400.0	16.1
S3	1165.5	31.4	689.7	29.9	544.8	24.5	337.9	18.9
Average	1006.9	29.1	726.4	27.6	505.7	23.1	340.2	16.8
StDv	178.38	2.02	128.16	1.99	86.23	1.18	58.65	1.85

Table F.26.1
Dynamic Modulus |E*| (MPa) and Phase angle, δ (degrees), test results for G2PB82 at 25°C

	10Hz		5Hz		1Hz		0.1Hz	
Sample	|E*| (MPa)	δ (deg.)	|E*| (MPa)	δ (deg.)	|E*| (MPa)	δ (deg.)	|E*| (MPa)	δ (deg.)
S1	6937.9	18.3	6103.4	20.1	3689.7	22.6	2269.0	25.8
S2	5731.0	20.9	5048.3	18.5	4241.4	25.1	1924.1	28.1
S3	7724.1	17.3	6289.7	19.3	4620.7	23.1	2303.4	27.4
Average	6797.7	18.8	5813.8	19.3	4183.9	23.6	2165.5	27.1
StDv	1003.9	1.9	669.5	0.8	468.2	1.3	209.8	1.2

Table F.26.2
Dynamic Modulus |E*| (MPa) and Phase angle, δ (degrees), test results for G2PB82 at 37.8°C

	10Hz		5Hz		1Hz		0.1Hz	
Sample	|E*| (MPa)	δ (deg.)	|E*| (MPa)	δ (deg.)	|E*| (MPa)	δ (deg.)	|E*| (MPa)	δ (deg.)
S1	3137.9	26.8	2600.0	27.3	1510.3	30.1	531.0	30.2
S2	3089.7	27.1	2531.0	28.2	1448.3	28.7	620.7	29.4
S3	3469.0	25.1	2793.1	26.8	1634.5	29.1	606.9	30.4
Average	3232.2	26.3	2641.4	27.4	1531.0	29.3	586.2	30.0
StDv	206.47	1.08	135.85	0.71	94.81	0.72	48.28	0.53

Table F.26.3
Dynamic Modulus |E*| (MPa) and Phase angle, δ (degrees), test results for G2PB82 at 45.4°C

	10Hz		5Hz		1Hz		0.1Hz	
Sample	|E*| (MPa)	δ (deg.)	|E*| (MPa)	δ (deg.)	|E*| (MPa)	δ (deg.)	|E*| (MPa)	δ (deg.)
S1	937.9	33.6	710.3	32.5	379.3	31.5	137.9	29.1
S2	965.5	33.1	731.0	32.9	406.9	31.1	165.5	28.4
S3	889.7	34.2	689.7	33.1	337.9	32.9	151.7	29.1
Average	931.0	33.6	710.3	32.8	374.7	31.8	151.7	28.9
StDv	38.40	0.55	20.69	0.31	34.71	0.95	13.79	0.40

Table F.27.1
Dynamic Modulus |E*| (MPa) and Phase angle, δ (degrees), test results for G3U64 at 25°C

	10Hz		5Hz		1Hz		0.1Hz	
Sample	|E*| (MPa)	δ (deg.)	|E*| (MPa)	δ (deg.)	|E*| (MPa)	δ (deg.)	|E*| (MPa)	δ (deg.)
S1	4600.0	22.8	3813.8	25.5	2300.0	30.4	1062.1	31.9
S2	5148.3	22.7	4203.4	24.8	2555.2	29.6	1124.1	32.4
S3	4686.2	23.5	3924.1	26.3	2231.0	31.8	1020.7	33.3
Average	4811.5	23.0	3980.5	25.5	2362.1	30.6	1069.0	32.5
StDv	294.83	0.44	200.84	0.78	170.75	1.12	52.07	0.71

Table F.27.2
Dynamic Modulus |E*| (MPa) and Phase angle, δ (degrees), test results for G3U64 at 37.8°C

	10Hz		5Hz		1Hz		0.1Hz	
Sample	|E*| (MPa)	δ (deg.)	|E*| (MPa)	δ (deg.)	|E*| (MPa)	δ (deg.)	|E*| (MPa)	δ (deg.)
S1	1572.4	31.5	1175.9	32.4	634.5	32.0	286.2	26.5
S2	1627.6	31.0	1286.2	31.8	665.5	31.5	310.3	26.4
S3	1506.9	32.1	1106.9	33.2	558.6	32.0	265.5	25.0
Average	1569.0	31.5	1189.7	32.5	619.5	31.8	287.4	26.0
StDv	60.42	0.55	90.45	0.73	54.99	0.26	22.44	0.82

Table F.27.3
Dynamic Modulus |E*| (MPa) and Phase angle, δ (degrees), test results for G3U64 at 54.4°C

	10Hz		5Hz		1Hz		0.1Hz	
Sample	|E*| (MPa)	δ (deg.)	|E*| (MPa)	δ (deg.)	|E*| (MPa)	δ (deg.)	|E*| (MPa)	δ (deg.)
S1	400.0	31.2	303.4	29.6	182.8	25.4	127.6	17.7
S2	437.9	32.9	772.4	30.8	203.4	26.4	134.5	18.4
S3	386.2	30.3	579.3	28.6	196.6	24.5	134.5	17.3
Average	408.0	31.4	551.7	29.7	194.3	25.4	132.2	17.8
StDv	26.78	1.32	235.70	1.08	10.53	0.95	3.98	0.53

Table F.28.1
Dynamic Modulus |E*| (MPa) and Phase angle, δ (degrees), test results for G3S70 at 25°C

	10Hz		5Hz		1Hz		0.1Hz	
Sample	|E*| (MPa)	δ (deg.)	|E*| (MPa)	δ (deg.)	|E*| (MPa)	δ (deg.)	|E*| (MPa)	δ (deg.)
S1	7153.9	19.7	5863.3	21.9	4192.8	25.7	2198.9	28.9
S2	7438.3	19.3	6335.9	21.3	4473.6	26.1	2408.9	28.2
S3	8125.2	17.9	6842.1	19.9	4550.7	23.9	2649.9	26.2
Average	7572.5	19.0	6347.1	21.1	4405.7	25.2	2419.2	27.8
StDv	499.33	0.97	489.50	1.03	188.33	1.19	225.72	1.37

Table F.28.2
Dynamic Modulus |E*| (MPa) and Phase angle, δ (degrees), test results for G3S70 at 37.8°C

	10Hz		5Hz		1Hz		0.1Hz	
Sample	|E*| (MPa)	δ (deg.)	|E*| (MPa)	δ (deg.)	|E*| (MPa)	δ (deg.)	|E*| (MPa)	δ (deg.)
S1	2672.2	27.7	2178.2	29.1	1255.8	31.2	600.9	27.4
S2	2993.1	27.6	2483.8	28.5	1388.8	29.9	690.3	26.8
S3	3115.8	25.1	2514.9	26.2	1615.5	28.3	765.8	25.6
Average	2927.0	26.8	2392.3	27.9	1420.0	29.8	685.7	26.6
StDv	229.10	1.48	186.10	1.52	181.85	1.43	82.54	0.88

Table F.28.3
Dynamic Modulus |E*| (MPa) and Phase angle, δ (degrees), test results for G3S70 at 54.4°C

	10Hz		5Hz		1Hz		0.1Hz	
Sample	|E*| (MPa)	δ (deg.)	|E*| (MPa)	δ (deg.)	|E*| (MPa)	δ (deg.)	|E*| (MPa)	δ (deg.)
S1	870.2	28.0	697.2	28.7	473.6	27.4	317.5	21.2
S2	1009.2	27.4	802.4	29.1	500.5	27.7	295.7	21.4
S3	1151.9	26.2	932.4	26.6	620.1	26.6	395.4	22.0
Average	1010.4	27.2	810.7	28.1	531.4	27.2	336.2	21.5
StDv	140.81	0.91	117.84	1.31	77.97	0.56	52.43	0.39

Table F.29.1
Dynamic Modulus |E*| (MPa) and Phase angle, δ (degrees), test results for G3CR70 at 25°C

	10Hz		5Hz		1Hz		0.1Hz	
Sample	|E*| (MPa)	δ (deg.)	|E*| (MPa)	δ (deg.)	|E*| (MPa)	δ (deg.)	|E*| (MPa)	δ (deg.)
S1	8143.7	16.8	6852.9	19.0	4632.2	23.0	2589.7	27.1
S2	8275.9	17.2	7147.1	17.8	5406.9	23.4	3018.4	27.1
S3	9604.6	14.6	7873.6	16.6	5604.6	20.5	3267.8	23.8
Average	8674.7	16.2	7291.2	17.8	5214.6	22.3	2958.6	26.0
StDv	808.01	1.39	525.37	1.21	513.95	1.59	343.01	1.91

Table F.29.2
Dynamic Modulus |E*| (MPa) and Phase angle, δ (degrees), test results for G3CR70 at 37.8°C

	10Hz		5Hz		1Hz		0.1Hz	
Sample	|E*| (MPa)	δ (deg.)	|E*| (MPa)	δ (deg.)	|E*| (MPa)	δ (deg.)	|E*| (MPa)	δ (deg.)
S1	3001.1	26.9	2458.6	28.3	1405.7	31.2	580.5	29.2
S2	3696.6	26.0	3064.4	27.5	1698.9	29.7	798.9	29.0
S3	4049.4	22.5	3264.4	24.4	2166.7	27.1	981.6	27.1
Average	3582.4	25.1	2929.1	26.7	1757.1	29.3	787.0	28.4
StDv	533.38	2.33	419.55	2.07	383.79	2.08	200.84	1.13

Table F.29.3
Dynamic Modulus |E*| (MPa) and Phase angle, δ (degrees), test results for G3CR70 at 54.4°C

	10Hz		5Hz		1Hz		0.1Hz	
Sample	|E*| (MPa)	δ (deg.)	|E*| (MPa)	δ (deg.)	|E*| (MPa)	δ (deg.)	|E*| (MPa)	δ (deg.)
S1	949.4	30.6	743.7	30.2	441.4	27.7	236.8	22.3
S2	1248.3	31.0	959.8	30.5	546.0	28.3	295.4	23.1
S3	1465.5	28.5	1189.7	27.7	778.2	27.2	411.5	23.5
Average	1221.1	30.0	964.4	29.5	588.5	27.7	314.6	22.9
StDv	259.12	1.34	223.02	1.51	172.37	0.55	88.92	0.57

Table F.30.1
Dynamic Modulus |E*| (MPa) and Phase angle, δ (degrees), test results for G3EE70 at 25°C

	10Hz		5Hz		1Hz		0.1Hz	
Sample	|E*| (MPa)	δ (deg.)	|E*| (MPa)	δ (deg.)	|E*| (MPa)	δ (deg.)	|E*| (MPa)	δ (deg.)
S1	5602.6	21.5	4624.9	23.2	2843.4	28.6	1269.4	31.0
S2	6476.3	23.3	5639.9	25.8	3381.7	29.4	1532.8	30.6
S3	5566.9	23.4	4698.8	25.4	2812.6	31.0	1280.7	31.8
Average	5882.0	22.7	4987.8	24.8	3012.6	29.7	1360.9	31.1
StDv	515.06	1.05	565.87	1.40	320.07	1.23	148.94	0.61

Table F.30.2
Dynamic Modulus |E*| (MPa) and Phase angle, δ (degrees), test results for G3EE70 at 37.8°C

	10Hz		5Hz		1Hz		0.1Hz	
Sample	|E*| (MPa)	δ (deg.)	|E*| (MPa)	δ (deg.)	|E*| (MPa)	δ (deg.)	|E*| (MPa)	δ (deg.)
S1	1974.1	28.9	1661.2	30.9	809.0	30.6	369.4	24.8
S2	2449.2	30.3	1805.0	31.9	965.1	32.0	449.2	26.0
S3	1877.1	31.1	1536.0	36.0	783.3	32.2	346.0	26.3
Average	2100.2	30.1	1667.4	32.9	852.5	31.6	388.2	25.7
StDv	306.17	1.14	134.59	2.67	98.39	0.87	54.11	0.77

Table F.30.3
Dynamic Modulus |E*| (MPa) and Phase angle, δ (degrees), test results for G3EE70 at 54.4°C

	10Hz		5Hz		1Hz		0.1Hz	
Sample	|E*| (MPa)	δ (deg.)	|E*| (MPa)	δ (deg.)	|E*| (MPa)	δ (deg.)	|E*| (MPa)	δ (deg.)
S1	590.4	30.8	455.2	29.3	270.9	26.0	162.1	18.7
S2	706.9	30.3	530.0	28.7	345.3	23.5	213.8	15.7
S3	546.8	31.3	413.9	30.0	244.8	24.2	169.0	16.4
Average	614.7	30.8	466.4	29.3	287.0	24.5	181.6	16.9
StDv	82.78	0.50	58.83	0.65	52.12	1.29	28.08	1.57

Table F.31.1
Dynamic Modulus |E*| (MPa) and Phase angle, δ (degrees), test results for G3PB70 at 25°C

	10Hz		5Hz		1Hz		0.1Hz	
Sample	|E*| (MPa)	δ (deg.)	|E*| (MPa)	δ (deg.)	|E*| (MPa)	δ (deg.)	|E*| (MPa)	δ (deg.)
S1	5061.3	23.3	4242.1	25.0	2505.5	30.0	1028.0	31.5
S2	4997.0	25.7	4281.2	28.3	2405.9	32.1	1008.7	30.7
S3	4914.0	25.2	4148.2	27.3	2429.8	32.3	1026.7	31.3
Average	4990.8	24.7	4223.9	26.8	2447.0	31.5	1021.1	31.1
StDv	73.83	1.27	68.36	1.67	51.98	1.30	10.79	0.42

Table F.31.2
Dynamic Modulus |E*| (MPa) and Phase angle, δ (degrees), test results for G3PB70 at 37.8°C

	10Hz		5Hz		1Hz		0.1Hz	
Sample	|E*| (MPa)	δ (deg.)	|E*| (MPa)	δ (deg.)	|E*| (MPa)	δ (deg.)	|E*| (MPa)	δ (deg.)
S1	1643.1	29.7	1388.8	32.1	629.7	31.1	307.3	22.6
S2	1680.3	30.9	1246.4	33.1	644.4	31.1	325.0	22.7
S3	1589.8	31.1	1165.9	36.4	620.1	31.6	309.2	23.1
Average	1637.7	30.5	1267.0	33.9	631.4	31.3	313.8	22.8
StDv	45.48	0.78	112.87	2.27	12.25	0.30	9.74	0.28

Table F.31.3
Dynamic Modulus |E*| (MPa) and Phase angle, δ (degrees), test results for G3PB70 at 54.4°C

	10Hz		5Hz		1Hz		0.1Hz	
Sample	|E*| (MPa)	δ (deg.)	|E*| (MPa)	δ (deg.)	|E*| (MPa)	δ (deg.)	|E*| (MPa)	δ (deg.)
S1	476.6	30.3	372.4	27.0	253.7	22.2	182.8	15.4
S2	413.8	29.1	340.3	25.1	224.6	18.9	165.5	15.9
S3	428.4	30.7	332.3	27.2	226.4	20.3	174.7	14.6
Average	439.6	30.0	348.4	26.4	234.9	20.4	174.3	15.3
StDv	32.88	0.84	21.21	1.14	16.28	1.65	8.63	0.66

Table F.32.1
Dynamic Modulus |E*| (MPa) and Phase angle, δ (degrees), test results for G3S76 at 25°C

	10Hz		5Hz		1Hz		0.1Hz	
Sample	|E*| (MPa)	δ (deg.)	|E*| (MPa)	δ (deg.)	|E*| (MPa)	δ (deg.)	|E*| (MPa)	δ (deg.)
S1	8779.3	14.3	7675.9	16.7	5586.2	21.5	3103.4	26.3
S2	10469.0	13.6	8613.8	15.7	6862.1	20.4	4206.9	25.1
S3	11324.1	11.1	9572.4	13.1	6675.9	16.3	4296.6	19.2
Average	10190.8	13.0	8620.7	15.2	6374.7	19.4	3869.0	23.5
StDv	1295.02	1.68	948.29	1.86	689.18	2.74	664.47	3.80

Table F.32.1
Dynamic Modulus |E*| (MPa) and Phase angle, δ (degrees), test results for G3S76 at 37.8°C

	10Hz		5Hz		1Hz		0.1Hz	
Sample	|E*| (MPa)	δ (deg.)	|E*| (MPa)	δ (deg.)	|E*| (MPa)	δ (deg.)	|E*| (MPa)	δ (deg.)
S1	3220.7	25.8	2613.8	27.7	1517.2	31.4	682.8	29.8
S2	4600.0	24.1	3751.7	26.1	2131.0	30.0	979.3	30.1
S3	4827.6	18.8	4089.7	21.4	2765.5	25.1	1379.3	26.1
Average	4216.1	22.9	3485.1	25.1	2137.9	28.8	1013.8	28.7
StDv	869.52	3.65	773.22	3.27	624.17	3.31	349.55	2.23

Table F.32.1
Dynamic Modulus |E*| (MPa) and Phase angle, δ (degrees), test results for G3S76 at 54.4°C

	10Hz		5Hz		1Hz		0.1Hz	
Sample	|E*| (MPa)	δ (deg.)	|E*| (MPa)	δ (deg.)	|E*| (MPa)	δ (deg.)	|E*| (MPa)	δ (deg.)
S1	1034.5	29.5	827.6	30.1	503.4	27.2	289.7	20.3
S2	1586.2	30.1	1227.6	29.5	682.8	27.9	400.0	21.5
S3	2041.4	24.7	1689.7	24.7	1172.4	25.1	620.7	22.8
Average	1554.0	28.1	1248.3	28.1	786.2	26.7	436.8	21.5
StDv	504.22	2.96	431.41	2.96	346.27	1.46	168.55	1.25

Table F.33.1
Dynamic Modulus |E*| (MPa) and Phase angle, δ (degrees), test results for G3CR76 at 25°C

	10Hz		5Hz		1Hz		0.1Hz	
Sample	|E*| (MPa)	δ (deg.)	|E*| (MPa)	δ (deg.)	|E*| (MPa)	δ (deg.)	|E*| (MPa)	δ (deg.)
S1	7391.8	18.5	6913.4	20.5	4269.0	25.5	2256.5	29.1
S2	8483.1	18.0	6972.0	19.5	5068.6	25.0	2737.2	28.2
S3	9082.0	17.0	7388.9	18.8	5031.4	23.5	2782.2	26.8
Average	8319.0	17.9	7091.4	19.6	4789.7	24.7	2592.0	28.0
StDv	856.99	0.77	259.26	0.89	451.31	1.04	291.37	1.18

Table F.33.2
Dynamic Modulus |E*| (MPa) and Phase angle, δ (degrees), test results for G3CR76 at 37.8°C

	10Hz		5Hz		1Hz		0.1Hz	
Sample	|E*| (MPa)	δ (deg.)	|E*| (MPa)	δ (deg.)	|E*| (MPa)	δ (deg.)	|E*| (MPa)	δ (deg.)
S1	2696.7	28.2	2296.7	29.5	1213.2	31.5	584.5	28.1
S2	3364.0	27.2	2583.9	28.2	1580.5	30.1	701.7	27.6
S3	3392.5	25.3	2713.8	26.8	1734.7	28.7	798.9	26.3
Average	3151.1	26.9	2531.5	28.1	1509.5	30.1	695.0	27.3
StDv	393.73	1.49	213.41	1.35	267.88	1.42	107.34	0.92

Table F.33.3
Dynamic Modulus |E*| (MPa) and Phase angle, δ (degrees), test results for G3CR76 at 54.4°C

	10Hz		5Hz		1Hz		0.1Hz	
Sample	|E*| (MPa)	δ (deg.)	|E*| (MPa)	δ (deg.)	|E*| (MPa)	δ (deg.)	|E*| (MPa)	δ (deg.)
S1	900.8	29.6	702.9	28.9	440.2	25.4	256.3	19.0
S2	1129.1	29.5	875.7	28.4	532.0	25.4	312.8	18.7
S3	1217.8	27.7	976.8	26.7	655.7	24.4	374.3	18.9
Average	1082.6	28.9	851.8	28.0	542.7	25.1	314.5	18.9
StDv	163.57	1.05	138.53	1.19	108.15	0.58	59.02	0.15

Table F.34.1
Dynamic Modulus |E*| (MPa) and Phase angle, δ (degrees), test results for G3EE76 at 25°C

	10Hz		5Hz		1Hz		0.1Hz	
Sample	|E*| (MPa)	δ (deg.)	|E*| (MPa)	δ (deg.)	|E*| (MPa)	δ (deg.)	|E*| (MPa)	δ (deg.)
S1	8648.3	21.3	5882.8	23.6	3655.2	28.4	1689.7	32.0
S2	6786.2	20.8	6944.8	22.5	3372.4	29.2	1641.4	31.2
S3	8206.9	19.9	5944.8	21.5	4358.6	27.9	2110.3	30.4
Average	7880.5	20.7	6257.5	22.5	3795.4	28.5	1813.8	31.2
StDv	973.01	0.71	596.08	1.05	507.84	0.66	257.95	0.80

Table F.34.2
Dynamic Modulus |E*| (MPa) and Phase angle, δ (degrees), test results for G3EE76 at 37.8°C

	10Hz		5Hz		1Hz		0.1Hz	
Sample	|E*| (MPa)	δ (deg.)	|E*| (MPa)	δ (deg.)	|E*| (MPa)	δ (deg.)	|E*| (MPa)	δ (deg.)
S1	2069.0	30.1	1710.3	31.9	862.1	32.9	372.4	25.1
S2	2200.0	29.4	2069.0	30.1	903.4	30.5	613.8	24.9
S3	2875.9	28.1	1731.0	28.3	1434.5	29.1	537.9	23.6
Average	2381.6	29.2	1836.8	30.1	1066.7	30.8	508.0	24.5
StDv	433.02	1.01	201.34	1.80	319.21	1.92	123.43	0.81

Table F.34.3
Dynamic Modulus |E*| (MPa) and Phase angle, δ (degrees), test results for G3EE76 at 54.4°C

	10Hz		5Hz		1Hz		0.1Hz	
Sample	|E*| (MPa)	δ (deg.)	|E*| (MPa)	δ (deg.)	|E*| (MPa)	δ (deg.)	|E*| (MPa)	δ (deg.)
S1	717.2	27.7	558.6	26.1	379.3	21.6	275.9	14.90
S2	800.0	29.4	613.8	28.4	413.8	23.9	241.4	17.00
S3	889.7	28.4	689.7	26.1	475.9	22.1	303.4	14.10
Average	802.3	28.5	620.7	26.9	423.0	22.5	273.6	15.3
StDv	86.23	0.85	65.79	1.33	48.93	1.21	31.10	1.50

TableF.35.1
Dynamic Modulus |E*| (MPa) and Phase angle, δ (degrees), test results for G3PB76 at 25°C

	10Hz		5Hz		1Hz		0.1Hz	
Sample	|E*| (MPa)	δ (deg.)	|E*| (MPa)	δ (deg.)	|E*| (MPa)	δ (deg.)	|E*| (MPa)	δ (deg.)
S1	7430.1	18.6	6116.5	20.9	4307.3	25.4	2230.5	28.3
S2	7948.3	17.9	6914.6	19.6	4794.3	24.5	2792.3	27.4
S3	8593.9	16.7	7090.8	18.8	4971.6	22.7	2891.8	25.0
Average	7990.7	17.7	6707.3	19.8	4691.1	24.2	2638.2	26.9
StDv	583.06	0.95	519.19	1.07	344.00	1.42	356.58	1.69

Table F.35.2
Dynamic Modulus |E*| (MPa) and Phase angle, δ (degrees), test results for G3PB76 at 37.8°C

	10Hz		5Hz		1Hz		0.1Hz	
Sample	|E*| (MPa)	δ (deg.)	|E*| (MPa)	δ (deg.)	|E*| (MPa)	δ (deg.)	|E*| (MPa)	δ (deg.)
S1	2713.6	27.6	2220.1	28.8	1271.5	30.5	588.3	27.0
S2	3252.9	26.2	2681.2	27.4	1503.1	29.7	723.2	27.3
S3	3538.9	23.8	2856.3	25.3	1889.5	27.5	907.7	25.5
Average	3168.5	25.9	2585.9	27.1	1554.7	29.2	739.7	26.6
StDv	419.07	1.93	328.64	1.74	312.22	1.55	160.32	0.93

Table F.35.3
Dynamic Modulus |E*| (MPa) and Phase angle, δ (degrees), test results for G3PB76 at 54.4°C

	10Hz		5Hz		1Hz		0.1Hz	
Sample	|E*| (MPa)	δ (deg.)	|E*| (MPa)	δ (deg.)	|E*| (MPa)	δ (deg.)	|E*| (MPa)	δ (deg.)
S1	851.0	27.9	685.2	29.6	444.8	27.5	247.9	21.3
S2	1129.9	28.9	878.0	29.0	506.7	28.2	326.6	22.8
S3	1318.2	26.6	1077.2	27.1	735.4	27.0	424.1	22.7
Average	1099.7	27.8	880.1	28.6	562.3	27.6	332.9	22.3
StDv	235.08	1.15	195.99	1.32	153.08	0.59	88.29	0.88

Table F.36.1
Dynamic Modulus |E*| (MPa) and Phase angle, δ (degrees), test results for G3S82 at 25°C

	10Hz		5Hz		1Hz		0.1Hz	
Sample	|E*| (MPa)	δ (deg.)	|E*| (MPa)	δ (deg.)	|E*| (MPa)	δ (deg.)	|E*| (MPa)	δ (deg.)
S1	11491.4	22.4	8887.9	26.6	5836.2	33.5	2905.2	38.1
S2	12181.0	22.0	9431.0	24.3	7672.4	30.1	3939.7	35.6
S3	12000.0	22.6	9137.9	25.5	6327.6	32.1	3189.7	35.5
Average	11890.8	22.3	9152.3	25.5	6612.1	31.9	3344.8	36.4
StDv	357.56	0.31	271.84	1.19	950.58	1.70	534.41	1.48

Table F.36.2
Dynamic Modulus |E*| (MPa) and Phase angle, δ (degrees), test results for G3S82 at 37.8°C

	10Hz		5Hz		1Hz		0.1Hz	
Sample	|E*| (MPa)	δ (deg.)	|E*| (MPa)	δ (deg.)	|E*| (MPa)	δ (deg.)	|E*| (MPa)	δ (deg.)
S1	3819.0	37.1	2646.6	39.6	1439.7	42.9	698.3	32.4
S2	4069.0	35.4	3069.0	36.8	1637.9	40.9	784.5	31.8
S3	3931.0	36.6	3155.2	35.1	1741.4	39.0	862.1	32.6
Average	3939.7	36.4	2956.9	37.2	1606.3	40.9	781.6	32.3
StDv	125.22	0.90	272.20	2.28	153.33	1.94	81.93	0.45

Table F.36.3
Dynamic Modulus |E*| (MPa) and Phase angle, δ (degrees), test results for G3S82 at 54.4°C

	10Hz		5Hz		1Hz		0.1Hz	
Sample	|E*| (MPa)	δ (deg.)	|E*| (MPa)	δ (deg.)	|E*| (MPa)	δ (deg.)	|E*| (MPa)	δ (deg.)
S1	1017.2	35.4	775.9	33.0	508.6	28.1	353.4	19.3
S2	1301.7	34.5	1086.2	33.1	706.9	28.0	500.0	20.1
S3	1456.9	39.3	862.1	37.4	681.0	30.6	422.4	23.6
Average	1258.6	36.4	908.0	34.5	632.2	28.9	425.3	21.0
StDv	222.97	2.53	160.20	2.49	107.79	1.48	73.32	2.32

Table F.37.1
Dynamic Modulus |E*| (MPa) and Phase angle, δ (degrees), test results for G3CR82 at 25°C

	10Hz		5Hz		1Hz		0.1Hz	
Sample	|E*| (MPa)	δ (deg.)	|E*| (MPa)	δ (deg.)	|E*| (MPa)	δ (deg.)	|E*| (MPa)	δ (deg.)
S1	8555.7	18.0	6942.5	20.2	4802.3	24.4	2538.5	29.0
S2	8966.7	17.0	7824.1	19.1	5440.2	23.7	3082.8	27.2
S3	9760.9	15.8	8035.6	17.3	5694.3	21.6	3264.9	25.3
Average	9094.4	16.9	7600.8	18.8	5312.3	23.3	2962.1	27.2
StDv	612.66	1.11	579.78	1.46	459.54	1.47	377.96	1.85

Table F.37.2
Dynamic Modulus |E*| (MPa) and Phase angle, δ (degrees), test results for G3CR82 at 37.8°C

	10Hz		5Hz		1Hz		0.1Hz	
Sample	|E*| (MPa)	δ (deg.)	|E*| (MPa)	δ (deg.)	|E*| (MPa)	δ (deg.)	|E*| (MPa)	δ (deg.)
S1	2889.1	28.4	2362.6	30.0	1330.5	32.9	559.2	30.2
S2	3519.5	27.5	2956.3	28.8	1608.0	31.4	768.4	30.1
S3	3746.6	24.2	3040.2	25.8	1970.7	28.2	906.9	27.3
Average	3385.1	26.7	2786.4	28.2	1636.4	30.8	744.8	29.2
StDv	444.27	2.22	369.37	2.16	321.06	2.43	175.04	1.68

Table F.37.3
Dynamic Modulus |E*| (MPa) and Phase angle, δ (degrees), test results for G3CR82 at 54.4°C

	10Hz		5Hz		1Hz		0.1Hz	
Sample	|E*| (MPa)	δ (deg.)	|E*| (MPa)	δ (deg.)	|E*| (MPa)	δ (deg.)	|E*| (MPa)	δ (deg.)
S1	952.9	28.7	751.1	28.2	465.5	24.6	290.8	17.6
S2	1249.4	29.2	977.6	28.8	574.1	25.9	339.7	19.0
S3	1385.6	26.2	1120.1	25.5	766.1	23.5	437.9	18.0
Average	1196.0	28.0	949.6	27.5	601.9	24.7	356.1	18.2
StDv	221.27	1.62	186.07	1.77	152.20	1.19	74.93	0.70

Table F.38.1
Dynamic Modulus |E*| (MPa) and Phase angle, δ (degrees), test results for G3EE82 at 25°C

	10Hz		5Hz		1Hz		0.1Hz	
Sample	|E*| (MPa)	δ (deg.)	|E*| (MPa)	δ (deg.)	|E*| (MPa)	δ (deg.)	|E*| (MPa)	δ (deg.)
S1	8746.6	16.1	7227.6	18.4	5103.4	23.2	2750.0	27.7
S2	9548.3	15.4	8196.6	17.4	5989.7	22.6	3565.5	26.6
S3	10544.8	13.3	8665.5	15.2	6096.6	19.2	3750.0	22.0
Average	9613.2	14.9	8029.9	17.0	5729.9	21.7	3355.2	25.5
StDv	900.90	1.44	733.31	1.65	545.14	2.17	532.15	3.04

Table F.38.2
Dynamic Modulus |E*| (MPa) and Phase angle, δ (degrees), test results for G3EE82 at 37.8°C

	10Hz		5Hz		1Hz		0.1Hz	
Sample	|E*| (MPa)	δ (deg.)	|E*| (MPa)	δ (deg.)	|E*| (MPa)	δ (deg.)	|E*| (MPa)	δ (deg.)
S1	2932.8	26.9	2387.9	28.8	1353.4	31.8	605.2	28.6
S2	4000.0	25.4	3331.0	27.1	1824.1	30.1	887.9	28.8
S3	4339.7	21.1	3500.0	23.1	2432.8	26.1	1169.0	25.5
Average	3757.5	24.5	3073.0	26.3	1870.1	29.3	887.4	27.6
StDv	734.14	2.99	599.26	2.89	541.12	2.92	281.90	1.87

Table F.38.3
Dynamic Modulus |E*| (MPa) and Phase angle, δ (degrees), test results for G3EE82 at 54.4°C

	10Hz		5Hz		1Hz		0.1Hz	
Sample	|E*| (MPa)	δ (deg.)	|E*| (MPa)	δ (deg.)	|E*| (MPa)	δ (deg.)	|E*| (MPa)	δ (deg.)
S1	955.2	29.1	760.3	29.1	472.4	25.8	286.2	19.0
S2	1389.7	29.9	1074.1	29.2	615.5	26.9	360.3	20.4
S3	1753.4	25.6	1439.7	25.1	998.3	24.4	541.4	20.6
Average	1366.1	28.2	1091.4	27.8	695.4	25.7	396.0	20.0
StDv	399.66	2.27	339.98	2.38	271.88	1.28	131.26	0.90

Table F.39.1
Dynamic Modulus |E*| (MPa) and Phase angle, δ (degrees), test results for G3PB82 at 25°C

	10Hz		5Hz		1Hz		0.1Hz	
Sample	|E*| (MPa)	δ (deg.)	|E*| (MPa)	δ (deg.)	|E*| (MPa)	δ (deg.)	|E*| (MPa)	δ (deg.)
S1	8713.8	17.8	6779.3	20.2	4620.7	25.0	2396.6	29.2
S2	8627.6	17.2	7779.3	19.1	5117.2	24.8	2924.1	28.2
S3	9765.5	15.5	7758.6	17.3	5517.2	22.1	3203.4	24.8
Average	9035.6	16.8	7439.1	18.9	5085.1	24.0	2841.4	27.4
StDv	633.57	1.19	571.47	1.44	449.14	1.60	409.76	2.28

Table F.39.2
Dynamic Modulus |E*| (MPa) and Phase angle, δ (degrees), test results for G3PB82 at 37.8°C

	10Hz		5Hz		1Hz		0.1Hz	
Sample	|E*| (MPa)	δ (deg.)	|E*| (MPa)	δ (deg.)	|E*| (MPa)	δ (deg.)	|E*| (MPa)	δ (deg.)
S1	2644.8	28.0	2162.1	29.8	1189.7	32.2	527.6	27.5
S2	3400.0	26.8	2910.3	28.1	1517.2	30.3	796.6	27.5
S3	3851.7	23.5	2910.3	24.9	2100.0	27.1	958.6	24.9
Average	3298.9	26.1	2660.9	27.6	1602.3	29.8	760.9	26.6
StDv	609.77	2.33	432.02	2.52	461.09	2.55	217.72	1.52

Table F.39.3
Dynamic Modulus |E*| (MPa) and Phase angle, δ (degrees), test results for G3PB82 at 54.4 °C

	10Hz		5Hz		1Hz		0.1Hz	
Sample	|E*| (MPa)	δ (deg.)	|E*| (MPa)	δ (deg.)	|E*| (MPa)	δ (deg.)	|E*| (MPa)	δ (deg.)
S1	875.9	28.6	693.1	28.1	441.4	24.4	282.8	17.6
S2	1193.1	29.8	920.7	29.0	548.3	25.9	320.7	19.3
S3	1465.5	26.6	1189.7	25.4	824.1	23.6	462.1	18.5
Average	1178.2	28.3	934.5	27.5	604.6	24.6	355.2	18.4
StDv	295.11	1.62	248.56	1.85	197.50	1.17	94.50	0.83

APPENDIX G

Results of Fatigue Life Test

Table G.1
Results of Fatigue Life Test of Gradation #1 samples

Mix	Beam	Stress kPa	Strain εi	Nf
G1U64	1	500	82.5	225,698
	2	550	133.1	176,091
	3	600	140.14	90,423
	4	700	176.22	12,591
G1S70	1	550	149.38	807,290
	2	650	215.6	506,440
	3	750	275	152,982
	4	850	338.9467	36,142
G1S76	1	700	159.5	1,033,232
	2	850	213.4	754,423
	3	950	227.7	417,655
	4	980	308	105,224
G1S82	1	800	191.4	1,415,527.84
	2	850	256.08	1,033,559.51
	3	900	273.24	572,187.35
	4	980	369.6	144,156.88
G1CR70	1	600	136.4	101,303
	2	650	143	81,770
	3	700	149.6	62,092
	4	750	170.5	16,943
G1CR76	1	650	132	81,992
	2	750	159.5	63,376
	3	850	181.5	16,032
	4	900	257.07	7,676
G1CR82	1	800	158.4	118,068.48
	2	850	191.4	91,261.44
	3	900	217.8	23,086.08
	4	980	308.484	11,053.44
G1EE70	1	550	157.3	490,344
	2	600	442.2	191,943
	3	700	586.3	177,233
	4	750	444.4	53,322
G1EE76	1	700	138.6	288,431
	2	750	214.5	174,313
	3	850	256.3	147,664
	4	950	320.8333	37,054
G1EE82	1	800	158.004	400,919.09
	2	850	244.53	242,295.07
	3	900	292.182	205,252.96
	4	980	365.75	51,505.06
G1Pb70	1	550	138.48	187,432
	2	650	167.33	160,432
	3	700	190.41	88,432
	4	750	269.6898	35,642
G1Pb76	1	700	222.722	120,554
	2	750	288.5	70,321
	3	800	303.502	37,983
	4	900	762.794	30,984
G1Pb82	1	800	244.9942	155,514.66
	2	850	317.35	90,714.09
	3	900	333.8522	48,998.07
	4	980	839.0734	39,969.36

Table G.2
Results of Fatigue Life Test of Gradation #2 samples

Mix	Beam	Stress kPa	Strain εi	Nf
G2U64	1	600	75	189987
	2	700	121	14818
	3	800	127	9723
	4	850	160	6557
G2S70	1	650	136	502,775
	2	750	196	84,798
	3	850	250	27,941
	4	950	308	14,334
G2S76	1	600	145	1,799,822
	2	700	194	1,566,606
	3	800	207	490,748
	4	850	280	79,884
G2S82	1	800	174	2,465,756.14
	2	850	232.8	2,146,250.22
	3	900	248.4	672,324.76
	4	980	336	109,441.08
G2CR70	1	500	116	897,907
	2	600	169	306,440
	3	700	222	200,733
	4	800	470	36,142
G2CR76	1	600	124	766,554
	2	700	130	324,422
	3	800	136	90,099
	4	900	155	41,334
G2CR82	1	800	148.8	1,050,178.98
	2	850	156	444,458.14
	3	900	163.2	123,435.63
	4	980	186	56,627.58
G2EE70	1	700	120	160,455
	2	800	145	81,673
	3	900	165	64,902
	4	950	234	13,442
G2EE76	1	700	193	918,919
	2	800	250	525,316
	3	900	263	198,499
	4	1000	661	58,552
G2EE82	1	800	231.6	1,258,919.03
	2	850	300	719,682.92
	3	900	315.6	271,943.63
	4	980	793.2	80,216.24
G2Pb70	1	700	143	1,904,856
	2	800	402	345,040
	3	900	533	133,980
	4	980	404	28,045
G2Pb76	1	600	126	1,400,190
	2	700	195	178,480
	3	800	233	28,444
	4	900	292	19,887
G2Pb82	1	800	151.2	1,918,260.30
	2	850	234	244,517.60
	3	900	279.6	38,968.28
	4	980	350	27,245.19

Table G.3
Results of Fatigue Life Test of Gradation #3 samples

Mix	Beam	Stress kPa	Strain εi	Nf
G3U64	1	600	67	155789.34
	2	700	108	12150.76
	3	800	113	7972.86
	4	850	143	5376.74
G3S70	1	650	598	412275.5
	2	750	178	69534.36
	3	850	228	22911.62
	4	950	280	11753.88
G3S76	1	600	132	1475854.04
	2	700	177	1284616.92
	3	800	188	402413.36
	4	850	255	65504.88
G3S82	1	800	158	2021920.035
	2	850	212	1759925.18
	3	900	226	551306.3032
	4	980	306	89741.6856
G3CR70	1	500	85	736283.74
	2	600	123	251280.8
	3	700	162	164601.06
	4	800	343	29636.44
G3CR76	1	600	91	628574.28
	2	700	95	266026.04
	3	800	99	73881.18
	4	900	113	33893.88
G3CR82	1	800	109	861146.7636
	2	850	114	364455.6748
	3	900	119	101217.2166
	4	980	136	46434.6156
G3EE70	1	700	102	131573.1
	2	800	123	66971.86
	3	900	140	53219.64
	4	950	199	11022.44
G3EE76	1	700	164	753513.58
	2	800	213	430759.12
	3	900	224	162769.18
	4	1000	562	48012.64
G3EE82	1	800	197	1032313.605
	2	850	255	590139.9944
	3	900	268	222993.7766
	4	980	674	65777.3168
G3Pb70	1	700	122	1561981.92
	2	800	342	282932.8
	3	900	453	109863.6
	4	980	343	22996.9
G3Pb76	1	600	107	1148155.8
	2	700	166	146353.6
	3	800	198	23324.08
	4	900	248	16307.34
G3Pb82	1	800	129	1572973.446
	2	850	199	200504.432
	3	900	238	31953.9896
	4	980	298	22341.0558

Vitae

Name	: Khaleel J. Al-Adham.
Nationality	: Jordanian
Date of Birth	: April 30, 1985.
Email	: Khaleel.aladham@gmail.com.
Address	: Palestine, Nablus.
Academic Background	: PhD in Transportation Engineering.

Khaleel J. Al-Adham has a PhD degree in Transportation Engineering, with excellent knowledge of all issues related to planning, traffic and pavement engineering. Khaleel is specialized in highway materials and design. His areas of interest include materials testing and evaluation of polymer modified asphalt binders and mixes, analysis and design of pavement, mathematical modeling, and pavement maintenance and management techniques. He will be working for full period on this proposed study.

He obtained his Master's degree (MS) in Civil Engineering at KFUPM (with specialization in Pavement Engineering) in 2014, and his BS in Civil Engineering from An-Rajah National University, Nablus, and Palestine in 2008. Before joining KFUPM, he served as a Teaching and Research Assistant for the An-Rajah University in Transportation research projects and courses. Since joining the Civil Engineering Department in KFUPM, he has been actively involved in research projects of transportation engineering. His MS thesis has the title of "Elastic Recovery evaluation of Saudi Asphalt Modified with Commercial Polymers".

He has been associated with a number of funded research projects related to modified asphalts, to name a few are:

- "Performance Grading Evaluation of Saudi Asphalt Modified With Honeywell Titan™ Polymers" (KFUPM-RI, 2013).

- "Effect of Riyadh Refinery Bitumen Variability on the Loadings of Honeywell Titan™ Polymers" (KFUPM-RI, 2014).
- "Investigation and modeling of Moisture Damage in Asphalt Binders at Nanoscale".(KFUPM-DSR, 2012).

Khaleel has some related publications, they are:

- Al-Adham, KH. & Arrifuzzaman MD. (2014). Moisture damage evaluation in carbon nanotubes reinforced asphalts. In Losa & Papagiannkis. *Sustainability, Eco-efficiency and conservation in Transportation Infrastructure Asset Management.* Paper presented at3rd International Conference on Transportation Infrastructure, Pisa, Italy. April 22-25 (pp. 103-109).

- Khaleel Al-Adham & Hamad Al-Abdul Wahhab (2015). Effect of Polymer type on improving rheological parameters related to Rutting resistance of Asphalt binders. *Bituminous Mixtures & Pavements VI – Nikolaides (Ed.)*. 6th International Conference, Thessaloniki, Greece. June 10-12 (pp. 89-95).

- MD. Abubaker, Al-Adham KH and H.I AlbdulWahhab (2016) Dynamic Refinement and Estimation of Asphalt Flow Number by Partial Load History Analysis. *Road Materials and Pavement Design* (Submitted: RMPD-16-07-10).

- Al-Adham KH, MD. Abubaker and H.I AlbdulWahhab (2017) Strain Recovery Rate and Absolute Percent Recovery of Polymer Modified Asphalt Binders. *Construction & Building Materials*. (Submitted: CONBUILDMAT-D-17-05400).

- Al-Adham, KH and H.I AlbdulWahhab (2017) Influence of Temperature on Jnr values of Polymer Modified Asphalt Binders. *International Journal of Pavement Research and Technology*. (Accepted: IJPRT_2017_158).

- MD. Abubaker, Al-Adham KH and H.I AlbdulWahhab (2017) Polyacrylonitrite Fiber Reinforced Styrene Butadiene Styrene Modified Asphalt Concrete. *Construction & Building Materials*. (Submitted: CONBUILDMAT-D-17-06360).